REPUBLIC OF TÜRKİYE
ANKARA UNIVERSITY
GRADUATE SCHOOL OF HEALTH SCIENCES

USE OF NEURAL STEM CELLS DIFFERENTIATED FROM HUMAN IPS CELLS AND TISSUE SCAFFOLDS OBTAINED BY 3D BIOPRINTING OF DIFFERENT NANOMATERIALS IN NEURAL REGENERATION

Cansu GÜRCAN KARATEPE

DEPARTMENT OF INTERDISCIPLINARY STEM CELL AND REGENERATIVE MEDICINE

DOCTORAL THESIS

SUPERVISOR

Assoc. Prof. Dr. Açelya YILMAZER AKTUNA

ANKARA

2025

REPUBLIC OF TÜRKİYE
ANKARA UNIVERSITY
GRADUATE SCHOOL OF HEALTH SCIENCES

USE OF NEURAL STEM CELLS DIFFERENTIATED FROM HUMAN IPS CELLS AND TISSUE SCAFFOLDS OBTAINED BY 3D BIOPRINTING OF DIFFERENT NANOMATERIALS IN NEURAL REGENERATION

Cansu GÜRCAN KARATEPE

DEPARTMENT OF INTERDISCIPLINARY STEM CELL AND REGENERATIVE MEDICINE

DOCTORAL THESIS

SUPERVISOR

Assoc. Prof. Dr. Açelya YILMAZER AKTUNA

CoHE 100/2000 SCHOLARSHIP

ANKARA
2025

ETHICAL STATEMENT

To Ankara University

Directorate of the Graduate School of Sciences,

The doctoral dissertation entitled " Use of Neural Stem Cells Differentiated from Human iPS Cells and Tissue Scaffolds Obtained by 3D Bioprinting of Different Nanomaterials in Neural Regeneration" was written by me in accordance with scientific ethics and values. The idea/hypothesis of the thesis belongs entirely to my thesis supervisors and me. The experimental study/research in the thesis was conducted by myself, and all sentences and comments belong to me.

I declare that the above-mentioned statements are true.

Student's Name and Surname: Cansu GÜRCAN KARATEPE

Date: 28/10/2025

Signature:

ACCEPTANCE AND APPROVAL

Ankara University Directorate of the Graduate School of Sciences

The thesis titled " Use of Neural Stem Cells Differentiated from Human iPS Cells and Tissue Scaffolds Obtained by 3D Bioprinting of Different Nanomaterials in Neural Regeneration" written by Cansu GÜRCAN KARATEPE from the Department of Interdisciplinary Stem Cell And Regenerative Medicine in Graduate School of Health Science, Ankara University, has been accepted UNANIMOUSLY as a DOCTORAL THESIS by the assesment committee whose members are listed below.

Defense Date: 28/10/2025

Prof. Dr. Asuman Özen
Ankara University
Chair

Doç. Dr. Açelya YILMAZER AKTUNA
Ankara University
Reporter

Prof. Dr. K. Can AKÇALI
Ankara University
Member

Prof. Dr. Eda Ayşe AKSOY
Hacettepe University
Member

Prof. Dr. Elif YALÇIN TOPÇUOĞLU
University of Health Science
Member

The decision of the jury regarding the thesis has been approved by the Board of Directors of Graduate School of Health Science Ankara University.

Prof. Dr. Fügen AKTAN
Graduate School Director

SUMMARY

Use of Neural Stem Cells Differentiated from Human iPS Cells and Tissue Scaffolds Obtained by 3D Bioprinting of Different Nanomaterials in Neural Regeneration

Spinal cord injury (SCI) is a life changing condition that affects millions of people worldwide. The global impact of spinal cord injury is significant, not only in terms of personal and family struggles, but also because of its economic burden on health systems and societies. With millions of people affected worldwide, spinal cord injury has led to an urgent need for innovative treatments to improve outcomes for spinal cord injury patients. While conventional therapies focus on managing symptoms and preventing further damage, stem cell therapies have emerged as a promising frontier in regenerative medicine. In this PhD thesis, neural stem cells differentiated from human iPS cells were treated with neural growth factors and different nanomaterials to differentiate into neural cells in 2-Dimensional (2D) culture medium. At the same time, tissue scaffolds were created from a 3-Dimensional (3D) bioprinter with bioink containing neural stem cells and nanomaterials and cultured with neural growth factors. Both 2D and 3D cultures were subjected to electric current to enhance neural differentiation potential. In addition, tissue scaffolds containing neural stem cells and MXene Quantum Dot (MQD), an electrically conductive nanomaterial, were implanted in rats with spinal cord injury. The regeneration process of the spinal cord damage created by utilizing this feature of MQD with electrical conductivity was followed. Thus, the effect of MQD with electrical conductivity on neural differentiation was investigated. Nerve regeneration studies involving cells and nanomaterials produced by bioprinting are limited in the literature. In this thesis, simultaneous 3D bioprinting of neural stem cells differentiated from human iPS cells, MQD and natural/synthetic polymers was performed for the first time. It was observed that MQD, which is known to have high electrical conductivity, was able to transfer the action potential between neurons more easily by applying electric current. In conclusion, this study highlights the potential of a multidisciplinary approach combining neural stem cells, MQD and electrical stimulation to enhance neural differentiation and promote functional recovery in spinal cord injury models. The results showed that electrical stimulation significantly enhanced neural differentiation by upregulating key neuronal markers, while MQD contributed to cell viability and neuroprotection. *In vivo* studies with functional assessments confirmed increased motor and sensory recovery in the combined treatment group, suggesting a synergistic effect of these interventions. Immunofluorescence and gene expression analyses confirmed the successful differentiation of neural stem cells into mature neurons and supported their integration into the injured spinal cord tissue. The thesis outputs are expected to support and pioneer stem cell studies, nanomaterial studies and nerve regeneration studies.

Keywords: Human iPS cells, Nanomaterials, Neural differentiation, 3-Dimensional bioprinting, Spinal cord injury

ÖZET

İnsan uPK Hücrelerinden Farklılaştırılmış Nöral Kök Hücreler ve Farklı Nanomalzemelerin 3-Boyutlu Biyobaskılanması ile Elde Edilen Doku İskelelerinin Nöral Rejenerasyonda Kullanımı

Omurilik yaralanması (OY), dünya çapında milyonlarca insanı etkileyen ve hayatlarını değiştiren bir durumdur. Omurilik yaralanmasının küresel etkisi, sadece kişisel ve ailevi mücadeleler açısından değil, aynı zamanda sağlık sistemleri ve toplumlar üzerindeki ekonomik yükü nedeniyle de önemlidir. Dünya çapında milyonlarca kişinin etkilendiği omurilik yaralanması, omurilik yaralanması hastalarının sonuçlarını iyileştirmek için yenilikçi tedavilere acil ihtiyaç duyulmasına neden olmuştur. Geleneksel tedaviler belirtileri yönetmeye ve daha fazla hasarı önlemeye odaklanırken, kök hücre tedavileri rejeneratif tıpta umut verici bir sınır olarak ortaya çıkmıştır. Bu doktora tezinde; insan uPK hücrelerinden farklılaştırılmış nöral kök hücrelerin nöral büyüme faktörleri ve farklı nanomalzemeler ile muamele edilerek 2-Boyutlu (2B) kültür ortamında nöral hücrelere farklılaşması sağlanmıştır. Aynı zamanda nöral kök hücre ve nanomalzeme içeren biomürekkep ile 3-Boyutlu (3B) biyoyazıcıdan doku iskeleleri oluşturulmuştur ve nöral büyüme faktörleri ile kültür edilmiştir. Nöral farklılaşma potansiyelini arttırmak için hem 2B hem de 3B kültürlere elektrik akım verilmiştir. Ayrıca omurilik hasarı verilmiş ratlara; nöral kök hücre ve elektrik iletkenliği olan nanomalzemelerden MXene Quantum Dot (MQD) içeren doku iskeleleri yerleştirilmiştir. Elektrik iletkenliği özelliğine sahip MQD'nin bu özelliğinden faydalanarak oluşturulan omurilik hasarının rejenerasyon sürecinin takip edilmiştir. Böylece elektrik iletkenliğini özelliğine sahip MQD'nin nöral farklılaşmaya etkisi araştırılmıştır. Biyobaskılamayla üretilmiş, hücre ve nanomalzeme içeren sinir rejenerasyon çalışmaları literatürde sınırlıdır. Bu tez çalışması ile birlikte ilk kez insan uPK hücrelerinden farklılaştırılmış nöral kök hücrelerin, MQD ve doğal/sentetik polimerlerin eş zamanlı 3B biyobaskılanması yapılmıştır. Yüksek elektrik iletkenliği olduğu bilinen MQD'nin elektrik akımı verilerek nöronlar arasındaki aksiyon potansiyelinin daha kolay aktarılması sağlandığı görülmüştür. Sonuç olarak, bu çalışma nöral kök hücreler, MQD ve elektrik stimülasyonunu birleştiren multidisipliner bir yaklaşımın nöral farklılaşmayı arttırma ve omurilik yaralanması modellerinde fonksiyonel iyileşmeyi teşvik etme potansiyelini vurgulamaktadır. Sonuçlar, elektrik stimülasyonunun temel nöronal belirteçleri yukarı doğru düzenleyerek nöral farklılaşmayı önemli ölçüde artırdığını, MQD'nin ise hücre canlılığına ve nöroproteksiyona katkıda bulunduğunu göstermiştir. Fonksiyonel değerlendirmeler yapılan *in vivo* çalışmalarda, kombine tedavi grubunda motor ve duyusal iyileşmenin arttığını doğrulayarak bu müdahalelerin sinerjik bir etkisi olduğunu düşündürmüştür. İmmünofloresan ve gen ekspresyonu analizleri, nöral kök hücrelerin olgun nöronlara başarılı bir şekilde farklılaşmaya başladığını doğrulamış ve yaralı omurilik dokusuna bütünleşmesini desteklemiştir. Tez çıktılarının kök hücre çalışmaları, nanomalzeme çalışmaları ve sinir rejenerasyon çalışmalarına destek ve öncü model olması beklenmektedir.

Anahtar Sözcükler: İnsan uPK hücrelerinden farklılaştırılmış nöral kök hücreler, Nanomalzemeler, Nöral farklılaşma, 3-Boyutlu biyobaskılama, Omurilik hasarı

TABLE OF CONTENTS

Ethics Statement ii
Acceptance and Approval iii
Summary iv
Özet v
Table of Contents vi
Acknowledgments viii
Symbols And Abbreviations ix
Index of Figures xi
Index of Tables xiii

1. INTRODUCION 1
1.1. Spinal Cord Injury 1
1.2. Stem Cells 7
1.3. Induced Pluripotent Stem Cells 7
1.3.1. iPSC-derived Neural Stem Cells 9
1.4. 3D-Bioprinting 12
1.5. Nanomaterials 15
1.5.1. Classification of Nanomaterials According To Their Size 15
1.5.2. 2D Nanomaterials and Derivatives 17
1.5.2.1. Types of 2D Nanomaterials 17
1.5.2.2. MXene Quantum Dots 18

2. MATERIALS AND METHODS 22
2.1. Materials 22
2.2. Methods 23
2.2.1. Cell Culture and Differentiation 23
2.2.1.1. Mesenchymal Stem Cell Culture and Differentiation 23
2.2.1.2. Human Neural Stem Cell (HNSC) Culture and Differentiation 24
2.2.1.3. Induced Pluripotent Stem Cell Culture (iPSC), Characterisation and Differentiation 25
2.2.2. Nanomaterials Treatment 29
2.2.3. Electrical Current Application 30
2.2.3.1. Electrical Current Application 30
2.2.3.2. Magnetic Field Application 30
2.2.4. 3D-Bioprinting Processes 31
2.2.4.1. Scaffold Design 31
2.2.4.2. Bioink Preparation 31
2.2.4.3. 3D Bioprinting and Crosslinking 32
2.2.5. Real Time Polymerase Chain Reaction 33
2.2.5.1. RNA Isolation 33
2.2.5.2. cDNA Synthesis 34
2.2.5.3. qRT-PCR 34
2.2.6. Immunohistochemical Staining 35
2.2.6.1. Live-Dead Staining 35
2.2.6.2. Immunofluorescence Staining 35
2.2.6.3. Alkaline Phosphatase Staining 35
2.2.7. Animal Experiment 36
2.2.7.1. Electromyography (EMG) Test 37
2.2.7.2. Basso, Beattie and Bresnahan (BBB) Locomotor Test 38

2.2.7.3. Hot Plate Locomotor Test 39
2.2.8. Histological Analysis 39
2.2.8.1. Sample Preparation for Scanning Electron Microscope (SEM) Imaging 40
2.2.9. Statistical Analysis 41

3. RESULTS 42
3.1. Mesenchymal Stem Cell Differentiation and Characterization 42
3.1.1. Determination of the Effect of sGO and Electric Current Application on the Viability of Mesenchymal Stem Cells by Live-Dead Staining Analysis 43
3.1.2. Determination of the Effect of sGO and Electric Current Application on Neural Markers in Mesenchymal Stem Cells by Gene Expression (qRT-PCR) Analysis 44
3.1.3. Determination of the Effect of sGO and Electric Current Treatment on Neural Proteins in Mesenchymal Stem Cells by Fluorescence Microscopy 45
3.2. Culturing, Dissociating and Differentiating Human Neural Stem Cell 46
3.2.1. Light Microscopy Images of Neurons Derived from Human Neural Stem Cell Lines 46
3.3. Induced Pluripotent Stem Cell (iPSC) Characterisation and Differentiation 47
3.3.1. PBMC Isolation, Transduction and Colony Growth 47
3.3.2. Characterization of Induced Pluripotent Stem Cells by Gel Electrophoresis and Gene Expression (qRT-PCR) Analysis 48
3.3.3. Characterization of Induced Pluripotent Stem Cells by Immunohistochemical Staining 51
3.3.3.1. Determination of Protein Expression of Pluripotent Cell Markers by Immunohistochemical Methods 51
3.3.3.2. Alkaline Phosphatase Live Staining to Confirm the Presence of Pluripotency 52
3.3.4. Embryoid Body Formation, Differentiation, qPCR and Immunofluorescence Staining 53
3.3.5. iPSC Culture for Neural Differentiation 56
3.3.5.1. iPSC Derived Neural Differentiation Characterization 57
3.4. Nanomaterials Treatment and Cytotoxicity Test 59
3.5. 3D-Bioprinting Processes 60
3.5.1. Determination of the Effect of sGO and Electric Current Application on the Viability of Scaffolds Cultured with Mesenchymal Stem Cells by Live-Dead Staining Analysis 60
3.5.2. Determination of the Effect of sGO and Electric Current Application on Neural Markers in scaffolds with Mesenchymal Stem Cells by Gene Expression (qRT-PCR) Analysis 61
3.5.3. Determination of The Morphological Properties of Neural Stem Cells Using Scanning Electron Microscope on Scaffolds 62
3.6. Animal Experiments Results 64
3.6.1. BBB Locomotor Test Results 64
3.6.2. Hot Plate Locomotor Test Results 65
3.6.3. Electromyography (EMG) Measurement Results 66
3.6.4. Immunofluorescence Staining of Spinal Cord Tissue Obtained From Rats 67

4. DISCUSSION 69
5. CONCLUSION AND FUTURE ASPECTS 85
REFERENCES 87
APPENDIXS 97
Appendix-1 97
Appendix-2 98
Appendix-3 99

ACKNOWLEDGMENTS

I am honored to do my PhD as a student of Ankara University Stem Cell Institute. I would like to thank my esteemed professors and colleagues who shared their scientific knowledge with us throughout my higher education.

I would like to express my endless gratitude to my advisor, Assoc. Prof. Dr. Açelya YILMAZER AKTUNA, who shared her life experiences, scientific knowledge and experiences throughout my doctoral thesis study; who brought me awareness, matured and supported me.

I would like to thank the Scientific and Technical Research Council of Turkey for providing financial support for my PhD thesis study within the scope of the 1004 project (Project No. 20AG003-P8), as well as Ankara University Stem Cell Institute and Ankara University Biomedical Engineering Department, from whose materials and equipment I benefited during my thesis study. I would also like to thank the Council of Higher Education for the YÖK 100/2000 scholarship in the priority area of stem cell studies.

I would like to thank Berfin İlayda Öztürk, Buse Altun, Esen Kirit, Hande Yavuz, Cemile Gökçe and my other teammates for their help and contributions throughout my thesis study. I would like to thank Prof. Dr. Asuman ÖZEN and Assoc. Dr. Ahmet CEYLAN, faculty members of Ankara University, Faculty of Veterinary Medicine, who contributed to obtaining ultra-thin sections for my thesis study. I would like to thank Prof. Kostas Kostarelos, member of the National Graphene Institute at the University of Manchester for the supply of graphene oxide material used in my thesis study and Prof. Sanjiv Dhingra, member of the University of Manitoba for the supply of MXene Quantum Dot material.

I would like to express my respect, love and gratitude to my precious mother Meryem GÜRCAN and my father Fikret GÜRCAN, who spent all their labor and love for me throughout their lives, and I would like to express my love and thanks to my precious sister Ceyda GÜRCAN, who is one of the most precious people in my life and with whom I share every moment.

My dear son Sarp Kaan KARATEPE, he is still very young, but you have always given me strength with your presence. The happiness of your presence is worth everything. Thank you so much for being in my life.

My dear husband Fatih KARATEPE, I would like to thank you for listening to me patiently and guiding me at every moment of my life, opening new horizons for me, and never withholding your help from me. Your sacrifices are very precious to me. Thank you so much for being in my life.

SYMBOLS AND ABBREVIATIONS

2D	2 Dimensional
3D	3 Dimensional
AF	Attechment Factor
BBB	The Basso, Beattie and Bresnahan
BDNF	Human Brain-Derived Neurotrophic Factor
BSA	Bovine Serum Albumin
$CaCl_2$	Calcium Chloride
CAD	Computer Aided Design
cDNA	Complementary DNA
CO_2	Carbon Dioxide
DMEM	Dulbecco's Modified Eagle's Medium
DMSO	Dimethyl Sulfoxide
DNA	Deoxyribose Nucleic Acid
DPBS	Dulbecco’s Phosphate Buffered Saline
EDTA	Ethylenediaminetetraacetic Acid
EGF	Epidermal Growth Factor
EMG	Electromyography
ESC	Embriyonic Stem Cell
FBS	Fetal Bovine Serum
FGF	Fibroblast Growth Factors
g	Gravitiy
HNSC	Human Neural Stem Cell
hβ-NGF	Human β-Nerve Growth Factor
iPSC	Induced Pluripotent Stem Cell
mA	Milliampere
MF	Magnetic Field
mL	Milliliter
mm	Millimeter
mM	Millimolar
MQD	MXene Quantum Dot
MSC	Mesenchymal Stem Cell
NSC	Neural Stem Cell
PBMC	Peripheral Blood Mononuclear Cell
PCR	Polymerase Chain Reaction
PSC	Pluripotent Stem Cell
RNA	Ribonucleic Acid

RPM	Revolutions Per Minute
SCI	Spinal Cord Injury
SEM	Scanning Electron Microscopy
sGO	Small Graphene Oxide
µl	Microliter
µm	Micrometre
°C	Degrees Celsius

FIGURES

Figure 1.1. Spinal cord anatomy 1

Figure 2.1. Timeline of mesenchymal stem cell differentiation 24

Figure 2.2. Timeline for obtaining induced pluripotent stem cells 27

Figure 2.3. ARM-based microcontroller designed to apply electric current to cells 30

Figure 2.4. Magnetic circuit designed to non-invasively apply electric current to rats 31

Figure 2.5. Snapshot of scaffolds printed on a 3D bioprinter, taken from each layer during printing 32

Figure 2.6. Schematic of 3D-Bioprinting processes 32

Figure 2.7. Spinal cord injury in rats and scaffold placement at the damaged area 37

Figure 2.8. Implantation of EMG probes in rats and delivery of stimulation 38

Figure 2.9. Specially prepared test boxes for BBB locomotor testing 38

Figure 2.10. Hot plate specially prepared for locomotor testing, special table that can provide stable heat 39

Figure 2.11. Emitech K550x Sputter Coater used to coat scaffolds with gold 40

Figure 2.12. Images of scaffolds uncoated and coated with gold prior to SEM imaging 41

Figure 3.1. Live-dead images of MSC cells treated with sGO and electric current. MSC cells were visualized under fluorescence microscopy at 1, 7 and 14 days after sGO and electric current treatment (10X) 43

Figure 3.2. Real time PCR analysis of MSC cells at days 1, 7 and 14 after treatment with sGO and electric current. Gene expression levels were calculated and normalized to the control group $p<0.05$ 44

Figure 3.3. Fluorescence microscope images of MSC cells at days 1, 7 and 14 after treatment with sGO and electric current. DAPI (blue), Nestin-FITC (green), b-III-tubulin-AF594 (red) (20X) 45

Figure 3.4. Differentiated culture images of HNSC cell line. The HNSC cell line was imaged under inverted light microscopy on days 2, 5, 11, 15, 18 and 21 after differentiation media treatment (10X) and (20X) 46

Figure 3.5. Culture images of PBMC cells on days 1 and 3 under light microscope after isolation 47

Figure 3.6. Changes of PBMC cells at days 1, 3, 5, 10 and 15 after transduction under light microscope 48

Figure 3.7. Images of the growth of colonies after colony selection on days 2, 3, 7 and 10 under the light microscope 48

Figure 3.8. PCR gel image demonstration of the presence of virus transgenes (SeV) expression in PBMC cells after transduction 49

Figure 3.9. Measurement of gene expression by qPCR at subsequent passages (A. SOX2 Expression, B. Oct4 Expression and C. Nanog Expression). Gene expression levels were calculated and normalized to the control group $p<0.05$ 50

Figure 3.10. PCR gel image demonstration of reduced gene expression of viral vectors (Sev) in iPSC colonies 50

Figure 3.11. SeV qPCR Results (A. SeV Expression, B. KOS Expression, C. Klf4 Expression and D. c-Myc Expression) Results were analyzed using GraphPad Prism (9.0.0). Two-way ANOVA test was used and significance level was accepted as $p<0.05$ 51

Figure 3.12. 4th iPS Cell Colony Stained with PSC 4-Marker Immunocytochemistry Kit (A. blue DAPI, red oct4 (20X), B. blue DAPI, red TRA-1-60, (20X) C. Red Oct4, Green SSEA4, (10X), D. blue DAPI, Green SSEA4, (10X) E. blue DAPI, Green Sox2, (40X) F. Red TRA-1-60, Green SOX2) (20X) 52

Figure 3.13. C2p10, c3p18, C4p22 Alkaline Phosphatase Staining 53

Figure 3.14. C4p25 Embryoid Body Formation 53

Figure 3.15. C4p25 Embryoid body spontaneous differentiation 54

Figure 3.16. qPCR Results for EB Formation (A. AFP Expression, B. Brachury Expression and C.FGF5 Expression.) Results were analyzed using GraphPad Prism (9.0.0). Two-way ANOVA test was used and significance level was accepted as $p<0.05$ 55

Figure 3.17. C4p25 EB Spontan Farklılaşma, 20X (A. DAPI, B. DAPI +AFP, C. DAPI +FGF5, D. DAPI +Brachury) 55

Figure 3.18. iPSC culture light microscopy images 56

Figure 3.19. iPS cells exposed to induction medium for 7 days 56

Figure 3.20. Light microscopy image of cells differentiating from iPSC into neural stem cells 57

Figure 3.21. Real-time PCR analysis of iPSC-derived neural stem cells at days 7, 14 and 21 after treatment with MQD and electric current. Gene expression levels were calculated and normalized to the control group $p<0.05$ 57

Figure 3.22. Live-Dead staining image of neural stem cells differentiated from iPSC 58

Figure 3.23. Immunofluorescent staining image of neural stem cells differentiated from iPSC 59

Figure 3.24. Cell viability analysis of iPS cells 24 hours after treatment with MQD. Normalized to control group $p<0.05$ 60

Figure 3.25. After 14 days, Live-Dead staining image of sGO and electrically treated scaffolds analyzing the number of viable cells 61

Figure 3.26. Real-time PCR analysis of MSC-derived neural stem cells isolated from scaffold on days 1, 7 and 14 after treatment with sGO and electric current. Gene expression levels were calculated and normalized to the control group $p<0.05$ 62

Figure 3.27. SEM images of scaffolds printed with neural stem cells 63

Figure 3.28. Analysis of the evaluation of functional motor recovery with the BBB score test 64

Figure 3.29. Analysis of hot plate test showing pain response 65

Figure 3.30. Peak image of the shock repeated at 0.1 s intervals to the experimental groups in the LabChart interface 66

Figure 3.31. Analysis of the EMG frequency of the experimental groups by analyzing all responses in terms of peak amplitude and frequency using the peak analysis feature of the LabChart interface 67

Figure 3.32. Immunofluorescence images of spinal cord tissue obtained from rats 68

TABLES

Table 2.1. Materials used in the experiments and their catalog numbers 22

1. INTRODUCTION

1.1. Spinal Cord Injury

The spinal cord is a long, tube-like structure made up of nerve tissue. It is located within the vertebral column and extends from the brainstem down to the lower back. The spinal cord transmits messages between the brain and many body parts, including muscles, skin, and organs. The spinal cord is segmented into four primary sections.

The cervical region is the uppermost part of the spinal cord located in the neck area and controls head and neck movements, the diaphragm and the arms. Thoracic region Located in the upper back, this part of the spinal cord helps control the chest muscles and abdominal muscles. Lumbar region Located in the lower back, this part is responsible for leg movements and some of the lower abdominal muscles. The sacral region is the lowest part of the spinal cord and controls the bowel, bladder and sexual functions.

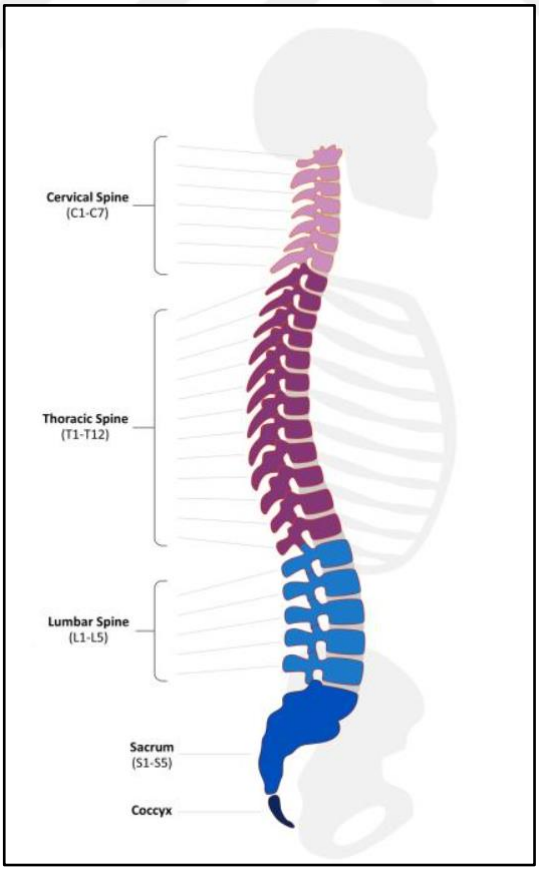

Figure 1.1. Spinal cord anatomy (National Institutes of Neurological Disorders and Stroke, 2025)

A spinal cord injury (SCI) is a serious condition affecting the central nervous system, leading to significant and often permanent changes in strength, sensation, and various bodily functions below the area of the injury. The spinal cord is an essential component of the body, serving as a conduit for communication between the brain and the peripheral system. Disruption of this route due to trauma or disease might result in profound repercussions (Dumont et al., 2001; W. R. Kim et al., 2017).

Spinal cord injuries are often categorized into two types based on their etiology. Traumatic spinal cord injury results from a sudden, traumatic incident that fractures or dislocates vertebrae, leading to compression or damage of the spinal cord. Common causes of traumatic spinal cord injury include: Motor vehicle accidents, which are a leading cause of spinal cord injuries worldwide, and can cause severe damage to the spinal cord. Falls, particularly prevalent among elderly persons, can result in vertebral fractures, subsequently causing spinal cord paralysis. High-impact sports such as soccer, gymnastics or diving can cause spinal cord damage. Gunshot wounds, stabbings and other acts of violence can also cause spinal cord trauma. Non-Traumatic Spinal Cord Injury is caused by underlying medical conditions or diseases that gradually weaken or damage the spinal cord. Tumors growing abnormally in or around the spinal cord can compress nerves and cause injury. Conditions such as meningitis or abscesses can cause inflammation around the spinal cord, leading to damage. Degenerative diseases such as multiple sclerosis or arthritis can slowly wear down the spinal cord over time. Stroke or other blood vessel problems in the spinal cord area can also lead to spinal cord paralysis (Alizadeh et al., 2019).

The severity and type of spinal cord injury largely determine the level of damage and the chances of recovery. A complete spinal cord injury results in a full loss of sensation and movement below the point of injury. This transpires when the spinal cord is entirely cut or significantly impaired. Individuals with a full spinal cord damage typically endure irreversible paralysis (paraplegia or quadriplegia), contingent upon the injury's location. In an incomplete spinal cord injury, certain impulses continue to transmit between the brain and the regions inferior to the lesion site. This indicates that the individual can preserve a degree of mobility or sensation. The degree of recuperation can significantly differ according on the severity of the harm.

Symptoms of a spinal cord injury can differ based on the type and location of the injury. Common symptoms can be listed as follows. Inability to move parts of the body, with

loss of movement ranging from mild weakness to complete paralysis. Sensory changes such as numbness, tingling or loss of feeling in certain areas. Depending on the level of injury, individuals may have difficulty urinating or controlling bowel movements. Higher level injuries, especially in the cervical region, may impair the ability to breathe, requiring mechanical ventilation. Some individuals may experience uncontrollable spasms or exaggerated reflexes below the level of injury. Damage to nerve fibers can lead to chronic pain or a burning sensation in the affected areas.

Spinal cord injury (SCI) is a life-changing condition that affects millions of people worldwide. An damage to the spinal cord can result in significant physical disability, loss of motor function, and several health issues. The global impact of SCI is significant, not only in terms of personal and family struggles, but also because of its economic burden on health systems and societies. Although pinpointing the exact percentage of the global population affected by spinal cord injuries is challenging, it is estimated that millions of people live with the effects of these injuries. Understanding the prevalence and global impacts of spinal cord injury can help shape better prevention, treatment and support strategies. Annually, it is estimated that between 250,000 and 500,000 individuals globally sustain a spinal cord injury. Exact figures vary due to under-reporting and variability in the quality of data collection in different countries. Research indicates that the global prevalence of spinal cord injuries ranges from 40 to 80 cases per million people each year (Ahuja et al., 2017).

The population of individuals with spinal cord injuries differs greatly across various regions. In developed countries with better health infrastructure, reported rates are often higher due to more comprehensive diagnostic and reporting systems. In contrast, many developing countries may under-report SCI cases due to limited medical facilities or lack of access to appropriate care. Determining the precise percentage of the global population affected by spinal cord injuries is challenging, but estimates indicate that around 0.005% to 0.01% of people worldwide experience this condition. This may seem like a small percentage, but given the current global population of more than 8 billion, it translates into millions of individuals worldwide (Lu et al., 2024).

Different regions show varying prevalence rates. Spinal cord injuries are more prevalent in high-income countries due to the frequency of accidents, such as vehicular incidents and sports-related injuries. In low-income countries where health systems are underdeveloped, many cases of spinal cord injury may go unreported or untreated.

Spinal cord injury affects people of all ages, but certain age groups are more at risk. The majority of new cases of spinal cord injury occur in people between the ages of 16 and 30. This demographic is more prone to engage in hazardous activities, such as high-speed driving or extreme sports, hence elevating the risk of severe injury. There is also a noticeable gender disparity in SCI cases. Men account for around 80% of all spinal cord injuries, which can be attributed to their greater involvement in activities such as driving, manual labor and contact sports. Men's predisposition to risk-taking behaviors further explains this gender gap (Parent et al., 2011).

Damage to the spinal cord has a profound impact on the quality of life for those affected. Individuals with spinal cord paralysis frequently encounter considerable physical and psychological health issues, including persistent pain, impaired bladder and bowel control, and sexual dysfunction. The psychological effects can be equally profound, with numerous patients experiencing sadness, anxiety, and social isolation as a result of their physical constraints.

The economic burden of SCI is also great. The cost of long-term care, rehabilitation and specialized medical equipment can be very high for both individuals and their families. In countries with inadequate healthcare coverage, this often leads to financial hardship. Access to appropriate health care for SCI patients varies significantly around the world. In high-income countries, patients often have access to specialized rehabilitation centers, advanced medical care and support services. Nevertheless, in numerous low- and middle-income nations, such facilities are limited, resulting in many patients not receiving sufficient therapy or follow-up care. Rehabilitation plays a crucial role in improving the quality of life for spinal cord injury patients; however, it is often inaccessible to many due to high costs or geographic limitations. The disparity in healthcare access substantially impacts the long-term prognosis of individuals with spinal cord injury (SCI) (Malekzadeh et al., 2022).

Innovative therapeutics for spinal cord injury (SCI) are being formulated to enhance recovery by facilitating neuronal regeneration, mitigating damage, and reinstating lost functions. These advanced medicines aim to address the restricted natural regenerative ability of the spinal cord, presenting promising opportunities in neuroregeneration. The following are the most promising novel therapies for spinal cord damage.

Stem cell therapy involves transplanting stem cells into the injured spinal cord to promote the regeneration of neurons, glial cells, and supportive tissues. Mesenchymal stem cells (MSCs), derived from bone marrow or adipose tissue, show promise in reducing inflammation and promoting tissue repair. Mesenchymal stem cells may create a more conducive environment for brain regeneration. Induced Pluripotent Stem Cells (iPSCs) are generated by reprogramming adult cells to an embryonic-like state. They can develop into multiple cell types, including neurons, rendering them optimal for spinal cord tissue regeneration. Since they can be derived from the patient's own cells, they offer a personalized treatment approach and minimize the risk of immune rejection. Neural Stem Cells (NSCs) have the ability to differentiate directly into neurons and glial cells, making them a promising option for repairing damaged spinal cord tissue (Montoto-Meijide et al., 2023).

Spinal cord stimulation employs implanted electrical devices to transmit impulses to the spinal cord, with the objective of restoring function or enhancing neural control. Epidural Electrical Stimulation (EES): Electrodes are positioned on the dura mater's surface to stimulate targeted regions of the spinal cord. This approach has resulted in enhancements in motor function and bladder control in certain patients with partial spinal cord injury. Transcutaneous Electrical Nerve Stimulation (TENS) is a non-invasive method that applies electrical stimulation to the skin's surface, potentially aiding in pain relief and minor functional improvement (Dorrian et al., 2023).

Gene therapy involves altering or introducing specific genes into the spinal cord to enhance repair processes. Gene delivery techniques are being investigated to reduce scarring (which can inhibit regeneration) and enhance axon growth. For example, gene editing techniques such as CRISPR are being investigated to repair or replace damaged genes that contribute to nerve damage and dysfunction. Genes that promote the expression of growth factors, such as brain-derived neurotrophic factor (BDNF), are being utilized to improve neuron survival and support neural regeneration (Zeng & Zhang, 2023).

Biomaterials and 3D bioprinting offer structural support to the damaged spinal cord, facilitating cellular proliferation and tissue regeneration. Hydrogels; soft, water-rich materials mimic the extracellular matrix and can be loaded with stem cells or growth factors to create an environment favorable for neural regeneration. 3D Bioprinting allows for the production of tailored scaffolds that match the spinal cord's structure, supporting cell growth

and tissue formation. These scaffolds can be engineered to support axon regeneration and enhance functional recovery (Deptuła et al., 2023).

Exosomes are diminutive vesicles released by cells that transport proteins, RNA, and various signaling chemicals. Exosome therapy involves using exosomes derived from stem cells to deliver healing factors to injured areas of the spinal cord. These exosomes can reduce inflammation and promote tissue repair by modulating the immune response and providing neuroprotective factors (Singh et al., 2024).

Neurotrophic factors, such as nerve growth factor (NGF) and glial cell line-derived neurotrophic factor (GDNF), are proteins that support the survival, growth, and repair of neurons. These substances are administered through injection or gene therapy into the damaged spinal cord to facilitate axonal regeneration and diminish cell mortality.

Nanomaterials can be used to deliver drugs, stem cells or growth factors directly to the site of injury with high precision. Nanoparticles can be used to deliver anti-inflammatory drugs, neuroprotective agents or stem cells directly into damaged tissue, helping to reduce secondary damage and promote healing. Nanofibers and nanoscaffolds create a structural framework that can guide regenerating axons, helping them grow in the right direction along the injury site (Wang et al., 2024).

Neuroprostheses and brain-machine interfaces aim to bypass the damaged spinal cord by creating a direct connection between the brain and external devices that can control movement. This approach is particularly helpful for patients with severe spinal cord injuries, giving them some autonomy by allowing them to control robotic limbs or computers with their thoughts.

Following a spinal cord injury, the development of scar tissue, referred to as glial scarring, can serve as both a physical and chemical impediment, obstructing neural regeneration. New treatments aim to reduce scarring and control inflammation that could otherwise make the injury worse. One enzyme, Chondroitinase ABC, is being investigated for its ability to degrade glial scar components and promote axon regrowth.

Robotic Exoskeletons, these wearable devices, support the body and assist controlled movements, enabling patients to stand, walk and exercise even with limited or no voluntary movement. Robotic exoskeletons not only aid rehabilitation, but also provide psychological

benefits, allowing patients to experience upright movement and improved mobility (Rodríguez-Fernández et al., 2021).

Next-generation therapies for spinal cord injuries are revolutionizing the approach to treatment and rehabilitation by focusing on regeneration, functional recovery and improving quality of life. While these therapies are still being developed and refined, they offer hope for further improvements in the future. The integration of stem cell therapy, biomaterials, gene therapy, and neuromodulation is expanding the possibilities for spinal cord repair.

1.2. Stem Cells

Stem cells have garnered significant attention in medicine and research for their remarkable ability to differentiate into various specialized cell types. Their unique regenerative properties make them a cornerstone of treatments aimed at repairing damaged tissues, combating degenerative diseases, and even generating new organs. Stem cells are unspecialized cells capable of self-renewal and differentiation into specific cell types. They function as a biological repair mechanism, capable of proliferating and producing similar stem cells or differentiating into specialized cells such as muscle, blood, or neuronal cells, contingent upon the body's requirements. The fundamental characteristics of stem cells are as follows. Self-renewal: The ability to divide and produce additional stem cells. Potency: The ability to differentiate into multiple cell types, depending on the specific type of stem cell. Stem cells form the foundational building blocks of all organs and tissues in the human body, making them essential for advancing developmental biology and therapeutic applications (Miller & Perin, 2016; Wobus, 2001).

1.3. Induced Pluripotent Stem Cells

Induced pluripotent stem cells (iPSCs) are a type of stem cell created by reprogramming adult somatic cells. Unlike embryonic stem cells, which are derived from embryos, induced pluripotent stem cells (iPSCs) are generated from differentiated cells, such as skin or blood cells, and reprogrammed to a pluripotent state. This means they have the remarkable ability to differentiate into almost any cell type in the body, similar to embryonic stem cells, but without the accompanying ethical concerns. Since their identification by Japanese scientist Shinya Yamanaka in 2006, iPSCs have transformed the domains of regenerative medicine, pharmacological research, and disease modeling. Yamanaka's pioneering research garnered him a Nobel Prize and unveiled numerous opportunities for

comprehending diseases and formulating individualized treatments. The pursuit to comprehend and exploit the capabilities of stem cells commenced well prior to the advent of iPSCs. Researchers have been fascinated by embryonic stem cells for their ability to differentiate into any cell type.

Nonetheless, the utilization of these cells has provoked considerable ethical dilemmas due to the destruction of human embryos.

In 2006, Shinya Yamanaka made a crucial discovery that changed the landscape of stem cell research. He discovered that adult cells could be reprogrammed into a pluripotent state by introducing only four specific genes. These reprogrammed cells, now known as iPSCs, exhibit the same basic properties as embryonic stem cells, but are produced from adult tissues, eliminating the need to use embryos. This breakthrough marked a major advancement by avoiding the ethical issues associated with embryonic stem cells and enabling the creation of patient-specific stem cells for personalized therapies.

The creation of induced pluripotent stem cells involves reprogramming adult differentiated cells, such as skin or blood cells, into a pluripotent state. This is achieved through a process called genetic reprogramming, which involves introducing specific genes that are highly expressed in embryonic stem cells. The primary method involves introducing four key transcription factors - Sox2, Klf4,Oct4 and c-Myc-into mature cells. These factors are administered by viral vectors that include reprogramming genes into the cell's DNA. Once inside the cell, these genes activate pathways that effectively reverse the cell's differentiation, putting it in a state where it can become almost any type of cell. After reprogramming, iPSCs exhibit two key characteristics. Pluripotency is the ability to differentiate into any of the three germ layers of the body (endoderm, mesoderm, and ectoderm), enabling the formation of all cell types. Self-renewal enables them to proliferate endlessly in the laboratory while retaining their capacity for specialization (Chehelgerdi et al., 2023).

The discovery of induced pluripotent stem cells (iPSCs) has had a profound impact on medicine and scientific research. Here are some of the most promising applications of these cells. In regenerative medicine, induced pluripotent stem cells (iPSCs) can be used to create tissues and organs genetically compatible with the patient, reducing the risk of immune rejection. Researchers are examining the potential of iPSCs to repair damaged

cardiac tissue following a myocardial infarction or to regenerate neurons in individuals afflicted with neurodegenerative disorders like Parkinson's disease. Induced pluripotent stem cells (iPSCs) are used in drug discovery and testing to produce disease-specific cells, allowing researchers to study disease progression at the cellular level and test new drugs in a controlled laboratory environment. Induced pluripotent stem cells (iPSCs) derived from patients with genetic disorders can be used to model these diseases and assess potential treatments. In disease modeling, researchers can create models of conditions like Alzheimer's, diabetes, and muscular dystrophy by generating induced pluripotent stem cells (iPSCs) from patients with specific genetic disorders. These models enable a deeper understanding of disease mechanisms and the development of targeted therapies. Induced pluripotent stem cells (iPSCs) offer great potential for personalized therapy, as they can be generated from a person's own cells (Moradi et al., 2019).

While iPSCs offer many of the same advantages as embryonic stem cells (ESCs), there are important differences between the two. One of the most important distinctions is ethical. Because ESCs are derived from embryos, their use has raised moral and ethical concerns, particularly in the context of the potential destruction of human life. iPSCs are a more ethically acceptable alternative because they do not contain embryos. In terms of functionality, both iPSCs and ESCs exhibit pluripotency and self-renewal. However, iPSCs are more prone to genetic abnormalities due to the reprogramming process, and researchers are still studying how these differences may affect their therapeutic potential. Despite these challenges, iPSCs have distinct advantages, including the ability to generate patient-specific cells that are less likely to be rejected by the patient's immune system when used in therapies (Halevy & Urbach, 2014).

1.3.1. iPSC-derived Neural Stem Cells

Induced pluripotent stem cells (iPSCs) have revolutionized stem cell research by providing a flexible platform for generating various cell types within the body. Neural stem cells (NSCs), which can be derived from induced pluripotent stem cells (iPSCs), are highly significant due to their broad applications in understanding and treating neurological disorders, as well as in repairing brain and spinal cord injuries. Neural stem cells derived from induced pluripotent stem cells are particularly important because they can differentiate into the main cell types of the nervous system: neurons, astrocytes, and oligodendrocytes. This offers exciting potential for developing treatments for conditions such as Parkinson's disease, Alzheimer's disease, and spinal cord injuries (Bahmad et al., 2017).

The production of iPSC-derived neural stem cells begins by reprogramming adult somatic cells, such as skin or blood cells, into induced pluripotent stem cells (iPSCs). After reprogramming to a pluripotent state, these cells can be guided to become neural stem cells by exposing them to specific growth factors and signaling molecules that simulate early brain development. Commonly used factors include retinoic acid and Sonic Hedgehog (Shh), which help guide iPSCs along the neural lineage. Once iPSCs are differentiated into NSCs, these cells exhibit characteristics similar to NSCs found naturally in the developing brain. They possess the ability for self-renewal, allowing them to proliferate and generate additional neural stem cells, and can differentiate into three primary categories of cerebral cells: neurons, which convey signals within the brain; astrocytes, which provide support and protection to neurons; and oligodendrocytes, which create the myelin sheath that insulates nerve fibers (Al Abbar et al., 2020).

iPS-derived NSCs share many key characteristics with naturally occurring neural stem cells. Like all stem cells, they possess the ability to self-renew, enabling them to produce more neural stem cells (NSCs) indefinitely. This feature is critical to generate sufficient numbers of cells for research and therapeutic applications. Furthermore, iPS-derived NSCs exhibit pluripotency, allowing them to differentiate into several cell types, especially those present in the nervous system. Under optimal conditions, iPS-derived NSCs can develop into many cell types. Neurons are specialized cells that conduct electrical signals within the brain and spinal cord. Astrocytes are glial cells that offer structural and metabolic support to neurons. Oligodendrocytes, cells that produce myelin, the insulating layer that helps neurons transmit signals more efficiently. These properties make iPS-derived NSCs an invaluable tool in the study of potential therapies for brain development, neurodegenerative diseases and neural injuries (Luciani et al., 2024).

The ability to generate neural stem cells from induced pluripotent stem cells (iPSCs) has led to numerous applications in both basic research and therapeutic settings. Neural stem cells derived from induced pluripotent stem cells (iPSCs) can be used in disease modeling to create models of neurodegenerative disorders such as Parkinson’s disease, Alzheimer’s disease, and amyotrophic lateral sclerosis (ALS). By creating patient-specific neural stem cells (NSCs), researchers can investigate how genetic mutations contribute to these diseases and evaluate potential treatments in a laboratory setting. Drug discovery and toxicity testing, iPS-derived NSCs are also used in drug development. By creating neurons and other brain cells from patients with certain diseases, researchers can test new drugs and treatments in a

controlled environment. This allows for more accurate predictions of how drugs will affect human neurons and reduces the need for animal testing. Repair of Brain and Spinal Cord Injuries: In regenerative medicine, neural stem cells derived from induced pluripotent stem cells (iPSCs) are being studied for their potential to restore damaged neural tissue. For instance, following a stroke or traumatic brain injury, neural stem cells may be implanted into affected regions to substitute missing neurons and rehabilitate function. Researchers are utilizing iPS-derived neural stem cells to investigate brain development and the pathways associated with neuropsychiatric illnesses, including schizophrenia and autism. This research elucidates the formation of brain circuits and the impact of abnormalities in these processes on the onset of mental diseases (Amin et al., 2019).

One of the most promising applications of iPSC-derived neural stem cells (NSCs) lies in the field of regenerative medicine. Researchers aim to use these cells to treat brain and spinal cord injuries, neurodegenerative diseases, and paralysis. In conditions like Parkinson's disease, where the loss of dopamine-producing neurons in the brain causes motor symptoms, iPSC-derived neural stem cells (NSCs) could be used to replace the lost neurons and restore dopamine production.In spinal cord injuries where nerve connections are severed, iPS-derived NSCs could potentially be transplanted to form new nerve connections and restore some degree of motor function. Although therapeutic applications remain in their nascent phases, numerous preclinical and preliminary clinical investigations are currently being conducted to assess the potential of iPS-derived NSCs for various disorders (Amin et al., 2019).

iPS-derived NSCs have become a valuable tool for modeling neurodegenerative diseases. For instance, in Parkinson's disease, researchers use iPSC-derived neural stem cells (NSCs) to produce dopaminergic neurons, the specific type of neurons that deteriorate in this condition. These neurons are being used to study how the disease progresses and to test drugs that could prevent or slow neuron loss. In Alzheimer's disease, iPS-derived neural stem cells are utilized to generate neurons that synthesize amyloid-beta and tau proteins, which are implicated in the pathology of Alzheimer's disease. Researchers aim to uncover novel targets for pharmacological development through the analysis of these neurons. In Amyotrophic Lateral Sclerosis (ALS), patient-derived induced pluripotent stem cells (iPSCs) are used to produce motor neurons that model the progression of the disease, providing insights into its effects on motor neurons and potential strategies to prevent their degeneration (Amin et al., 2019).

Utilizing iPS-derived NSCs in research and therapy presents numerous advantages. iPSCs, derived from adult cells, have ethical advantages over embryonic stem cells, which need the death of embryos, hence rendering them a more ethically acceptable source of pluripotent stem cells. Personalized therapy can employ iPSCs derived from the patient's own cells, enabling the creation of individualized neural stem cells (NSCs) that are genetically matched to the patient. This mitigates the likelihood of immunological rejection in cell-based therapy. Their adaptability allows iPS-derived NSCs to be utilized for investigating a broad spectrum of neurological disorders, rendering them an essential instrument in neuroscience research (Thanaskody et al., 2022).

Notwithstanding their potential, numerous obstacles and hazards are linked with iPS-derived NSCs. Genetic and epigenetic anomalies; the reprogramming process may induce genetic mutations or epigenetic modifications, thereby impacting the safety and efficacy of iPS-derived NSCs in therapeutic applications. Neoplasm development: Similar to other stem cells, iPS-derived neural stem cells has the capacity to generate tumors (teratomas) if not adequately regulated upon transplantation. Controlling differentiation to ensure that iPS-derived NSCs develop into the intended cell types and integrate effectively into existing brain networks presents a significant barrier for clinical use (Okita & Yamanaka, 2011).

1.4. 3D Bioprinting

The concept of bioprinting emerged in the early 2000s. The first major milestone was achieved in 2003 when Thomas Boland, a pioneer in the field, adapted an inkjet printer to dispense living cells instead of ink. Over the years, advancements in both biotechnology and 3D printing techniques have allowed the creation of increasingly complex and functional tissue structures. Recent developments include the successful printing of blood vessels, liver tissues, and early-stage human organ models (Gu et al., 2020; Mendoza-Cerezo et al., 2023).

3D bioprinting is an advanced technology that involves creating three-dimensional, biologically functional structures using living cells and bio-compatible materials. It builds tissues layer by layer in a way similar to how traditional 3D printers fabricate physical objects. The primary distinction is that bioprinting utilizes bioinks-composed of living cells, growth factors, and biopolymers-to create tissue-like structures that can be used in medical applications such as tissue repair, organ regeneration, or drug testing (Shiplu Roy et al., 2020).

Three-dimensional bioprinting is gaining substantial attention in the fields of regenerative medicine and tissue engineering. The process consists of two key components: the bioprinter and the bioink (Moroni et al., 2018). This technology utilizes digital technologies to fabricate complex tissues that closely resemble the organization and structure of genuine tissue. It facilitates accurate customisation of dimensional parameters and the sequential printing of intricate biomaterial architectures with computer-aided design (CAD) models (Ouyang et al., 2020).

In 3D bioprinting, bioinks play a very important role. They consist of biological materials such as collagen, gelatin, alginate or synthetic polymers in combination with living cells. The bioink must be formulated to maintain cell viability and promote cell differentiation after printing. Cells used in bioprinting are typically classified into three categories: autologous cells (obtained from the patient's own body), allogeneic cells (donor-derived), and stem cells (which can differentiate into specialized cell types) (Chen et al., 2023; Persaud et al., 2022).

3D bioprinting uses an additive manufacturing technique where tissues are created layer by layer based on a digital 3D model. The process usually follows the following steps in sequence. Pre-printing: A digital 3D model of the tissue or organ is designed using medical imaging data, such as CT or MRI scans. Printing: Bioink containing living cells is deposited layer by layer to create the desired shape. Post-printing: The printed structure undergoes maturation in a bioreactor where cells grow, differentiate and interact with the biomaterial scaffold to form functional tissue (Bishop et al., 2017).

3D bioprinting applications can be broadly classified as follows. A principal use of 3D bioprinting is tissue engineering. Scientists can print complex tissue structures such as skin, bone, cartilage and even liver or kidney. These tissues can be used for wound healing: creating skin grafts for burn victims. Orthopedics: printing cartilage for joint repair (Mirshafiei et al., 2024; Saini et al., 2021; Tripathi et al., 2023). The second is organ bioprinting. Early prototypes and partial organ structures are being developed, but fully functional organs such as kidneys or hearts are a long way from being printable. In the future, this technology could address the shortage of organ transplants by enabling the printing of personalized organs using the patient's own cells, thus eliminating the risk of rejection (Panja et al., 2022; Xia et al., 2018). The third is drug testing and development. 3D bioprinting is revolutionizing drug development. By mimicking human organs, bioprinted

tissues could offer a more accurate platform for testing new drugs. This approach could reduce reliance on animal models, which often do not translate well into human biology (Gao et al., 2021; Mihaylova et al., 2024).

There are basically four main types of 3D bioprinters. Extrusion-based bioprinting involves pushing bioink through a nozzle to create layers of tissue. It allows the use of various viscosities, making it suitable for printing both cells and scaffold materials. However, the resolution may not be as high as other methods (Davoodi et al., 2020). Inkjet bioprinting uses droplets of bioink that are deposited in a precise pattern onto a substrate. It's suitable for creating high-resolution structures but may not be ideal for more complex tissues due to limitations in the thickness of layers that can be deposited (Li et al., 2020). Laser-assisted bioprinting uses laser pulses to propel cells onto a substrate. It offers high precision and can print very delicate structures, but it's often slower and more expensive compared to extrusion and inkjet methods (Ventura, 2021). Stereolithography bioprinting use light to cross-link bio-inks within the reservoir through a layer-by-layer approach. This approach is constrained to photosensitive bio-inks due to its operational mechanism (Yu et al., 2020).

Despite the enormous potential in 3D Bioprinting, it faces several challenges. Issues such as vascularization, material limitations, scale and complexity are some of them. Despite these challenges, the future of 3D bioprinting remains promising, with ongoing research driving advancements. These include the creation of biomaterials that better mimic human tissue, small-scale organ models that can be used for drug testing and disease modeling, and the development of methods for bioprinting fully vascularized organs that can integrate with the human body. New developments in artificial intelligence and machine learning are also expected to play a role in optimizing bioprinting processes, increasing accuracy and reducing production times.

3D bioprinting signifies a revolutionary advancement in medicine and tissue engineering. This technique has the potential to transform drug testing and facilitate organ regeneration, addressing significant medical concerns of our era. Despite the technical and ethical hurdles still to be overcome, rapid advances in this field make it a promising tool for the future of personalized medicine and organ replacement therapies.

1.5. Nanomaterials

Nanomaterials are substances characterized by structural dimensions at the nanoscale, generally between 1 and 100 nanometers. At these size, materials frequently have distinct physical, chemical, and biological properties relative to their larger-scale equivalents. These distinctive properties emerge because, at the nanoscale, materials possess a greater surface area in relation to their volume, resulting in improved reactivity, strength, electrical conductivity, or optical performance (Altammar, 2023).

There are various types of nanomaterials, including nanoparticles, nanowires, nanotubes, and nanofilms. They can be made from metals, ceramics, polymers, and other materials. Nanomaterials are employed in various applications, including medicine (for drug delivery and cancer treatment), electronics (in transistors and sensors), energy (for more efficient solar panels and batteries), and environmental technologies (for water purification and pollution control)(Baig et al., 2021; Khan et al., 2019). In summary, nanomaterials represent a groundbreaking field of study with transformative potential across many industries due to their size-dependent properties and versatility.

1.5.1. Classification Of Nanomaterials According To Their Size

In zero-dimensional nanomaterials, all dimensions are at the nanoscale. The predominant types of 0D nanomaterials include nanoparticles (metallic nanoparticles like gold or silver, nanoparticles of semiconductors such as zinc oxide, and polymeric nanoparticles) and quantum dots (nanoscale semiconductor particles exhibiting quantum mechanical properties, rendering them highly effective for optoelectronic and biomedical applications). Owing to their diminutive dimensions, 0D nanomaterials possess a substantial surface-to-volume ratio, hence enhancing their reactivity and interactions with other substances. In quantum dots, electron energy levels are quantized, leading to distinctive optical and electrical characteristics, including size-tunable light emission (Adul-Rasool et al., 2024; Byakodi et al., 2022; Mekuye & Abera, 2023).

1D nanomaterials are characterized by one large dimension (length), while the other two dimensions (width and thickness) are on the nanoscale. This gives them a wire-like or tube-like structure. Common examples include nanowires (Materials such as silicon or gold nanowires are used in electronic devices due to their excellent conductivity), nanotubes

(Carbon nanotubes (CNTs) are cylindrical structures made of graphene sheets, known for their strength and electrical properties) and nanorods (Rod-like nanoparticles, typically made of metals such as gold or semiconductors). The long, thin shape of 1D nanomaterials gives them a high aspect ratio, which affects their mechanical and electrical behavior. Materials such as carbon nanotubes and nanowires offer superior electrical and thermal conductivity due to electron mobility along their length. Carbon nanotubes, for example, are renowned for their tensile strength, making them ideal for use in lightweight, high-strength materials (Adul-Rasool et al., 2024; Byakodi et al., 2022; Mekuye & Abera, 2023).

In two-dimensional nanomaterials, the length and width are markedly greater than the thickness, which is confined to the nanoscale. These materials are often planar, sheet-like entities. Examples include graphene, which is a monolayer of carbon atoms organized in a hexagonal lattice. The most renowned 2D material is transition metal dichalcogenides (TMDs), exemplified by molybdenum disulfide (MoS_2), which serves as a 2D semiconductor in optoelectronics and flexible electronics, alongside MXenes, a family of 2D transition metal carbides and nitrides distinguished by their unique electrical and chemical properties. Two-dimensional materials possess a high surface-to-volume ratio, hence augmenting their interaction with other substances. Numerous 2D materials, including transition metal dichalcogenides (TMDs), possess adjustable bandgaps, rendering them appropriate for various electrical and optoelectronic applications. Notwithstanding their little thickness, numerous 2D materials, including graphene, exhibit remarkable flexibility and strength (Adul-Rasool et al., 2024; Byakodi et al., 2022; Mekuye & Abera, 2023).

Three-dimensional nanomaterials are composed of nanostructures arranged in a three-dimensional pattern. While these materials have internal nanostructures, their overall bulk structure extends in all three dimensions. Examples include nanocomposites (materials composed of nanoparticles dispersed in a matrix, such as carbon nanotubes or polymers reinforced with metal nanoparticles) and nanocrystalline materials (materials in which the crystal grains are on the nanometer scale, altering their mechanical and thermal properties). Incorporating nanomaterials into 3D structures can significantly increase the strength, toughness and flexibility of the material. 3D nanomaterials such as aerogels have a highly porous structure, making them extremely lightweight while maintaining strength. 3D nanomaterials often combine several desirable properties such as electrical conductivity, mechanical strength and thermal stabilit (Adul-Rasool et al., 2024; Byakodi et al., 2022; Mekuye & Abera, 2023).

1.5.2. 2D Nanomaterials and Derivatives

Two-dimensional (2D) nanomaterials are a class of nanomaterials with one dimension confined to the nanometer scale, usually less than a few nanometers thick, while their other two dimensions extend significantly in length and width. These materials consist of only a few atomic layers, making them extraordinarily thin yet possessing a large surface area. Their unique atomic structure gives them distinct electronic, mechanical, and optical properties, which have sparked interest in various scientific and industrial fields.

1.5.2.1. Types of Two-Dimensional Nanomaterials

Graphene is arguably the most recognized two-dimensional nanomaterial. It comprises a monolayer of carbon atoms organized in a hexagonal lattice. Graphene demonstrates exceptional characteristics, including superior electrical conductivity, substantial mechanical strength, and flexibility. Its prospective applications encompass flexible electronics, batteries, sensors, and further areas (Geim & Novoselov, 2007; George & Bhattacharyya, 2023).

Transition Metal Dichalcogenides (TMDs), like molybdenum disulfide (MoS_2), are another class of 2D materials. These are semiconductors that exhibit a bandgap, unlike graphene, which makes them useful for electronics, photonics, and optoelectronic devices. They also have excellent catalytic and lubrication properties (Srivastava et al., 2024).

Hexagonal Boron Nitride (h-BN) also known as "white graphene," is structurally similar to graphene but made from alternating boron and nitrogen atoms. It is an excellent insulator with high thermal stability, making it suitable for high-temperature and dielectric applications (Ali et al., 2025).

MXenes are a category of two-dimensional transition metal carbides, nitrides, and carbonitrides. They exhibit excellent conductivity and possess potential for energy storage applications, including supercapacitors and batteries, as well as for electromagnetic shielding (Thakur et al., 2022).

Black phosphorus (Phosphorene) is another 2D material that has recently gained attention. It has tunable electronic properties and exhibits a direct bandgap, making it promising for transistors, photodetectors, and other semiconductor devices (Castellanos-Gomez, 2015).

1.5.2.2. MXene Quantum Dots

MXene quantum dots (MQDs) are a new class of nanomaterials that are attracting increasing attention in various fields of science and technology. Derived from a two-dimensional family of materials called MXene, these quantum dots have enormous potential due to their unique properties, including tunable electronic, optical and chemical properties. As quantum dots, they demonstrate size-dependent quantum confinement properties, rendering them appropriate for many applications including energy storage, environmental sensing, and healthcare (Dhamodharan et al., 2024).

MXenes constitute a category of two-dimensional materials initially identified in 2011 by scholars at Drexel University. They originate from a wider category of materials termed MAX phases, wherein “M” denotes an early transition metal (e.g., titanium or molybdenum), “A” signifies an element from groups 13 or 14 (e.g., aluminum), and “X” indicates carbon or nitrogen. MXenes are produced by the selective removal of the "A" layer from MAX phases via etching, resulting in layers of transition metal carbides or nitrides. One of the most intriguing characteristics of MXenes is their ability to be tailored regarding composition and surface chemistry (H. Kim et al., 2017). This adaptability renders them appropriate for various applications, including energy storage and water purification. MXenes show promise due to their metallic conductivity, hydrophilic nature and excellent mechanical properties. The discovery of MXenes has opened a new frontier in two-dimensional materials science, and their potential increases even further when these materials are transformed into quantum dots.

Quantum dots (QDs) are nanoscale semiconductor particles that display distinctive electrical and optical characteristics resulting from quantum confinement effects. When the size of a material is reduced to the nanoscale, typically to less than 10 nanometers in diameter, its electronic properties differ significantly from bulk materials. This leads to size-tunable light absorption and emission, making quantum dots highly attractive for optoelectronic, imaging and photovoltaic applications. Quantum dots are particularly known

for their fluorescence ability, meaning they can absorb and re-emit light in different colors depending on their size. Smaller quantum dots emit light in the blue or violet spectrum, but larger quantum dots emit light in the red or near-infrared spectrum. These tunable optical properties make quantum dots useful in applications ranging from LED displays to solar cells and biomedical imaging. However, conventional quantum dots, which are usually made from materials such as cadmium selenide, have limitations such as toxicity and high cost. This is where MXene quantum dots offer a new avenue for discovery with their unique composition and properties (Mimona et al., 2025).

The synthesis of MXene quantum dots involves breaking larger sheets of MXene into smaller, nanoscale particles while maintaining or enhancing their desirable properties. There are several methods used to synthesize MXene quantum dots, each with its own unique advantages and challenges. A prevalent technique for generating MXene quantum dots is hydrothermal synthesis. This technique use elevated temperature and pressure water to decompose bigger MXene sheets into quantum dots. The method can be optimized by modifying variables such as temperature, pressure, and reaction duration, enabling researchers to regulate the dimensions and characteristics of the resultant quantum dots. Hydrothermal synthesis is widely used because it is relatively simple and scalable. It enables the production of high-quality MXene quantum dots with consistent properties. However, this method can be time-consuming and the need for high-pressure equipment may limit its widespread adoption in some environments. Another popular method for synthesizing MXene quantum dots is chemical exfoliation. This involves treating MXene sheets with chemical agents that weaken the bonds between the layers and allow them to separate into nanoscale quantum dots. Chemical exfoliation is particularly useful for producing uniform, well-dispersed quantum dots with excellent optical and electronic properties. This method is advantageous as it can produce large quantities of quantum dots in a relatively short time. Furthermore, the process can be tailored to produce quantum dots with specific surface chemistries that are important for applications such as sensing and catalysis. However, the use of strong chemicals in the process can sometimes lead to unwanted side reactions or degradation of the material (J. Wang et al., 2022).

MXene quantum dots possess several distinctive features that render them appealing for various applications. These properties are primarily influenced by the quantum confinement effects that occur when the material is reduced to the nanoscale, as well as the inherent properties of the parent MXene material. One of the most remarkable properties of

MXene quantum dots is their photoluminescence - their ability to absorb and re-emit light. This property is highly tunable, meaning that the color of the light emitted by the quantum dots can be adjusted by changing their size or chemical composition. This makes MXene quantum dots highly suitable for optoelectronics such as light-emitting diodes (LEDs) and bio-imaging applications where their fluorescence can be used to monitor biological processes at the cellular level. MXenes are known for their excellent electronic conductivity, and this property is retained and even enhanced in quantum dot forms. The metallic characteristics of MXene quantum dots allow them to function as extremely efficient electrical conductors, rendering them suitable for applications including supercapacitors, sensors, and electronic devices. The surface chemistry of MXene quantum dots can be easily modified to allow the addition of various functional groups. This versatility is important for applications such as catalysis, where certain surface chemistries can increase reaction rates, and for biomedical applications where biocompatibility is essential. Furthermore, the chemical stability of MXene quantum dots under various environmental conditions makes them useful for long-term applications (Protyai & Bin Rashid, 2024).

There is a need for alternative methods that will contribute to traditional treatments in the world. Innovative approaches are being developed especially for use in regenerative medicine and tissue engineering. These innovative approaches are accompanied by nanotechnology, biomaterials and nanomaterials. These studies, which are one of the outputs of interdisciplinary studies, are of great importance especially in terms of developing new approaches for the treatment of injuries affecting the nervous system. Since natural nerve regeneration is very slow or almost nonexistent, peripheral and spinal nerve injuries place great burdens on societies. There is a need to develop innovative treatment methods for this type of nerve damage.

This PhD thesis has the main aim to develop an innovative tissue engineering product for nerve regeneration using a 3D bioprinted scaffold containing electrically conductive nanomaterials and neural growth factors.

Our initial goal was to demonstrate that mesenchymal stem cells (MSCs) and iPSCs can efficiently differentiate into neurons in a 2D culture system in the presence of neural growth factors and nanomaterials, and increase neuronal marker expression compared to conventional methods.

Our second goal was to provide a 3D bioprinted scaffold composed of nanomaterials and bio-ink containing iPSCs, a biomimetic microenvironment that promotes cell attachment, proliferation and differentiation into functional neurons.

Our third goal was that the presence of electrically conductive nanomaterials in the scaffold would facilitate the transmission of electrical signals and the application of an external electric field could further enhance neuronal differentiation by stimulating electrophysiological activity.

Our final goal was that the resulting differentiated neurons in the 3D scaffold would exhibit functional properties similar to native neural tissue and demonstrate the potential for direct neural tissue repair in clinical applications.

2. MATERIALS AND METHODS

2.1. Materials

The small graphene oxide (sGO) nanomaterial used in this thesis was provided by Prof. Kostas Kostarelos of the National Graphene Institute, University of Manchester. MXene Quantum Dot (MQD) material was provided by Prof. Dr. Sanjiv Dhingra from the University of Manitoba.

The materials used in this thesis are shown in **Table 2.1**.

Table 2.1. Materials used in the experiments and their catalog numbers

Stage in which the material is used		Material Name and Catalog Number
Cell Culture	MSC Culture	Pen Strep Penicillin Streptomycin (Cat. No. 15140-122.Gibco), FBS Fetal Bovine Serum (Cat. No.10500-064. Gibco, Life Technologies), DPBS (1X) Dulbecco's Phosphate Buffered Saline (Cat. No.14190-094. LifeTechnologies), Trypsin-EDTA (1X) (Cat. No. 25300-054. Gibco), Dimethyl Sulfoxide (Cat. No. D2650. Lot. No. RNBF0698SIGMA-ALDRICH), B-27 Supplement (Ref No:17504-044, gibco) HBDNF (Lot:7 , Cell Signaling), N2 Supplement 100X(Lot:1559091, Gibco)
	HNSC Culture	(HS820K-20, Cell Application)
	iPSC Culture	Essential 8 Supplement (50X) (lot 2313787, Gibco), Revitacell Supplement (Lot: 2466026, Gibco), StemPro Accutase (Ref:A11105-01,Gibco), Neural Induction Supplement (50X) (Ref: A16477-01,Gıbco), Neurobasal Medium (Lot: 2646164, Gibco)
RNA Isolation		Macherey-nagel NucleoSpinRNA Mini Kit (Cat. No. 740955.50), 2-Mercaptoethanol (Cat. No. 31350-010.Gibco)
cDNA Synthesis		iScript™ cDNA Synthesis Kit (Cat. No. 170-8891. BIORAD)
PCR		Sso AdvancedTM Universal SYBR® Green Supermix (Cat. No. 172-5271. BIO-RAD)
Immunofluorescence Staining		Bovine Albumin (Protease Free) (Lot. No. OK18665. BioShop), TRITON® X-100 (Cat. No. 1L22885. BioShop®),
Live-Dead Staining		Thermo Fisher Scientific LIVE/DEAD Cell Viability Assays LOT:2261453 REF: L3224

2.2. Methods

The experiments were carried out in the Stem Cell and Regenerative Medicine Research Laboratories of the Department of Biomedical Engineering and the Tissue Engineering Laboratories of the Stem Cell Institute, Ankara University. The study was supported by the Tübitak 1004 project titled Regenerative and Restorative Medicine Research and Applications (Project No. 20AG003-P8).

2.2.1. Cell Culture and Differentiation

2.2.1.1. Mesenchymal Stem Cell Culture and Differentiation

Growth of Mesenchymal Stem Cell Line in 2D Cell Culture Medium: Adipose-derived mesenchymal stem cells (MSC) were grown in appropriate cell culture medium. MSC High Glucose Dulbecco's Modified Eagle's Medium (DMEM) was grown in 5% CO2 medium at 37°C with the addition of 10% fetal bovine serum, 1% pen-strep, 1% glutamax and 1ng/mL FGF. Since it is important to obtain healthy cells in cell differentiation, the nucleus, cytoplasm structure and cell morphology of MSCs were checked under a light microscope.

Differentiation of Mesenchymal Stem Cells into Neurons in 2D Cell Culture Media: Differentiation of MSCs into neurons was accomplished in two steps **Figure 2.1**.

i. Induction Step: MSCs grown in cell culture medium were transferred to induction medium, which is the first step of differentiation. DMEM-F12, 10% FBS, 1% Pen-Strep, 1% Glutamax, 10ng/mL FGF, 10ng/mL EGF and 0,1% β-mercaptoethanol are used as components of this medium. The induction medium was changed every 2-3 days and fresh medium was added. MSC cells were cultured in this medium for 7 days.

ii. Differentiation Step: After 7 days, the induction step was stopped. Cells were removed with trypsin and plated onto 6-well plates ($3X10^4$ cells per well) coated with Attechment Factor (AF). Cells were expected to adhere to the 6-well plate within 24 hours. At the end of 24 hours, 4 hours of different nanomaterials treatment was applied according to the experimental groups and fresh differentiation medium was added. DMEM-F12, 10%

FBS, 1% Pen-Strep, 1% Glutamax, 10ng/mL FGF, 10ng/mL NGF, 10ng/mL EGF, 10ng/mL BDNF, 1X N2 and B27 supplement, 0,1% β-mercaptoethanol and retinoic acid are used as this medium. The differentiation medium was changed every 2-3 days. At the same time, 1 milliampere (mA) electric current was applied to the cells whose differentiation medium was changed for 1 minute according to the experimental groups determined. The differentiation step continued for 14 days.

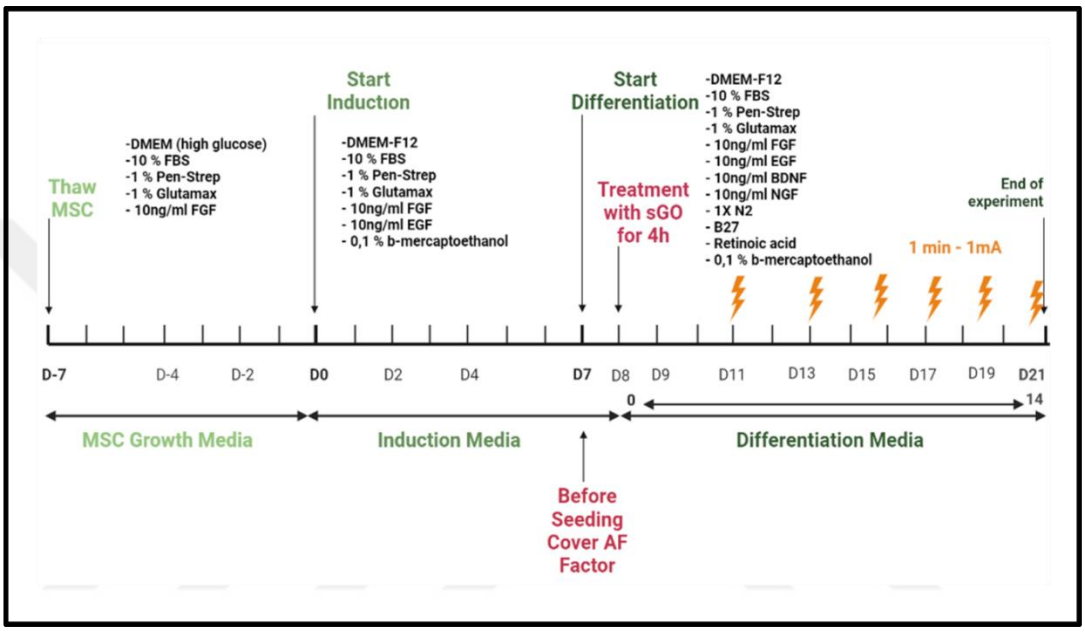

Figure 2.1. Timeline of mesenchymal stem cell differentiation

2.2.1.2. Human Neural Stem Cell (HNSC) Culture and Differentiation

Culturing Human Neural Stem Cells: Commercially available Human Neural Stem Cell (HNSC) line was cultured according to the protocol. The cells were thawed in a water bath until a small amount of ice remained in the cryovial tube. Cells were resuspended by gently pipetting 2 times with a pre-wetted pipette tip. The cell suspension was transferred from the cryotube into a 15mL flask and 9mL Neural Stem Cell Growth Medium was added. Cells were centrifuged at 200 x g for 5 min. The supernatant was aspirated and resuspended in Neural Stem Cell Growth Medium. A 10 cm petri dish (non-tissue culture) was added and prepared in advance for Neural Stem Cell Growth Medium seeding. 5 mL of HNSC was transferred to the prepared petri dish. HNSC were allowed to float in the Neural Stem Cell Growth Medium and not adhere to the dish. HNSC culture was incubated in a 37°C, 5% CO^2 humidified incubator. The culture was checked daily to ensure that all HNSCs had floated.

HNSC proliferated and formed floating neurospheres within 2 to 3 days. To prevent the formed neurospheres from sticking to the petri dish, flow was maintained by pipetting with medium. Every 2 or 3 days, half of the medium was removed and fresh medium was added. This process continued until the diameter of the neurospheres reached 100-200 μm.

Dissociatiation and Differentiation Human Neural Stem Cells:

i. Dissociatiation Step: Spheroids reaching a diameter of 100-200 μm were collected in a 15 mL conical tube and centrifuged at 800 rpm for 3-5 min. The aspirated cells were resuspended in Neural Stem Cell Dissociation Solution. Incubated in a 37°C water bath for 2 min and growth medium was added. Centrifuged again at 1,200 rpm for 5 min and aspirated. Neurospheres were resuspended in 1-2 mL growth medium and gently crushed 10-15 times. Gently 10-15 times with a glass pipette to break up the neurospheres. The cell suspension was seeded into a 10 cm Petri dish (non-tissue culture).

ii. Differentiation Step: The differentiated HNSC suspension was diluted to 100,000 cells per mL in Neural Stem Cell Growth Medium. The seeding density for differentiation is 50,000 cells per cm^2. HNSC were incubated in Neural Stem Cell Growth Medium overnight in a 37°C, 5 % CO^2 incubator. Differentiation medium was added the next day. The culture was checked daily and half of the differentiation medium was replaced every other day. Approximately 7 to 10 days to differentiate into astrocytes. 2 to 3 weeks were required to differentiate into neurons and 4 weeks to differentiate into oligodendrocytes.

2.2.1.3. Induced Pluripotent Stem Cell Culture (iPSC), Characterisation and Differentiation

Preparation of Peripheral Blood Mononuclear Cell Medium: 13mL StemPro-34 Supplement (Cat No: 10641-025) and 2 mM L-Glutamine were added into 500 mL StemPro-34 SFM Medium (Cat No: 10639-011 ThermFisher Scientific). It was then completed with the necessary cytokines in accordance with the kit protocol (IL3 (20ng/mL), IL6 (20ng/mL), FLT 3 (100ng/mL), SCF (100ng/mL)).

Peripheral Blood Mononuclear Cell Isolation (PBMC): Healthy individual blood collected into an EDTA tube was diluted with PBS at a ratio of 1:1. For PBMC isolation; blood diluted with PBS was slowly added onto 4 mL of ficoll. After centrifugation at 300 x g for 20 min, the buffy coat containing PBMCs was collected. The collected layer was washed by centrifuging in 10 mL of PBS at 300 x g for 8 min. Cells were suspended in 1 mL of PBMC medium prepared for PBMC culture and counted. The cells were distributed in 1 mL into a 24-well culture dish at 500,000 cells/well. They were cultured in a healthy manner under standard culture conditions of 37°C until transduction **Figure 2.2**.

Viral Transduction: PBMC cells isolated from blood were challenged by Sendai viruses carrying OKSM programming factors programming was performed. For this, the Cytotune iPSC 2.0 programming kit (Thermo Fisher Scientific) was used. In accordance with the kit's protocol; the virus, which varies depending on the lot number titration was determined and transduction was performed with an initial cell count of $5x10^4$.

Day 0 Cells cultured in PBMC medium were collected and centrifuged at 300 x g for 10 min. After the cells were suspended in PBMC medium, they were counted and 50,000 cells/500mL transferred to a 15 mL tube. After 1 mL of virus mixture (MOI KOS 2: cmyc 2: Klf4 1) was added to the cells, 1,000 x g for 30 min. Cells were transferred to a 6-well culture dish.

Day 1 Cells were collected from the transduced well and transferred to a 15 mL falcon tube. The viruses in the supernatant were removed by centrifugation at 200 x g for 10 min. Cells were transferred to a 24-well culture dish in 1 mL PBMC medium.

Day 3 6-well culture dishes were coated with vitronectin to a final concentration of 0.5 $\mu g/cm^2$. After 1 hour at room temperature, vitronectin was removed from the wells. Tranduced cells were collected and centrifuged at 200 x g 10 min. and then cytokine transferred to a vitronectin-coated well in Stem Pro 34 SFM medium without vitronectin.

Day 4-6 The medium of the cells was replaced with fresh cytokine-free medium.

Day 7 As of today, cells continue to be cultured with Essential 8 Medium (Cat No: A1517001) has been established.

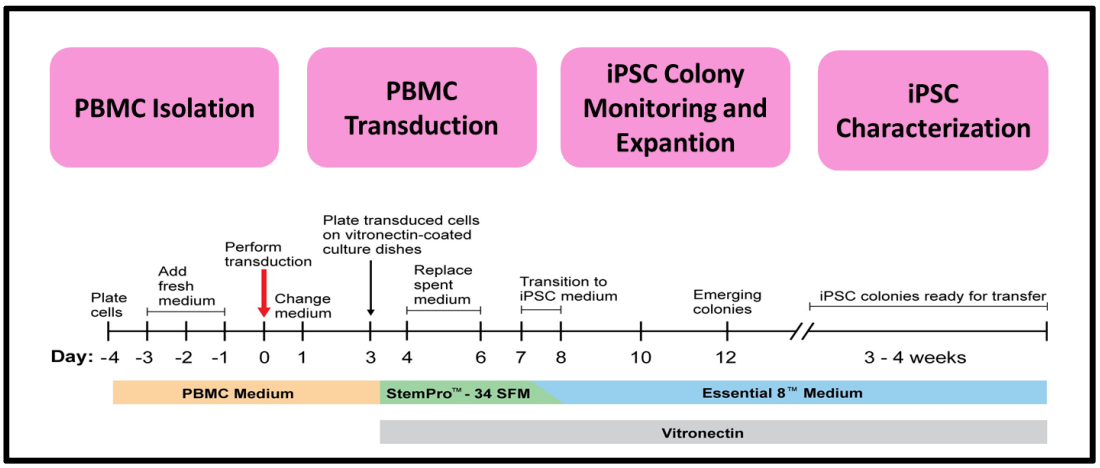

Figure 2.2. Timeline for obtaining induced pluripotent stem cells

Colony Collection: Following viral transduction (Day 0), the cells were monitored daily under a microscope. The colonies formed in the culture were collected under the microscope after their morphology became evident between days 15-18. Colonies were released from their surroundings with a 27G needle and collected with a 100 µL pipette. Collected and transferred to vitronectin-coated wells. Culturing was continued with Colony Essential 8 medium.

Expansion of Colonies: Colonies are left to grow in new wells after collection. 50-60% of the surface area of the colonies coating followed by passaging with EDTA. In this way, expansion and multiplication of colonies are ensured. To coat a 100 cm^2 petri dish with vitronectin, 60 µL vitronectin was added to 6 mL DPBS. Diluted and mixed well and placed in a petri dish. Incubate at room temperature for 1 hour to coat the dish and then store at +4°C for 1 week if not to be used. The medium of the cells to be passaged is collected and then the petri dish is washed with DPBS. Add 0.5mM EDTA according to the petri dish used (4mL for a 60mm 2 petri dish) and incubate at 37°C for 5 min. While waiting for the cells to rise, excess DPBS is removed from the vitronectin-coated petri dish and 6 mL of E8 medium is added to the petri dish to prevent the dish from drying out. Then, 0,5 mM EDTA is collected from the edge of the petri dish in such a way that it does not lift the cells and removed. The colonies lifted from the surface are collected with E8 medium and transferred to vitronectin-coated cell culture plates. The medium is changed every 24 hours until the cells are passaged again.

Freezing Colonies: Two methods for freezing colonies were tested. The first is freezing using E8. The medium of the cells was collected and then the petri dish was washed with DPBS. Depending on the petri dish used, 0,5 mM EDTA was added and incubated at 37 °C for 5 min. 0,5 mM EDTA was collected from the edge of the petri dish in such a way that it did not lift the cells and removed. Cells were collected with 900 µL E8 medium and placed in cryovial tubes and 100 µL DMSO was added to maintain DMSO concentration at 10%. The tubes were placed in a container containing isopropanol and stored at -80°C. The next day the cells were removed to liquid nitrogen.

The second is freezing using PSC Cryomedium. The medium of the cells was collected and then the petri dish was washed with DPBS. Depending on the petri dish used, 0.5 mM EDTA is added and incubated at 37°C for 5 min. 0.5 mM EDTA is collected from the edge of the petri dish so that it does not lift the cells and removed. Cells are collected with E8 medium, centrifuged at 200xg for 4 min and the supernatant is discarded (This step can be skipped and cells can be collected directly with PSC Cryomedium). Cells are collected with 1 mL PSC Cryomedium and placed in cryovial tubes. The tubes are placed in a container containing isopropanol and stored at -80°C. The next day the cells are removed to liquid nitrogen.

Thawing of Colonies: Petri dishes are coated with vitronectin. Add 3mL of E8 medium into a 50mL flask. In another flask, add 100 µL RevitaCell to 10 mL of medium. Thaw the frozen cells rapidly in a 37°C water bath, leaving a small portion frozen. Add E8 medium dropwise to the thawed cells and collect from the cryovial into a 50 mL flask containing medium. The cryovial is washed once more with medium and the remaining cells can be collected. Cells should not be collected in a give-and-take manner in order to avoid complete disintegration of the colony structure and separation of the cells from each other. The collected cells are centrifuged at 300xg for 4 min and the supernatant is collected and discarded. Cells are collected with RevitaCell containing medium and seeded in petri dishes. The medium containing RevitaCell should be replaced with E8 within 18-24 hours.

Induced Pluripotent Stem Cell (iPSC) Differentiation: In this thesis study, high quality human PSCs were used for neural differentiation. T25 flasks were coated with vitronectin and iPSC culture was continued until ~70-80% confluency was reached. The iPSC culture that reached appropriate confluency was passaged in accordance with the

passage protocol. To estimate the cell concentration in iPSC clumps, 1mL of the cell suspension was reserved. This separated suspension was centrifuged at 200 × g for 3 min and the supernatant was aspirated. 1 mL of pre-warmed StemPro® Accutase® was added to the pellet, then incubated at 37°C for 5 min. To turn the cells into a single cell suspension, they were pipetted vigorously 5 times and the cells were counted under a microscope. After aspirating vitronectin from T25 flasks, 750,000 cells were seeded per T25 flask and 4mL iPSC culture medium was added. Meanwhile, cells were treated with 10 μM ROCK inhibitor overnight to prevent cell death. Move the T25 flasks back and forth and side to side to distribute the cells evenly across the surface, then gently place the T25 flasks into a CO^2 incubator.

Neural Induction: On day 1 of PSC splitting (15-25% confluence), the medium used to remove non-attached cells was aspirated and pre-warmed PSC Neural Induction Media was added to T25 flasks. (Neural Induction Media consists of 490 mL Neurobasal® Medium + 10 mL Neural Induction Supplement). T25 flasks were placed in the incubator again. On the 2nd day of neural induction, it was checked under light microscope that the morphology of the cell colonies was uniform. Approximately 48 hours after the PSC were transferred to Neural Induction Medium, the used medium was aspirated from each flask and pre-warmed Neural Induction Medium was added. On day 4 of neural induction, cells reached confluency. Colonies with non-neural differentiation were marked and removed with a Pasteur glass pipette and the culture medium was renewed. On the 6th day of neural induction, the cells approached maximum confluency and the culture medium was again renewed.

2.2.2. Nanomaterials Treatment

Single iPS cells (5,000 cells/well) were seeded in a 96-well plate. After overnight incubation, cells were treated with MQD material at concentrations of 2,5, 5, 10, 20, 50, 100 μg/mL for 4 hours. LDH assay (Thermo) was performed at 24 hours according to the kit instructions. A graph showing the percentage of cell viability was then plotted.

2.2.3 Electrical Current Application

2.2.3.1. Electric Current Application

Graphene, one of the carbon-based nanomaterials known to have high electrical conductivity, will be provided with an electric current for easier transfer of the action potential between neurons. This process has been implemented with an ARM-based microcontroller as time-controlled and current-controlled. Thanks to the microcontroller, more than one current can be applied to the cells at different time intervals **Figure 2.3**. The electric current value chosen for this thesis proposal is 1 milliampere (mA) (Jaatinen et al., 2015). This current value was applied to cells and scaffolds for 1 minute. This procedure was applied every 2-3 days during the differentiation period.

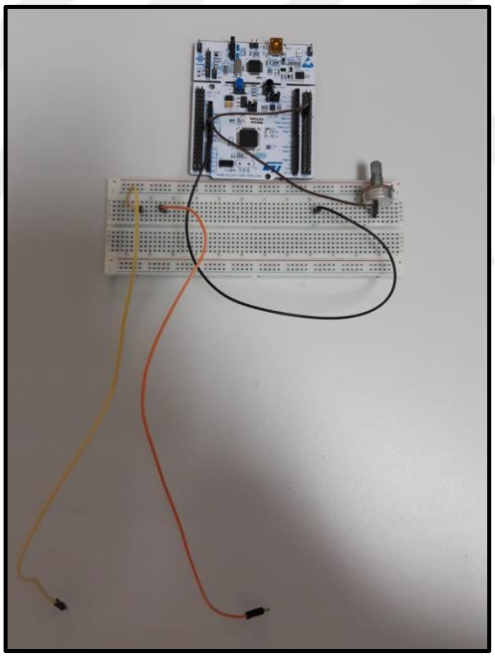

Figure 2.3. ARM-based microcontroller designed to apply electric current to cells

2.2.3.2. Magnetic Field Application

As a result of the positive results observed in cells to which electric current was applied, it was considered to apply this experiment on experimental animals, but since the effects of the probes used for the experiment on the experimental animal were not known, it was evaluated that the closest effect could be provided externally with a Magnetic Field

(MF). In order to create the magnetic field and observe its effect, a simple circuit was created and connected to a magnetic coil. In the circuit, a timer integration (LM555) was operated in astable mode. Thus, the timer integration was enabled to generate signal pulses at a certain frequency. In addition, the operating frequency can be changed with passive electronic materials connected to the timer integration. The pulses obtained at the output of the integrated were used for base triggering for one n-type BJT and one p-type BJT. Considering that the current level of the BJT2s used would not be sufficient, a mosfet was connected to the circuit in order to trigger the coil at higher current and the coil was triggered with this mosfet. Thus, a magnetic field was obtained at the desired frequency **Figure 2.4**.

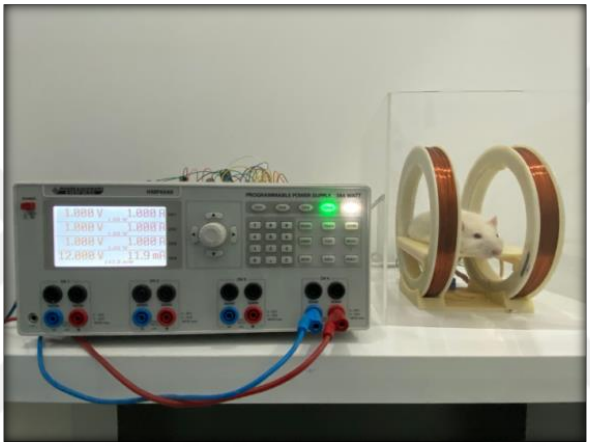

Figure 2.4. Magnetic circuit designed to non-invasively apply electric current to rats

2.2.4 3D-Bioprinting Processes

2.2.4.1. Scaffold Design

Considering the scaffolding structure, a 3x3 cm^2 structure was designed with the AutoCAD program. This design has been uploaded to the program of the Envisiontec Bioplotter brand Manufacturer series printer at Ankara University Stem Cell Institute in .stl format. After that, the pattern of the layers was selected and printing began.

2.2.4.2. Bioink Preparation

At this stage, 3% alginic acid was used. A bioink was prepared in a 30 cc bioprinter cartridge with a total volume of 20 mL. The prepared bioink was incubated and the air

bubbles were allowed to collect on the surface so that it could be printed smoothly during the printing stage.

2.2.4.3. 3D Bioprinting and Crosslinking

Envisiontec Bioplotter brand Producer series device was used for bioprinting. As mentioned above, cells grown in the induction step were printed with a 3D bioprinter for the differentiation step. Cells were grown in healthy condition and approximately 10-13x10^3 cells were dissolved and mixed in differentiation medium with 8% alginate solution and 100µg/mL sGO. This alginate-cell mixture was filled into 30 cc cartridges and 0.2 mm need types were used. This bio-ink was added to the cold head cartridge of the bioprinter and loaded into the device and then printed. The scaffold obtained after printing was kept in 100mM $CaCl^2$ solution for 15 min and crosslinked. After washing with PBS, the scaffold was taken into differentiation medium **Figure 2.5** and **Figure 2.6**.

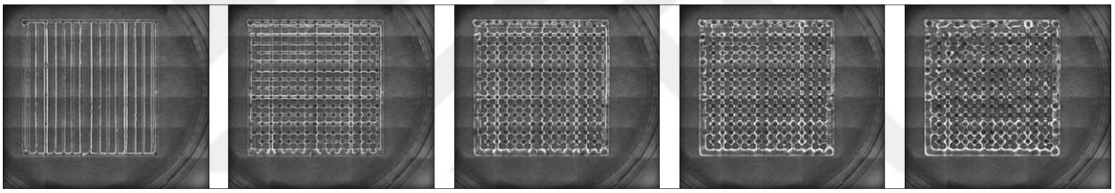

Figure 2.5. Snapshot of scaffolds printed on a 3D bioprinter, taken from each layer during printing

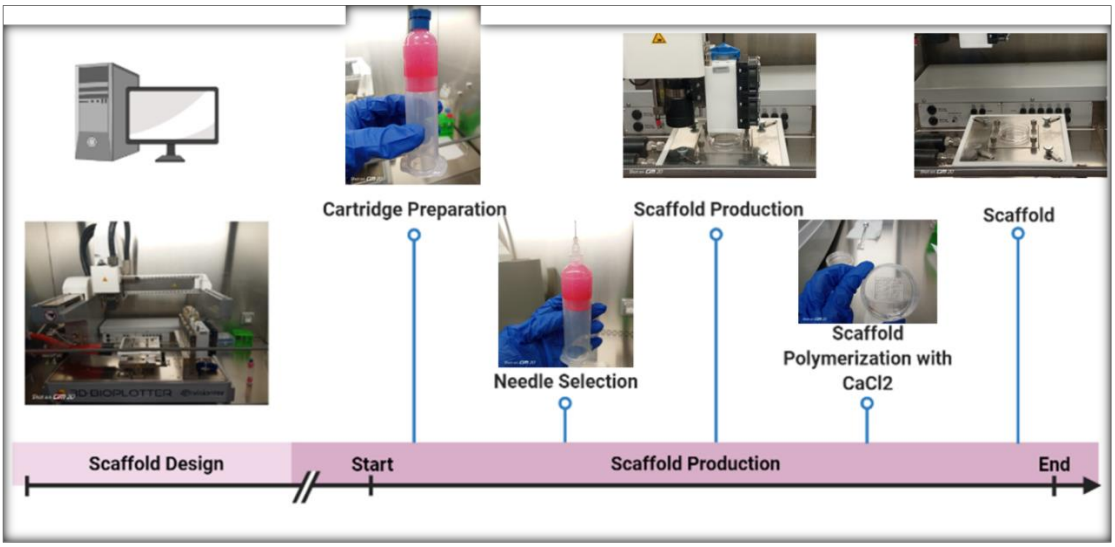

Figure 2.6. Schematic of 3D-Bioprinting processes

2.2.5. Real Time Polymerase Chain Reaction

Neural cell markers were determined by qRT-PCR method. At days 1, 7 and 14 after 2-D Culture, RNA was isolated with the QiagenRneasy Plus Mini Kit and cDNA was synthesized with the QiagenQuanti Reverse Transcription Kit. Then, the expression level of each gene was determined according to the reference GAPDH gene by qRT-PCR analysis with 2µg cDNA obtained from the 2-Dimensional culture.

2.2.5.1. RNA Isolation

Macherey-nagel Nucleo Spin RNA Mini Kit was used for RNA isolation of 2D and 3D cell cultures. For two-dimensional culture, the plates removed from the incubator were aspirated after treatment according to the experimental procedure. Cells were washed with 10 mL DPBS. Each plate was added trypsin-EDTA and placed in an incubator at 37°C with 5% CO2. The medium was added to the cells separated from the plate and mixed by pipetting. Cells were counted with a hemocytometry slide and transferred to tubes as 5×10^5 cells and centrifuged at 11,000 rpm for 5 min. After centrifugation, the supernatant was aspirated. 250 µL β-mercaptoethanol was added to 25 mL of lysis solution from the Macherey-nagel Nucleo Spin RNA Mini Kit and the lysis solution was prepared. 350 µL of lysis solution was added to the pellet remaining in the tube and the tubes were stored at -20°C. RNA was then isolated from the samples according to the protocol specified in the Macherey-nagel Nucleo Spin RNA Mini Kit. Finally, 50 µL of nuclease-free H2O was added to the isolated RNA in the tube and the samples were stored at -20°C.

For three-dimensional cultures (scaffolds), scaffolds were collected for RNA isolation after treatment according to the experimental procedure. The medium in the Petri was aspirated and removed. DPBS was added to cover the scaffold and washed 2 times. After the DPBS was aspirated, 2 mL of pre-prepared and 155 mM sodium citrate solution (sterile) was added to cover the scaffold well for isolation of the encapsulated cells in the scaffold. Petri were incubated in an incubator at 5% CO2 and 37°C for 50 min to dissolve the scaffold and release the cells. The cell suspension in the petri dishes was then collected in a 15 mL flask and centrifuged at 300 x g for 5 min. The supernatant was aspirated and discarded. The cell pellet was thawed by mechanical force. Cells were counted with a hemocytometry slide and transferred to tubes as 5×105 cells and centrifuged at 11,000 rpm for 5 min. The supernatant was aspirated. The lysis solution from the Macherey-nagel

Nucleo Spin RNA Mini Kit 24 was added 350 µL to each tube and the tubes were stored at -20°C. RNA was then isolated from the samples according to the protocol specified in the Macherey-nagel Nucleo Spin RNA Mini Kit. Finally, 50 µL of RNase-free H2O was added to the isolated RNA in the tube and the samples were stored at -20°C.

2.2.5.2. cDNA synthesis

The commercially available iscript cDNA Synthesis Kit was used for cDNA synthesis from the RNA obtained from 2-dimensional and 3-dimensional cultures. According to the iscript cDNA Synthesis Kit protocol, the amount of RNA was calculated as 1,000 nanograms (ng). The cDNA synthesis solution was prepared by taking 1 µL of iScript Reverse transcriptase enzyme + 4 µL of iScript reaction mix in the iscript cDNA Synthesis Kit per sample. 5 µL of the cDNA synthesis solution was added to the RNAs calculated as 1,000 ng. It was incubated with BIORAD thermal cycler device. Incubation was completed at 25°C for 25 min, 42°C for 30 min and 85°C for 5 min. The synthesized cDNAs were diluted 1:2 with RNase-free H2O and stored at -20°C.

2.2.5.3. qRT-PCR

Commercial primers designed for polymerase chain reaction (PCR) were used. Commercially available lyophilized primers were reconstituted with ionized water and a master stock was prepared. The stock primers were reconstituted to a final concentration of 5 pmol/µL. For the PCR reaction, the reaction mixture was prepared according to the commercially available SsoAdvanced™ Universal SYBR® Green Supermix protocol. Accordingly; 10 µL SsoAdvanced Universal SYBR® Green Supermix, 1 µL Forward Primer, 1 µL Reverse Primer, 6 µL Nuclease-free H2O was used for each sample. 25 For each sample, 18 µL of the PCR reaction mixture was dispensed into 96-well PCR plates. 2 µL of cDNA was added on top and the total volume was 20 µL per well. According to the protocol determined in BIO-RAD thermal cycler (CFX96) devices; initial denaturation was incubated at 95°C for 10 min, extension at 95°C for 15 seconds (40 cycles), final extension at 60°C for 1 min (40 cycles). After the PCR reaction, the ΔΔCt equation was used to calculate the mRNA amounts. The cycle threshold (ct) value was used to calculate the amount of gene expression for the samples obtained compared to the control group. The difference between the samples and the reference gene used was calculated (ΔCt). Then, the

difference between the ΔCt value of the samples to be analyzed and the ΔCt value of the control group was found and analyzed using the 2-ΔΔCt equation.

2.2.6. Immunohistochemical Staining

2.2.6.1. Live –Dead Staining

Non-toxic live-dead staining was performed to determine cell viability and mortality. The same procedure was applied for 2D and 3D culture. The media has been removed; cells and scaffolds were washed with PBS. The cells and scaffold were then treated with the mixture from the Thermo-LIVE / DEAD Cell Viability Assay kit at room temperature for 30 min and viewed under the EVOS fluorescence microscope. Live and dead cell density were calculated.

2.2.6.2. Immunofluorescence Staining

Immunofluorescence staining was performed to determine the expression of neural cell markers at the protein level. On days 1, 7 and 14 after culture, samples in 2D culture and 3D scaffold were fixed with cold methanol. The fixed cells were then stained with b-III-tubulin and nestin primary antibodies and incubated overnight, followed by staining using secondary antibodies labeled FITC, AF543. 4',6-Diamidino-2-Phenilindole (DAPI) was used to mark the cell nucleus. Stained cells were visualized with an EVOS fluorescent microscope. DAPI (blue), Nestin-FITC (green), b-III-tubulin AF543 (red).

2.2.6.3. Alkaline Phosphatase Staining

iPS cells were seeded in 2 wells of a 12-well plate previously coated with vitronectin and allowed to grow in their own medium. The medium was removed from iPS cells that reached sufficient size. Cells were washed with pre-warmed serum-free DMEM/F12 medium and kept for 2-3 min. The washing process was repeated. Alkaline Phosphatase Live Stain (Thermofisher, A14353) with 500X stock solution was diluted in serum-free DMEM-F12 and an appropriate amount of 1X Alkaline Phosphatase Live staining solution was prepared for each well. The prepared 1X Alkaline Phosphatase Live staining solution was applied directly to adherent iPS cells. Cells were incubated with this solution for approximately 1 hour in the dark and at room temperature. After incubation, the solution was removed and

the cells were washed twice with serum-free DMEM/F12 for 5 min each time. After washing, fresh serum-free DMEM/F12 medium was added to the cells. iPS cells were examined under a Zeiss Cell Discoverer microscope.

2.2.7. Animal Experiment

Spinal cord injury model was used for this doctoral thesis. A total of 100 rats (Wistar Albino), 50 females and 50 males, aged 4-6 weeks were used. For this model, rats under anaesthesia were subjected to hemisection spinal cord injury in the (T7-T10) region. Scaffolds containing neural stem cells and MQD in different combinations suitable for each group were created by 3-D bioprinting. After the spinal cord injury was created, scaffolds were placed to cover the injury. Following scaffold implantation, dorsal muscles and skin were sutured, antibiotics and analgesics were administered. In studies, it has been determined that analgesic administration before surgery reduces postoperative pain. Therefore, 1 mg/kg dose of analgesic (meloxicam) was administered half an hour before the operation. This application continued for 5 days. Wound care of the animals awakened from anaesthesia was continued in the following days until the end of the experiment. After the operation, antibiotic (enrofloxacin) was administered at a dose of 10 mg/kg and this application continued for 5 days. Electrical cytumisation was applied to the groups 1 week after the spinal cord injury. Electrical cytumlation to be applied 1 week after the spinal cord injury was repeated 3 times a week. This procedure is non-invasive and does not affect animal welfare. Since immune response would occur due to the use of neural stem cells differentiated from human iPS cells, Cyclosporin A 10mg/kg intraperitoneal injection was given to the animals every day until the end of the experiment to suppress the immune response. In addition, BBB score analysis and motor evoked potential measurements and hot plate test were performed at 2nd, 3rd, 4th, 5th, 5th, 6th, 7th and 8th weeks after spinal cord injury. At the end of 4 and 8 weeks determined in the experimental plan, EMG test was performed on the anaesthetised animals just before the experiment was terminated, and then the animals were euthanised and the tissues in the area of spinal cord injury were removed **Figure 2.7**.

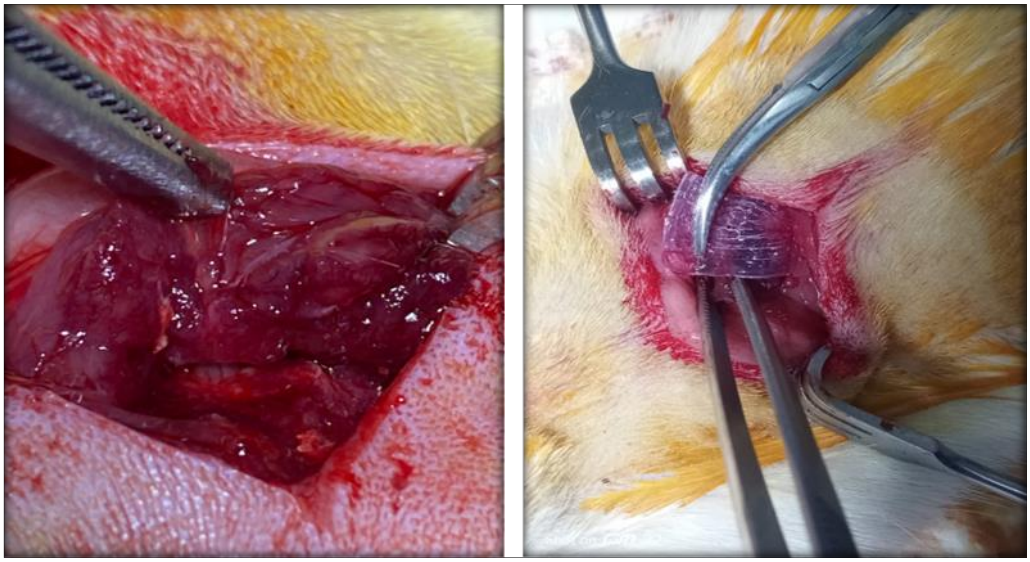

Figure 2.7. Spinal cord injury in rats and scaffold placement at the damaged area

2.2.7.1. Electromyographi (EMG) Test

EMG, often known as electromyography, is a neurological diagnostic technique that involves assessing the electrical activity of nerves and skeletal muscles. This investigation aimed to examine the electrical potentials of nerves and muscles between different treatment groups following spinal cord damage. EMG measurements were recorded for each animal in the treatment group using LabChart after 8 weeks. Prior to EMG, the animals were anesthetized using a ketamine cocktail and the adequacy of anesthesia was verified by the absence of paw withdrawal reflexes in response to intense foot compression. Subsequently, the posterior region of each animal was meticulously groomed through the process of shaving. In order to achieve precise and reliable measurements, a surgical cut was performed in the area between the shoulder blades, beginning 2 cm above the affected thoracic level (T7-T10). The measuring electrodes were positioned superiorly and inferiorly to the incision, while the ground electrode was affixed to the animal's tail and the animals were stimulated at the apex of the incision **Figure 2.8**. To eliminate unwanted interference from the original EMG signal, a band-pass filter was implemented within the LabChart interface, specifically set at a frequency range of 50-2000 Hz. The pulse height was adjusted to 4 V, and the animals were subjected to repeated shocks at intervals of 0.1 s. The peak analysis capability of LabChart was utilized to analyze all responses for their peak amplitude and frequency. The EMG responses of all animals within the same group were averaged during analysis.

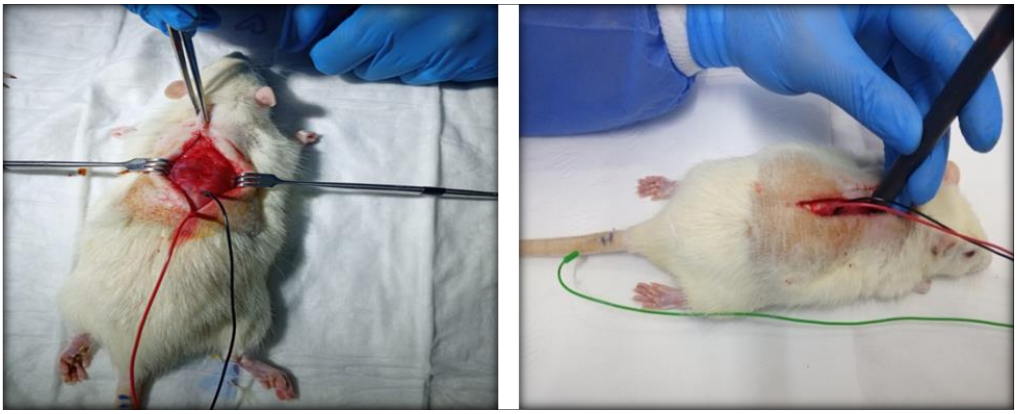

Figure 2.8. Implantation of EMG probes in rats and delivery of stimulation

2.2.7.2. Basso, Beattie and Bresnahan (BBB) Locomotor Test

The BBB test is a locomotor test established by Basso, Beattie and Bresnahan (BBB) to assess recovery after contusion injuries to the rat spinal cord. It tests locomotor function using an open-field locomotor scale defined from complete paralysis (score 0) to normal locomotion (score 21) (BASSO et al., 1995) **(Appendix-3)**. This is an efficient, extended and precise locomotor grading scale to standardise locomotor outcome measurements between laboratories. Prior to BBB testing, healthy animals and spinal cord injured animals were allowed to move freely in a transparent plastic box with a non-slip floor before and after the operation to assess locomotor outcomes **Figure 2.9**. For 4 min, two observers evaluated hind limb handling skills, joint movements, paw placement, weight support and front/back limb coordination according to the 0-21 point BBB locomotion scale. In the meantime, these observations were video recorded in order to be re-evaluated later. As a result of these observations, a scoring between 0-21 was made and comparison between the groups was provided. The evaluation of functional motor recovery is thought to be an indicator of regeneration of the lesioned spinal cord.



Figure 2.9. Specially prepared test boxes for BBB locomotor testing

2.2.7.3. Hot Plate Locomotor Test

The hot plate test is a test that measures pain response in animals. In this test, the plate was heated to 58°C **Figure 2.10** and the temperature of the plate was kept stable. Hot plate test was performed before and 1 week after spinal cord injury. The stopwatch was started as soon as the rat was placed on the hot plate and the stopwatch was stopped when the rat showed jumping or hind paw licking behaviour. The duration of jumping or hind paw licking behaviour with reflex was calculated. This time was compared between healthy animals and animals with spinal cord injury and the behavioural movements related to the improvement in spinal cord injury between the groups were interpreted.

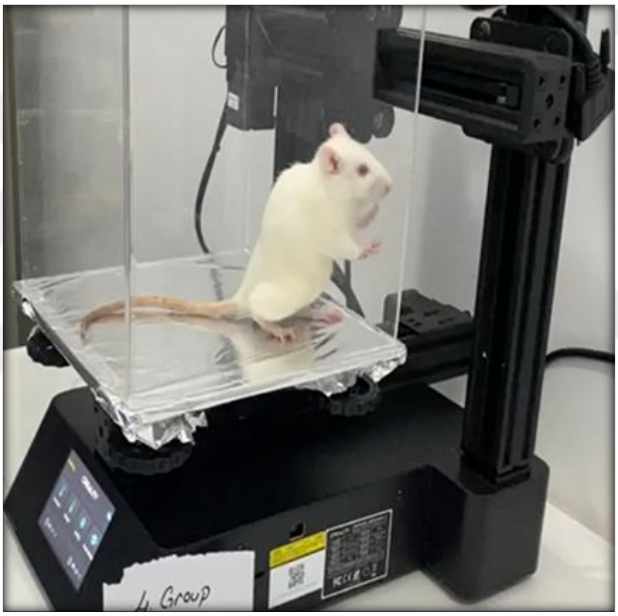

Figure 2.10. Hot plate specially prepared for locomotor testing, special table that can provide stable heat

2.2.8. Histological Analysis

Spinal cords were collected and fixed in 10% neutral buffered formalin (NBF). Fixed tissues were embedded in parafilm and blocks were then sectioned on poly-l-lysine microscope slides. Following dewaxing and rehydration, sections were stained with Mallory's trichrome stain and mounted in Entellan. Images were acquired with a microscope digital camera (DFC450, Leica, Wetzlar, Germany) integrated into a light microscope (DM2500, Leica, Wetzlar, Germany).

2.2.8.1. Sample Preparation for Scanning Electron Microscope (SEM) Imaging

The scaffolds printed by 3D bioprinting need to be dried in order to be visualised in Scanning Electron Microscope. For this purpose, the media of the cultured scaffolds were removed and washed 3 times with DPBS. A 4% paraformaldehyde solution was added to cover the scaffolds and kept at +4°C for 2 hours. Paraformaldehyde was removed and washed 3 times with distilled water. Scaffolds were kept at -80°C for 1 hour, then quickly transferred to freeze dryer and dried at -55°C for 2 days. These samples were then imaged in an SEM device.

Gold plating was performed before SEM examination. The samples were fixed on aluminum stubs with double-sided carbon tape. Insulating samples cannot be examined in the SEM device. Because in SEM, the sample is bombarded with electrons under high potential difference. If the surface of the sample is not conductive, the electrons sent to the sample will accumulate on the surface and will not be able to bring information about the surface by colliding with the electrons that follow. During the examination, electrons should only interact with surface atoms. Since the scaffold samples examined were insulators, the coating process was carried out for 2 min with the Emitech K550X model gold plating device to ensure electron transmission **Figure 2.11**. The plating process is achieved by impacting the argon gas in the environment on the gold plate target and depositing the broken gold particles on the sample surface. The samples with conductive surface were placed on the sample stage of the SEM device **Figure 2.12.** Imaging was performed under an accelerator potential of 20 kV in the SEM device with a tungsten filament.

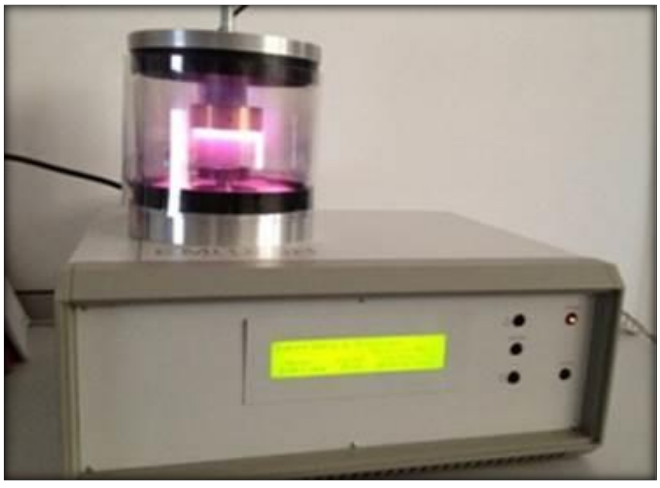

Figure 2.11. Emitech K550x Sputter Coater used to coat scaffolds with gold

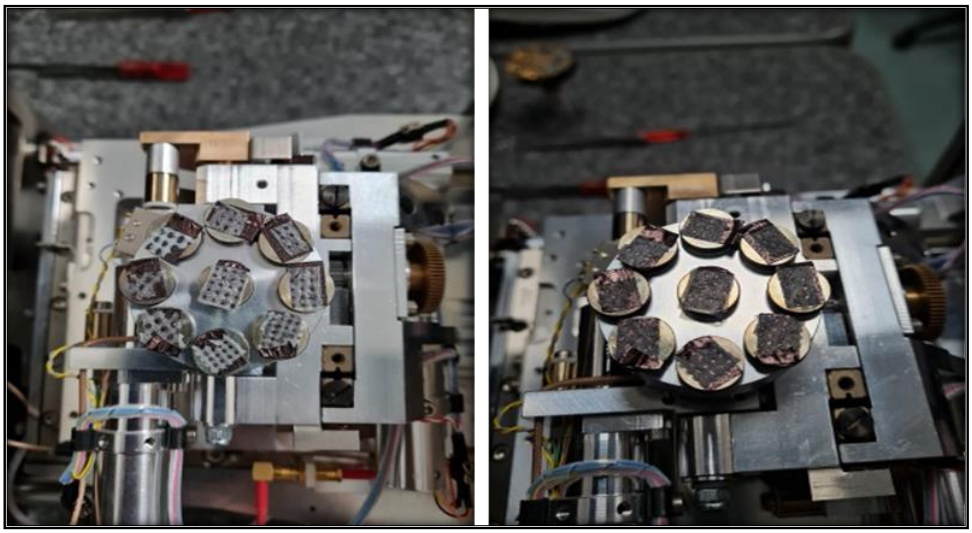

Figure 2.12. Images of scaffolds uncoated and coated with gold prior to SEM imaging

2.2.9. Statistical Analysis

In this thesis, the statistical analyses were evaluated by Assoc. Prof. Dr. Özlem KAYMAZ, Lecturer, Department of Statistics, Faculty of Science, Ankara University.

The measurements obtained by PCR analysis specific to neural stem cell genes will be used as the primary outcome variable in determining the sample size of the study. In the study, as a result of the power analysis for the "Repeated Measures ANOVA" method, the sample size was determined to be at least 15 units in total with 5 groups and 3 replications, large effect level (d=0.95) and 0.05 significance level. In this case, the power of the test is expected to be approximately 82.7%.

The mean±std. deviation and median (minimum and maximum) values for continuous variables, and frequency values for categorical variables (dead-live staining, immunohistochemical staining and SEM imaging) will be given. With these data, the levels of differentiation between the groups will be compared to the control group (group 1). Differences between the 5 groups and 3 time points (day 1, day 7, day 14) will be tested by two-way repeated measures analysis of variance (Two-way Repeated Measures ANOVA). $p< 0.05$ will be considered statistically significant.

Statistical analyses will be evaluated using (GraphPad Inc.) package programme and two-way data analysis programme (Anova Two Way Tukey). Results are given as mean SD. For analyses, p values less than 0.05 will be considered significant.

3. RESULTS

In this doctoral thesis; neural stem cells differentiated from human MSC, human NSC and human iPS cells were treated with neural growth factors and different nanomaterials and differentiated into neural cells in 2-D culture medium. At the same time, a bioink containing neural stem cells and nanomaterials was used to create a scaffold from a 3D bioprinter and cultured with neural growth factors. To increase the potential for neural differentiation, electric current was applied to both 2D and 3D cultures. Thus, the effect of nanomaterials with electrical conductivity on neural differentiation was investigated and the results obtained are given below.

3.1. Mesenchymal Stem Cell Differentiation and Characterization

Growth of Mesenchymal Stem Cell Line in 2D Cell Culture Media: Adipose-derived mesenchymal stem cells (MSCs) were grown in High Glucose Dulbecco's Modified Eagle's Medium (DMEM) with 10% fetal bovine serum, 1% pen-strep, 1% glutamax and 1ng/mL FGF at 37°C in 5% CO2.

Differentiation of MSCs into neurons in 2D cell culture medium was performed in two steps.

MSCs grown in cell culture medium were transferred to induction medium, which is the first step of differentiation. DMEM-F12, 10% FBS, 1% Pen-Strep, 1% Glutamax, 10 ng/mL FGF, 10 ng/mL EGF and 0.1% β-mercaptoethanol were used as components of this medium. Induction medium was changed every 2-3 days and fresh medium was added. MSC cells were cultured in this medium for 7 days.

After 7 days, the induction step was stopped and the differentiation step was initiated. For this step, cells were removed with trypsin and plated in 6-well plates (3X104 cells per well) coated with Attechment Factor (AF). Cells were expected to adhere to the 6-well plate within 24 hours. At the end of 24 hours, 100ug/mL sGO treatment was applied for 4 hours according to the experimental groups and fresh differentiation medium was added. DMEM-F12, 10% FBS, 1% Pen-Strep, 1% Glutamax, 10 ng/mL FGF, 10 ng/mL NGF, 10 ng/mL EGF, 10 ng/mL BDNF, 1X N2 and B27 supplement, 0.1% β-mercaptoethanol and

retinoic acid were used as this medium. The differentiation medium was changed every 2-3 days. At the same time, 1 mA electric current was applied to the cells in which the differentiation medium was changed for 1 minute according to the determined experimental groups. The differentiation phase continued for 14 days.

3.1.1. Determination of the Effect of sGO and Electric Current Application on the Viability of Mesenchymal Stem Cells by Live-Dead Staining Analysis

Non-toxic live-dead staining was performed to determine cell viability and death rate. Thermo-LIVE/DEAD Cell Viability Assay kit was used for this. The same procedure was performed for 2D and 3D culture. Media was removed; cells and scaffolds were washed with PBS. Cells and scaffold were then treated with the chitin content for 30 min at room temperature and imaged under an EVOS fluorescence microscope. Live and dead cell density was calculated. For this experiment, 4 different experimental groups were designed and images were obtained from days 1, 7 and 14. i) MSC (control), ii) MSC (differentiation media), iii) MSC (differentiation media + sGO), iv) MSC (differentiation medium + sGO + electric current). As shown in **Figure 3.1**, in the live-dead image obtained from 2D culture, a decrease in MSC (differentiation media + sGO + electric current) viability was observed in the group to which electric current was applied on day 14.

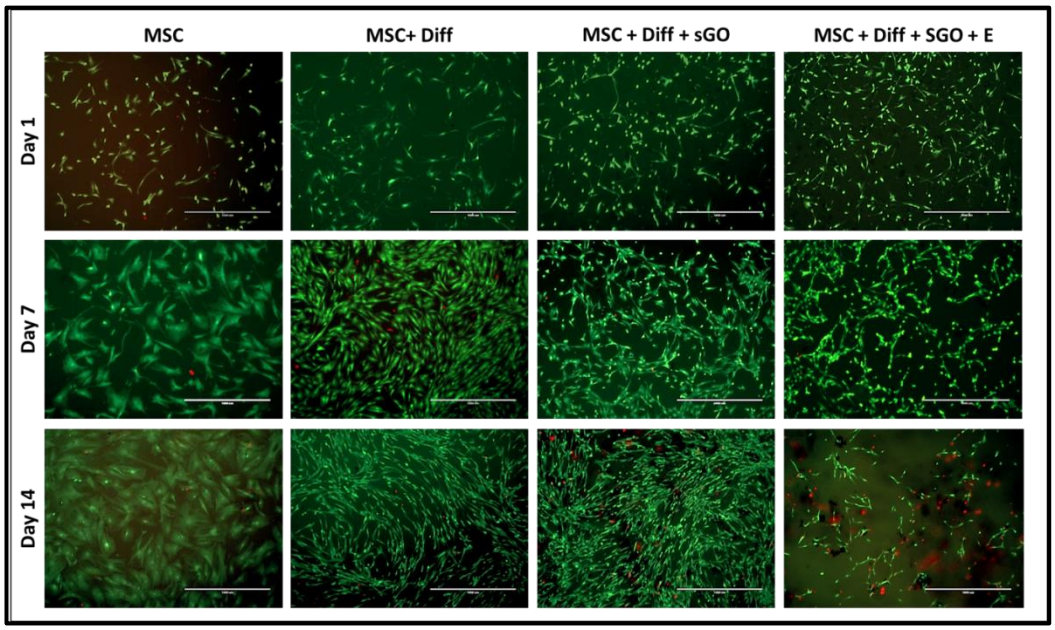

Figure 3.1. Live-dead images of MSC cells treated with sGO and electric current. MSC cells were visualized under fluorescence microscopy at 1, 7 and 14 days after sGO and electric current treatment (10X)

3.1.2. Determination of the Effect of sGO and Electric Current Application on Neural Markers in Mesenchymal Stem Cells by Gene Expression (qRT-PCR) Analysis

Neural cell markers were determined by qRT-PCR. On days 1, 7 and 14 after 2-D culture, RNA was isolated with Macherey-nagel NucleoSpinRNA Mini Kit and cDNA was synthesized with iScript™ cDNA Synthesis Kit. Then, qRT-PCR analysis was performed with 2µg of cDNA obtained from 2-D culture and the expression level of each gene was determined relative to the reference GAPDH gene. The neural cell markers used were nestin and b-III-tubulin. For this experiment, 4 different experimental groups were designed; i) MSC (control), ii) MSC (differentiation media), iii) MSC (differentiation media + sGO), iv) MSC (differentiation media + sGO + electric current). As shown in **Figure 3.2**, neural cell markers of these 4 different experimental groups were examined at days 1, 7 and 14. All groups were normalized to the control group during qRT-PCR analysis. It was observed that the electric field increased nestin gene expression in the 7th and 14th day groups.

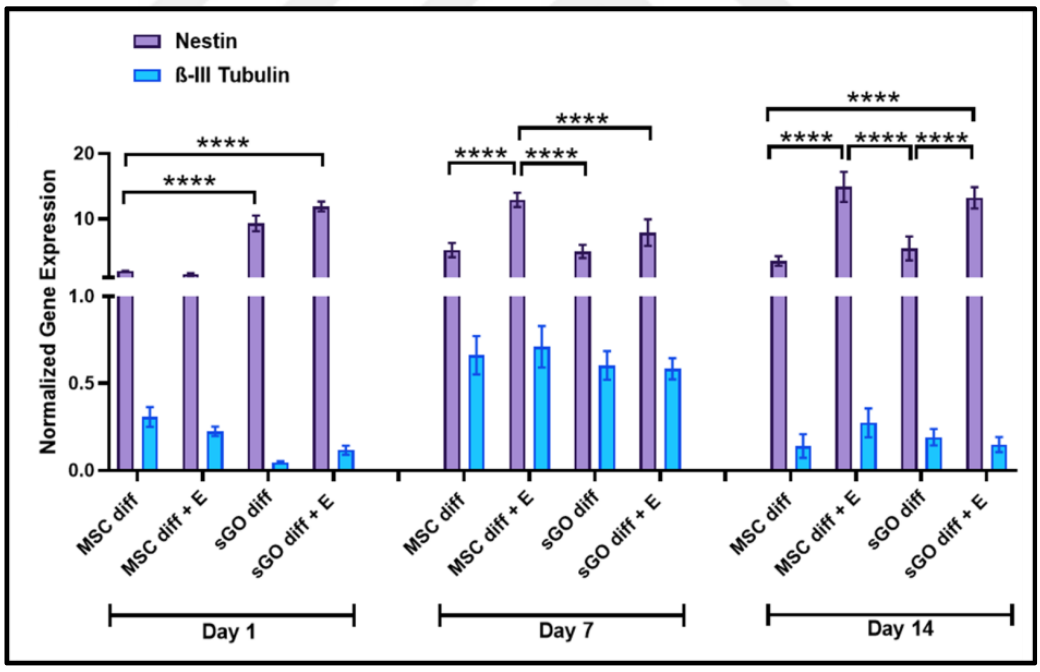

Figure 3.2. Real time PCR analysis of MSC cells at days 1, 7 and 14 after treatment with sGO and electric current. Gene expression levels were calculated and normalized to the control group $p<0.05$

3.1.3. Determination of the Effect of sGO and Electric Current Treatment on Neural Proteins in Mesenchymal Stem Cells by Fluorescence Microscopy

Immunofluorescent staining was performed to determine the expression of neural cell markers at the protein level. At days 1, 7 and 14 after culture, the samples in 2D culture **Figure 3.3** were fixed with cold methanol. The fixed cells were then stained with primary antibodies b-III-tubulin (1:50) ab18207 and nestin (1:100) ab6320 and incubated overnight, followed by staining using secondary antibodies labeled FITC (1:1000) ab6785, AF594 (1:500) ab150080. 4',6-Diamidino-2-Phenylindole (DAPI) was used to label cell nuclei. Stained cells were visualized with EVOS fluorescence microscopy. DAPI (blue), Nestin-FITC (green), b-III-tubulin-AF594 (red). The neural cell markers used were nestin and b-III-tubulin. For this experiment, 4 different experimental groups were designed; i) MSC (control), ii) MSC (differentiation environment), iii) MSC (differentiation environment + sGO), iv) MSC (differentiation medium + sGO + electric current). As shown in **Figure 3.3**, neural cell markers of these 4 different experimental groups were examined at days 1, 7 and 14. All groups were compared with the control group. At the end of the 14th day, it was observed that the cells in the other groups had elongated and thinned, i.e. morphologically changed compared to the control group. In particular iv) In the MSC (differentiation medium + sGO + electric current) group, nestin and b-III-tubulin protein expression was markedly observed.

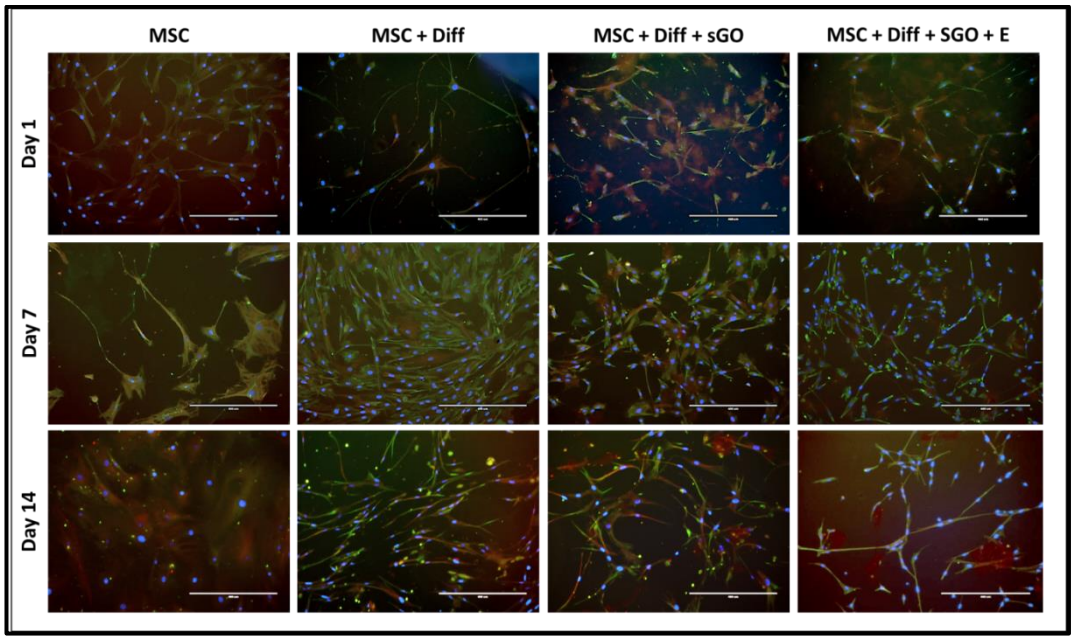

Figure 3.3. Fluorescence microscope images of MSC cells at days 1, 7 and 14 after treatment with sGO and electric current. DAPI (blue), Nestin-FITC (green), b-III-tubulin-AF594 (red) (20X)

3.2. Culturing, Dissociating and Differentiating Human Neural Stem Cell

Spheroid human neural stem cells were cultured in their own medium and under appropriate conditions until they reached 100-200 μm in diameter. The spheroids were checked daily to ensure they did not adhere to the culture dish and the mediums were changed every 2 or 3 days.

Spheroids reaching 100-200 μm in diameter were treated with dissotiation solution to become single cells. After counting the cells that became single cells, they were seeded at certain ratios and treated with differentiation medium. A new medium was added by changing half of the medium every day. Human neural stem cells were cultured for 2-3 weeks to differentiate into neurans.

3.2.1. Light Microscopy Images of Neurons Derived from Human Neural Stem Cell Lines

Neural stem cells treated with differentiation medium for 3 weeks differentiated into neurons at the end of 3 weeks. Below are images obtained **Figure 3.4** by light microscopy on days 2, 5, 11, 15, 18 and 21. At the end of the 21st day, HNSC cells were removed from the plan of this thesis because the amount of cells obtained was not sufficient for the experiments planned for this thesis. Instead of HNSC cells, iPS cells, which are thought to have high cell number productivity after differentiation, were preferred.

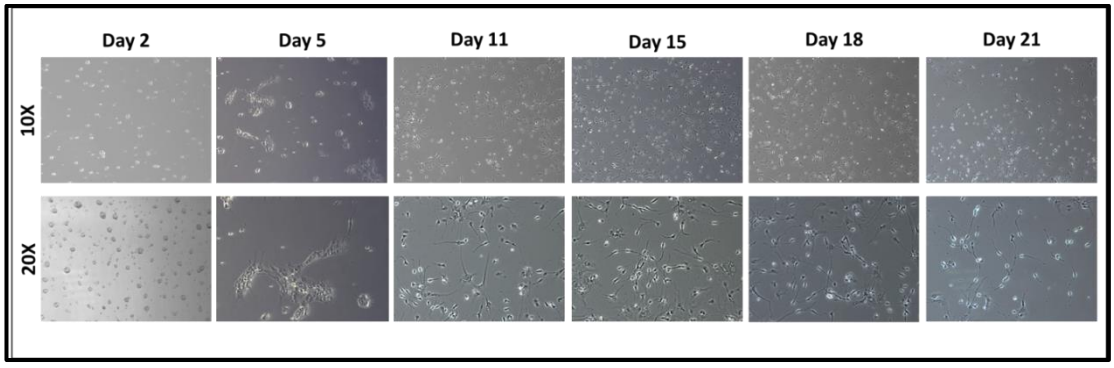

Figure 3.4. Differentiated culture images of HNSC cell line. The HNSC cell line was imaged under inverted light microscopy on days 2, 5, 11, 15, 18 and 21 after differentiation media treatment (10X) and (20X)

3.3. Induced Pluripotent Stem Cell (iPSC) Characterisation and Differentiation

3.3.1. PBMC Isolation, Transduction and Colony Growth

Special medium was prepared according to the protocol for PBMC cells isolated from healthy donors. To 500 mL StemPro-34 SFM Medium (Cat. No: 10639-011 ThermFisher Scientific), 13 mL StemPro-34 Supplement (Cat. No: 10641-025) and 2 mM L-Glutamine were added. Then, it was supplemented with the necessary cytokines (IL 3 20 ng/mL, IL 6 20 ng/mL, FLT 3 100 ng/mL, SCF 100 ng/mL) according to the kit protocol. Thus, PBMC medium was prepared**. Figure 3.5** shows the image of PBMC cells under a light microscope on days 1 and 3.

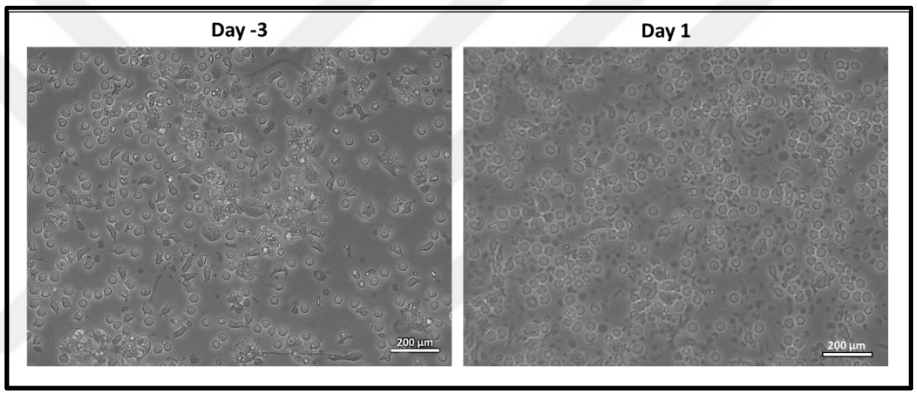

Figure 3.5. Culture images of PBMC cells on days 1 and 3 under light microscope after isolation

PBMC cells isolated from blood were subjected to programming by Sendai viruses carrying OKSM programming factors. Cytotune iPS 2.0 programming kit (ThermoFisher Scientific) was used for this purpose. Viral transduction was performed according to the protocol described in the method section. As can be seen in **Figure 3.6**; after transduction, the cells started to attach to the surface. Small cell communities were observed in about 10 days. These cell communities were replaced by colonies over time. They have the characteristics of typical pluripotent stem cell colonies mentioned in the literature: large nuclei, small cells, shiny colony wall.

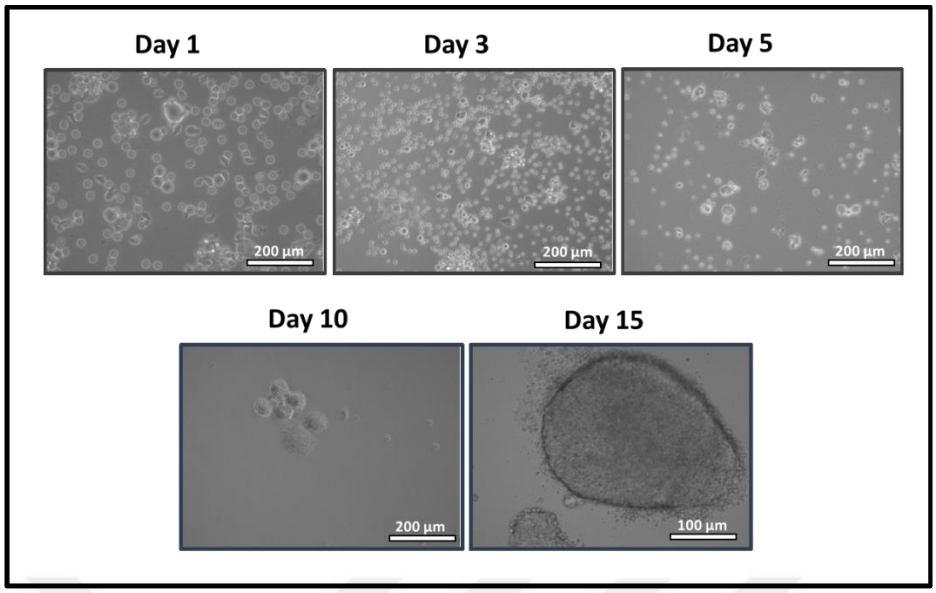

Figure 3.6. Changes of PBMC cells at days 1, 3, 5, 10 and 15 after transduction under light microscope

On the 15th-20th day of transduction, when the colonies were large enough to be collected, collection was performed under a microscope. The healthy colonies in the 6-well culture dishes were identified and collected. Each selected colony was transferred to each well of a 12-well culture dish. The growth, condensation and spontaneous differentiation of the colonies were monitored and the colonies were passaged with EDTA and the expansion was continued. The growth pattern of a colony after colony picking is shown in **Figure 3.7.**

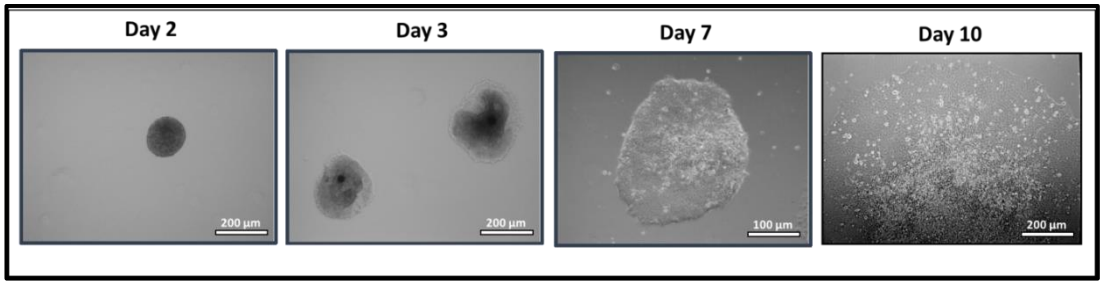

Figure 3.7. Images of the growth of colonies after colony selection on days 2, 3, 7 and 10 under the light microscope

3.3.2. Characterization of Induced Pluripotent Stem Cells by Gel Electrophoresis and Gene Expression (qRT-PCR) Analysis

In order to ensure colony multiplication, 3 colonies were selected as shown in **Figure 3.7** and iPSCs were multiplied from each colony with at least 10 stocks in nitrogen. In parallel with the multiplication process, characterization studies were started. In order to

prove the efficiency of the freeze thawing method mentioned in the method section, 1 cycle of freeze thawing of the colonies was performed. In order to prove the presence of viral transduction, it was analyzed whether the genes were expressed in the cells with the primer sets specified in the kit. For this purpose; total RNA was isolated from the cells collected on the 2nd day following transduction and cDNA synthesis was performed. The PCR products obtained were run on agarose gel. The presence of expression of virus transgenes in PBMC cells from which RNA was isolated after transduction was observed and the PCR gel image is shown in **Figure 3.8.**

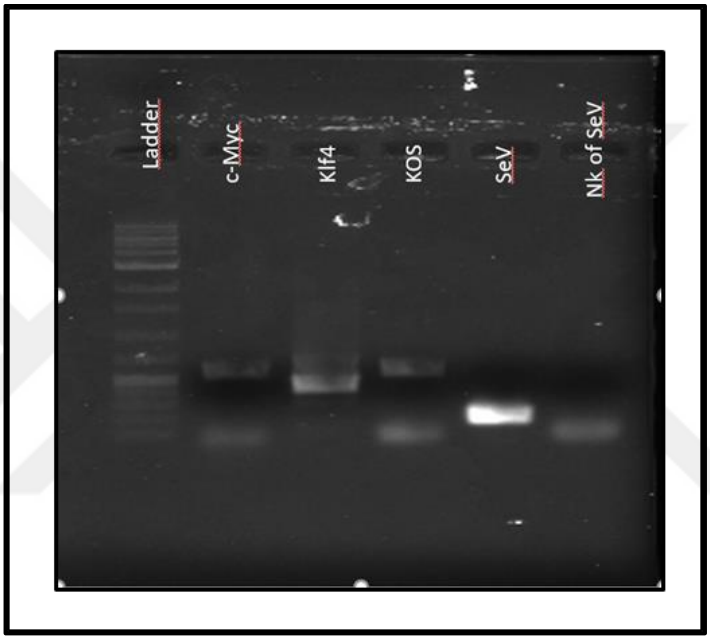

Figure 3.8. PCR gel image demonstration of the presence of virus transgenes (SeV) expression in PBMC cells after transduction

SOX2, OcT4 and Nanog are transcription factors that are crucial for inducing pluripotency in cells, often used in the production of induced pluripotent stem cells (iPSCs). SOX2: Maintains self-renewal and pluripotency by regulating other genes important for stem cell function. OCT4: Master regulator of pluripotency, which is required to maintain the undifferentiated state of stem cells. NANOG: Works with SOX2 and OCT4 to maintain the pluripotent state by suppressing differentiation. According to the PCR results from colonies 2, 3 and 4 in the following passage cycles, it is observed in **Figure 3.9** that pluripotency markers are expressed (SOX2, Oct4 and Nanog).

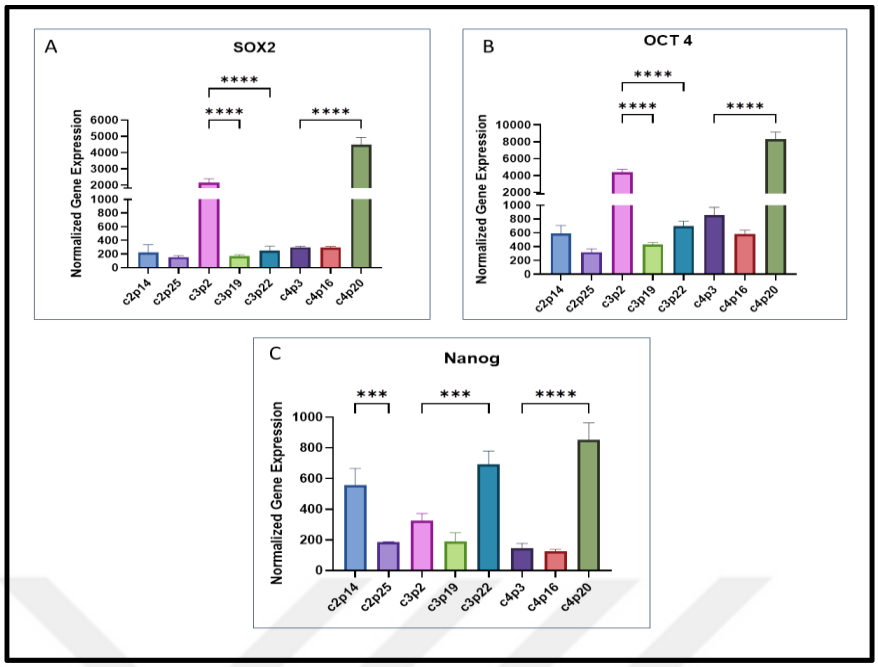

Figure 3.9. Measurement of gene expression by qPCR at subsequent passages (A. SOX2 Expression, B. Oct4 Expression and C. Nanog Expression). Gene expression levels were calculated and normalized to the control group $p<0.05$

For colony 4 passaged 16 times, it was analyzed whether the viral vectors were deleted or not and whether the genes were expressed in the cells with the primer sets specified in the kit. The decreased presence of viral vectors in the cells was shown by analyzing the decreased gene expression of viral vectors **Figure 3.10** and **Figure 3.11**.

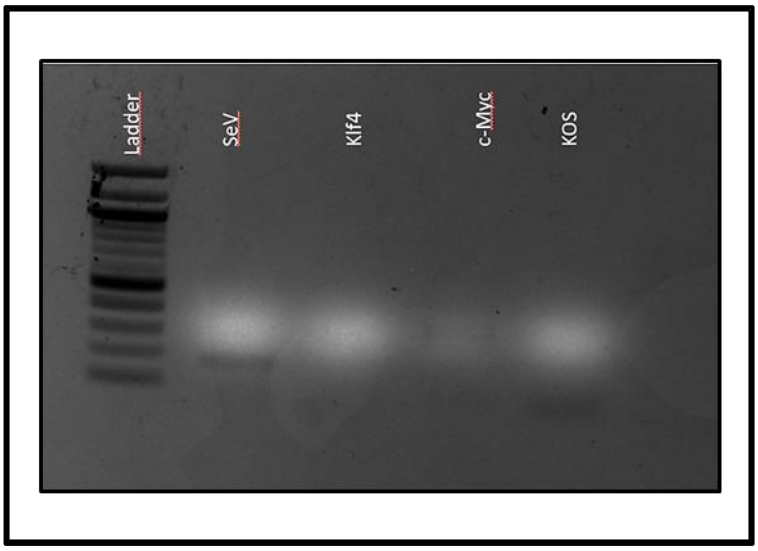

Figure 3.10. PCR gel image demonstration of reduced gene expression of viral vectors (Sev) in iPSC colonies

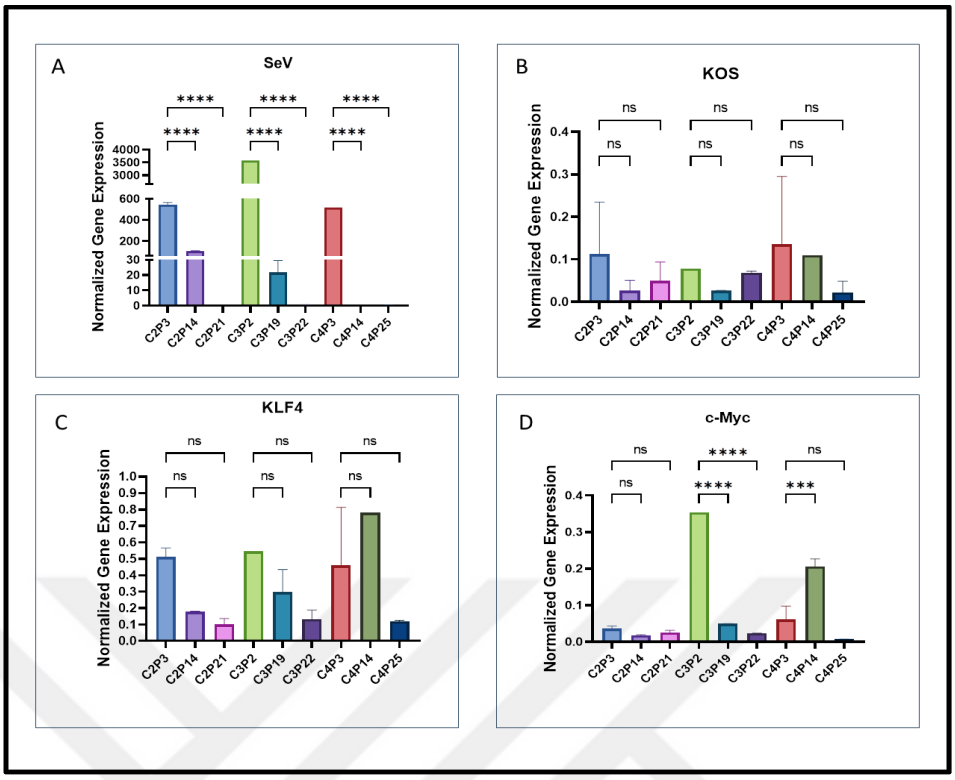

Figure 3.11. SeV qPCR Results (A. SeV Expression, B. KOS Expression, C. Klf4 Expression and D. c-Myc Expression, Results were analyzed using GraphPad Prism (9.0.0). Two-way ANOVA test was used and significance level was accepted as $p<0.05$)

3.3.3. Characterization of Induced Pluripotent Stem Cells by Immunohistochemical Staining

3.3.3.1. PSC-4 Marker Immunocytochemistry Kit

Immunostaining was continued after gene expression analysis. The 4th colony cells passaged 18 times were stained with PSC4-Marker Immunocytochemistry Kit. This kit is designed for the detection of four key markers of pluripotency in human pluripotent stem cells (PSCs). Oct4 is a transcription factor crucial for maintaining stem cell pluripotency. SSEA-4 a surface glycoprotein usually expressed in pluripotent cells. TRA-1-60 and TRA-1-81 - surface markers associated with undifferentiated pluripotent stem cells. The PSC4-Marker Immunocytochemistry Kit was used to confirm that the stem cell population remained pluripotent by confirming the expression of pluripotency markers. It was shown that iPS cells obtained in iPSC colonies stained with PSC4-Marker Immunocytochemistry Kit expressed pluripotent genes **Figure 3.12**.

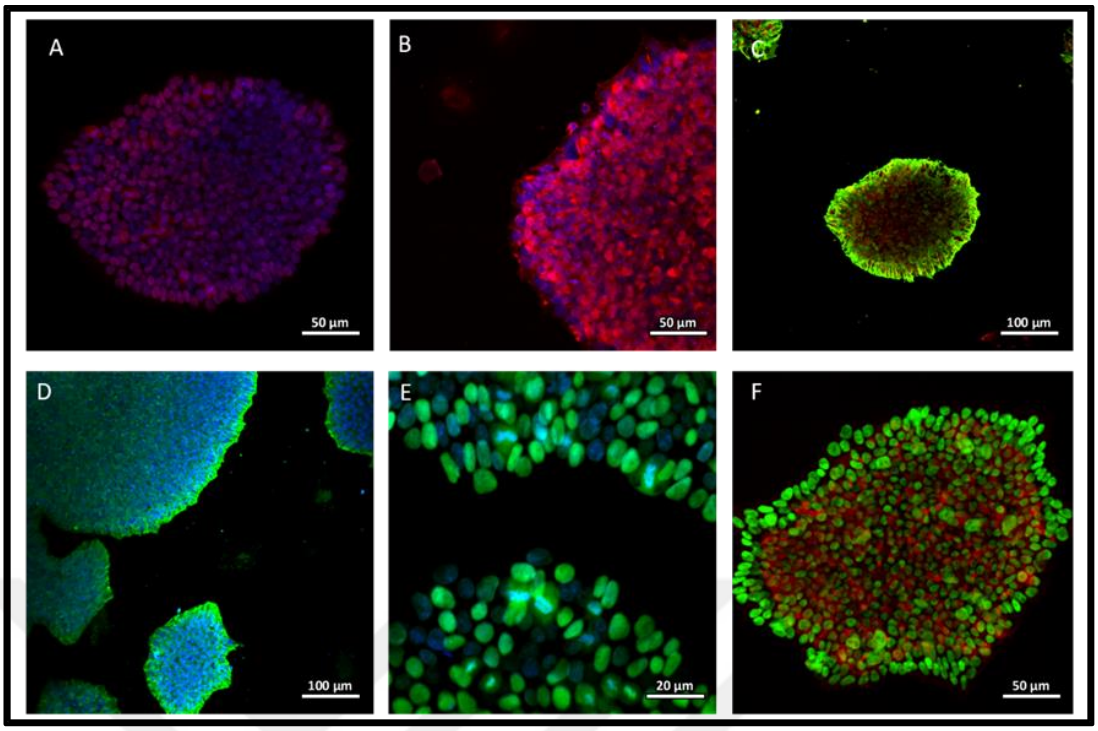

Figure 3.12. 4th iPS Cell Colony Stained with PSC 4-Marker Immunocytochemistry Kit (A. blue DAPI, red oct4 (20X), B. blue DAPI, red TRA-1-60, (20X) C. Red Oct4, Green SSEA4, (10X), D. blue DAPI, Green SSEA4, (10X) E. blue DAPI, Green Sox2, (40X) F. Red TRA-1-60, Green SOX2) (20X)

3.3.3.2. Alkaline Phosphatase Live Staining to Confirm the Presence of Pluripotency

Alkaline Phosphatase Live Staining of iPSC colonies to confirm the presence of pluripotency. Alkaline phosphatase staining, which is commonly expressed in undifferentiated cells (such as iPSC),allowed for confirmation of pluripotency and non-destructive evaluation. With this method, as shown in **Figure 3.13**, all colonies were shown to express alkaline phosphatase enzymes, a marker of pluripotency, ensuring that the cells retained stem cell-like properties.

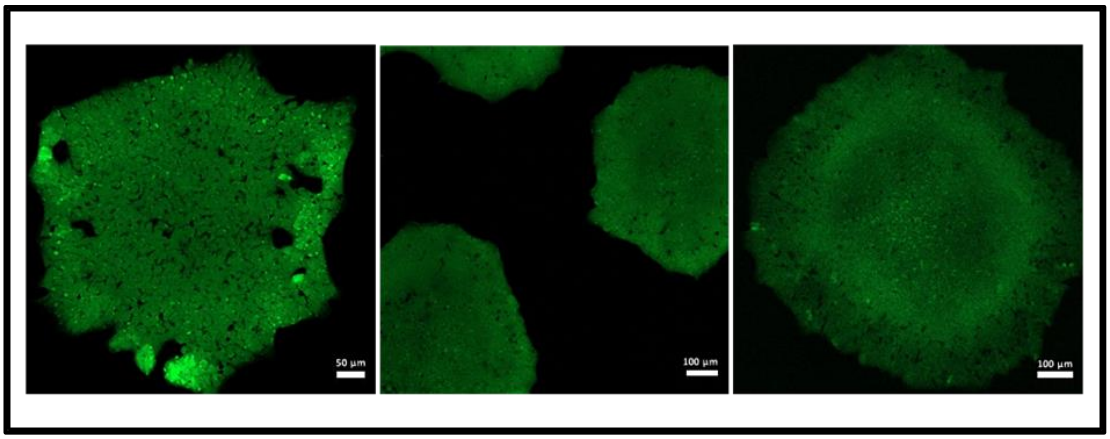

Figure 3.13. C2p10, c3p18, C4p22 Alkaline Phosphatase Staining

3.3.4. Embryoid Body Formation, Differentiation, qPCR and Immunofluorescence Staining

iPSCs form embryoid bodies to mimic early embryonic development, promote multilineage differentiation and test their pluripotent potential. Embryoid body formation experiments were performed during the 16th and 18th passaging **Figure 3.14**. Spontaneous differentiation of EBs is a natural, random process in which iPSCs or ESCs differentiate into a wide variety of cell types without external guidance. It reflects the cells' innate ability to mimic early embryonic development **Figure 3.15**.

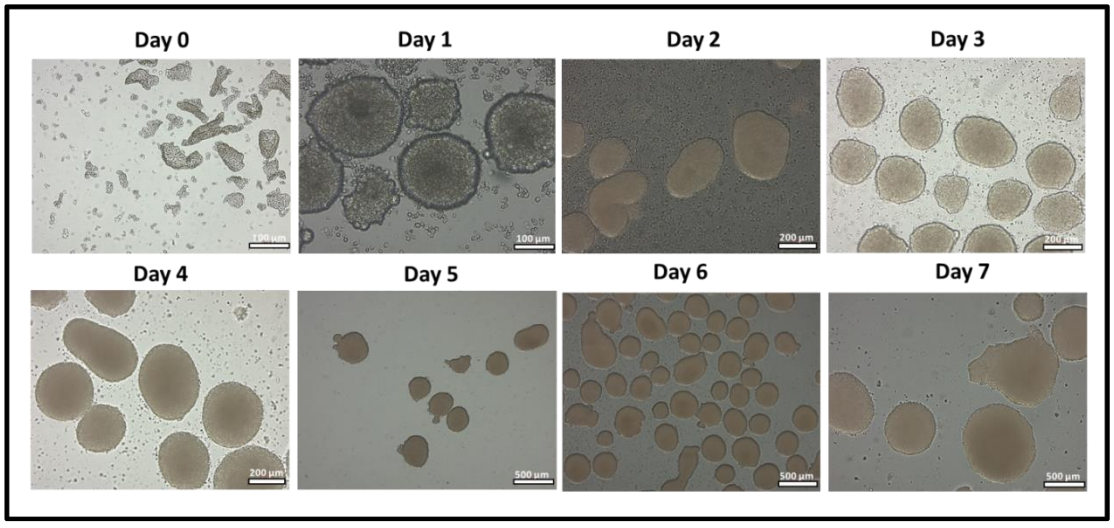

Figure 3.14. C4p25 Embryoid Body Formation

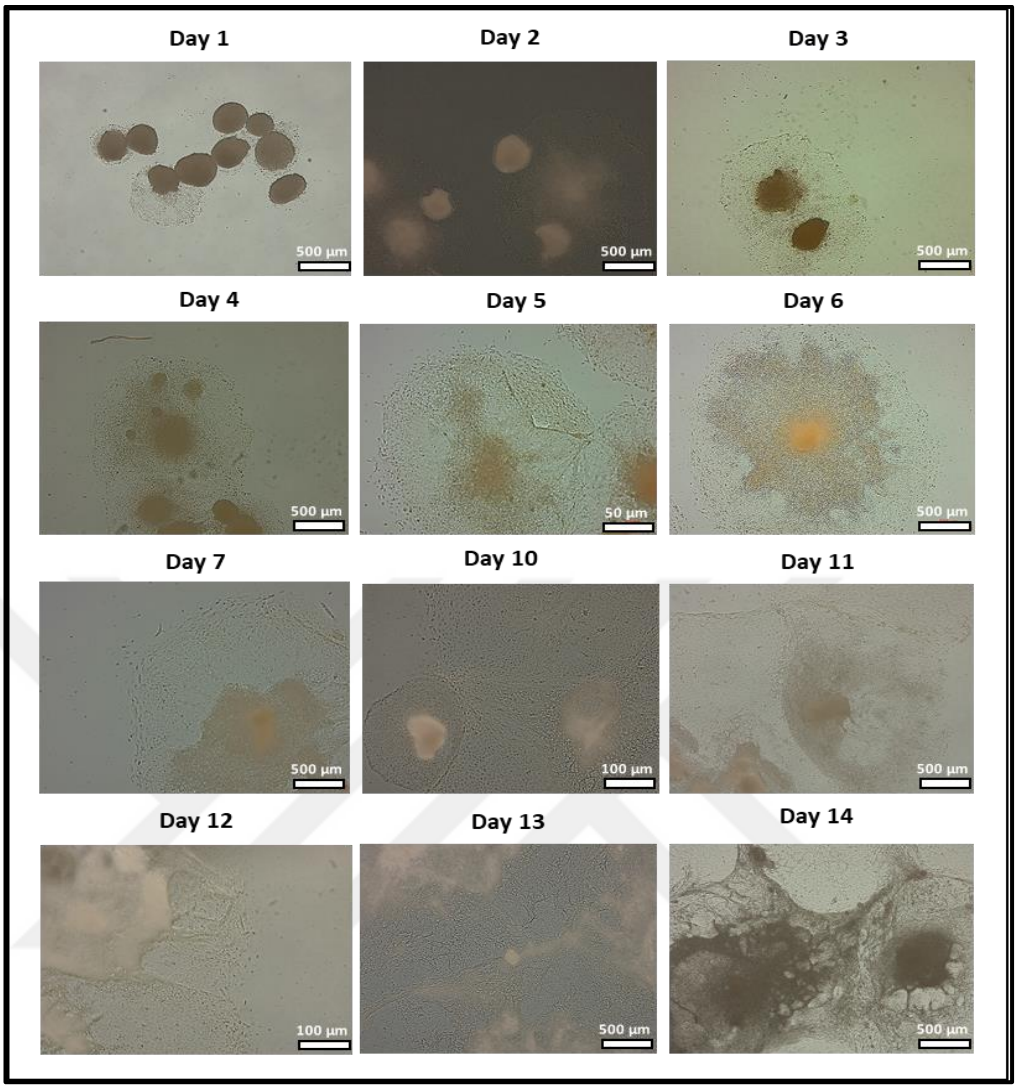

Figure 3.15. C4p25 Embryoid body spontaneous differentiation

In the context ofembryoid body (EB) formation, markers such as AFP, Brachury and FGF5 are important indicators of differentiation into the three germ layers (endoderm, mesoderm and ectoderm), respectively. Each of these markers reflects the commitment of cells to specific lineages during the differentiation process. AFP represents endodermal differentiation. Brachyury represents mesodermal differentiation. FGF5 represents ectodermal differentiation. These markers are critical in monitoring how embryoid bodies spontaneously differentiate into different germ layers during in vitro development, ensuring the proper formation of tissues that represent early embryonic development**. Figure 3.16** shows the qPCR results. Normalized AFP, Brachury and FGF5 expressions are significantly increased.

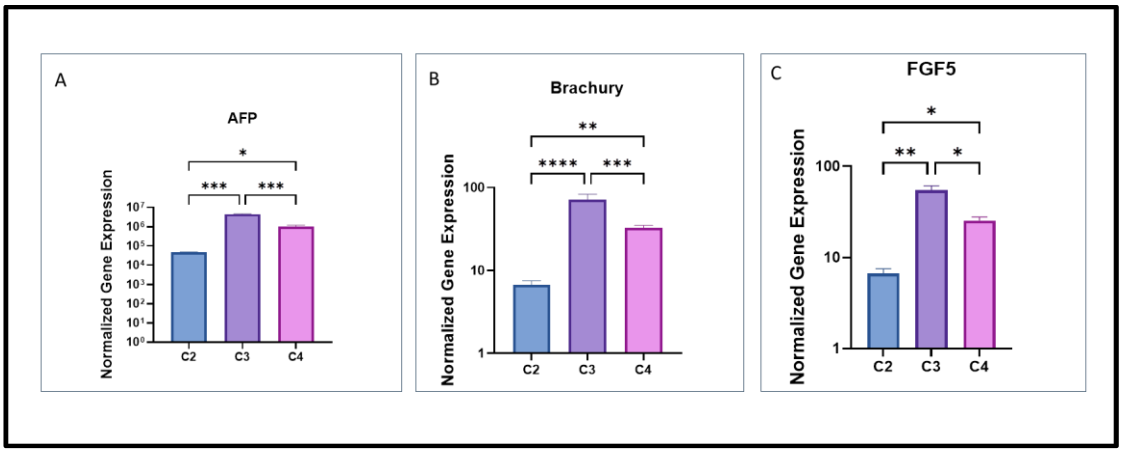

Figure 3.16. qPCR Results for EB Formation (A. AFP Expression, B. Brachury Expression and C.FGF5 Expression. Results were analyzed using GraphPad Prism (9.0.0). Two-way ANOVA test was used and significance level was accepted as $p<0.05$)

To support the qPCR results, the results of spontaneous differentiation staining of EBs (A. DAPI, B. DAPI +AFP, C. DAPI +FGF5, D. DAPI +Brachury) **Figure 3.17** are shown.

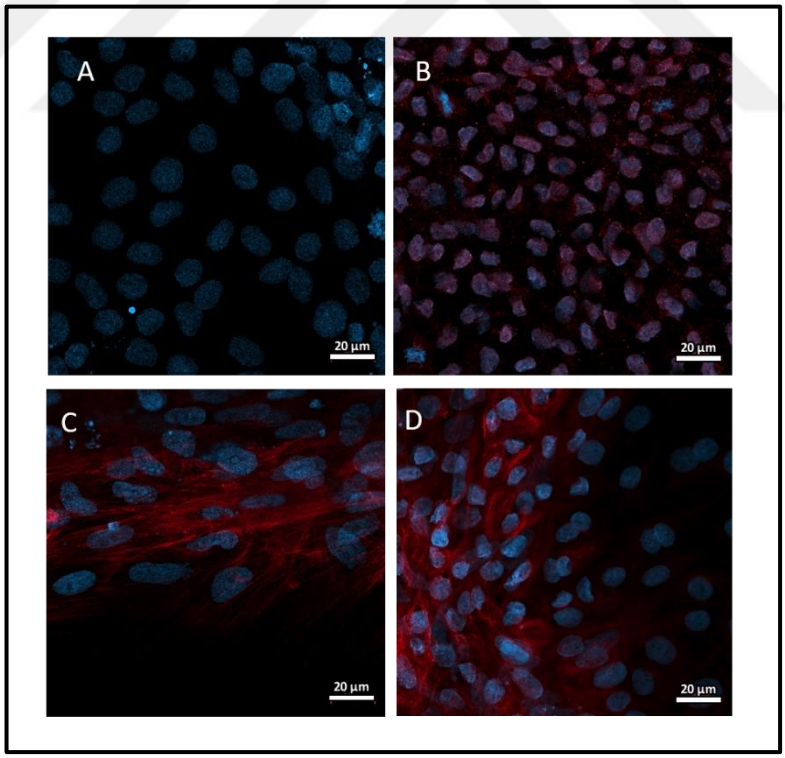

Figure 3.17. C4p25 EB Spontan Farklılaşma, 20X (A. DAPI, B. DAPI +AFP, C. DAPI +FGF5, D. DAPI +Brachury)

3.3.5. iPSC Culture for Neural Differentiation

iPS cells were used as a source for neural cell differentiation. The neural differentiation protocol was applied by culturing and propagating iPS cells **Figure 3.18**.

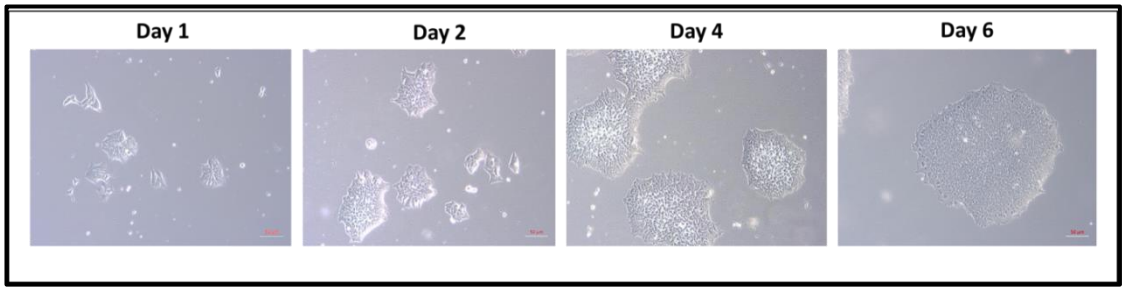

Figure 3.18. iPS culture light microscopy images

After iPS cultures were obtained, the final differentiation kit protocol was applied. According to this protocol, iPS cells were treated with induction medium for 7 days **(Figure 3.19)**.

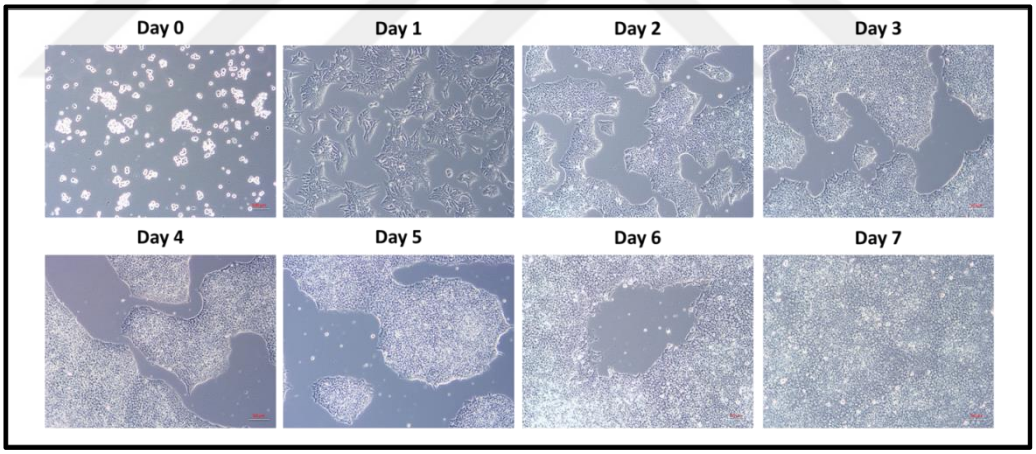

Figure 3.19. iPS cells exposed to induction medium for 7 days

After 7 days, the induced iPS cells were removed from the plate, washed, reseeded and treated with expantion medium **Figure 3.20**.

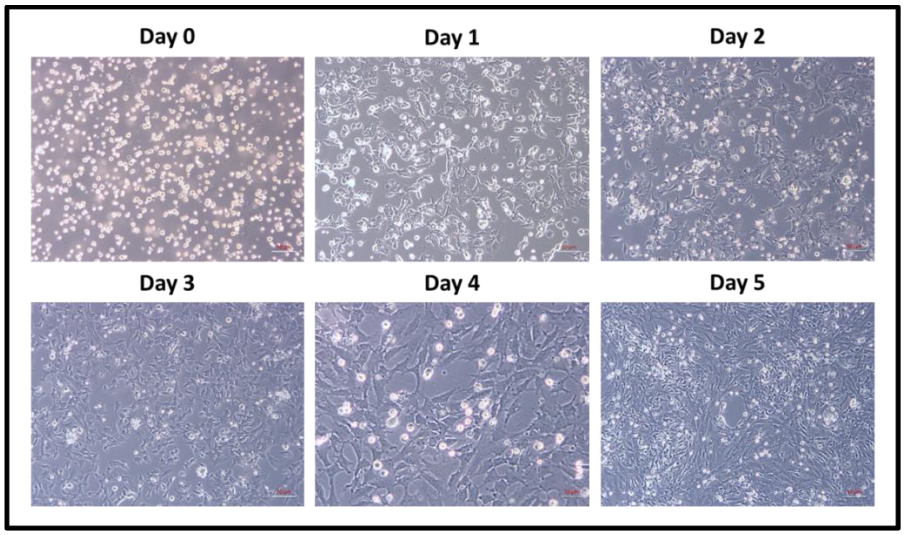

Figure 3.20. Light microscopy image of cells differentiating from iPSC into neural stem cells

3.3.5.1. iPSC Derived Neural Differentiation Characterization

Gene Expression (qRT-PCR)

Neural stem cells differentiated from iPSC were treated with electricity and MQD. At the end of the 21-day experiment, neural markers were analyzed by PCR. On day 21, a significant increase was observed in nestin and b-Tubulin III markers in the electrically treated group **Figure 3.21**.

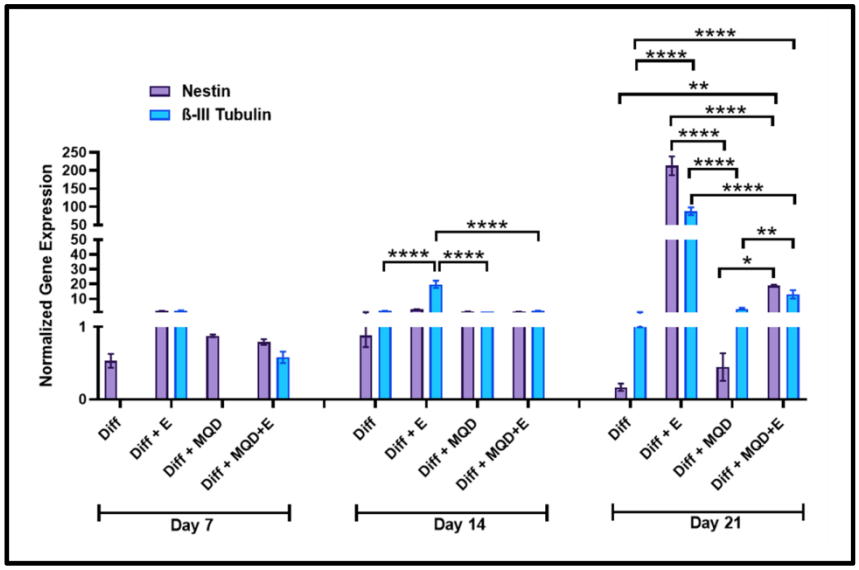

Figure 3.21. Real-time PCR analysis of iPSC-derived neural stem cells at days 7, 14 and 21 after treatment with MQD and electric current. Gene expression levels were calculated and normalized to the control group $p<0.05$

Live-Dead

Neural stem cells differentiated from iPSC were treated with electricity and MQD. During the 21-day experiment, Live-Dead staining was performed to determine whether these cells could survive. According to the results of this staining, a decrease in the number of viable cells was observed in the groups treated with electricity **Figure 3.22**.

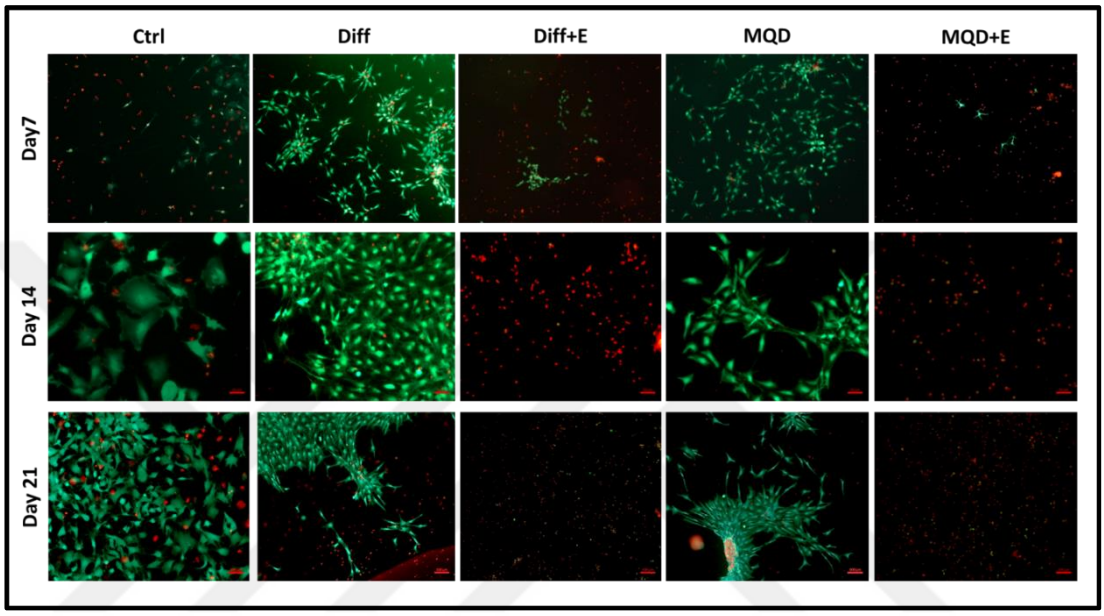

Figure 3.22. Live-Dead staining image of neural stem cells differentiated from iPSC

Immunofluorescent staining was performed to prove neural marker expression of neural stem cells differentiated from iPSC. According to this staining result, the cells were found to express neural protein **Figure 3.23**.

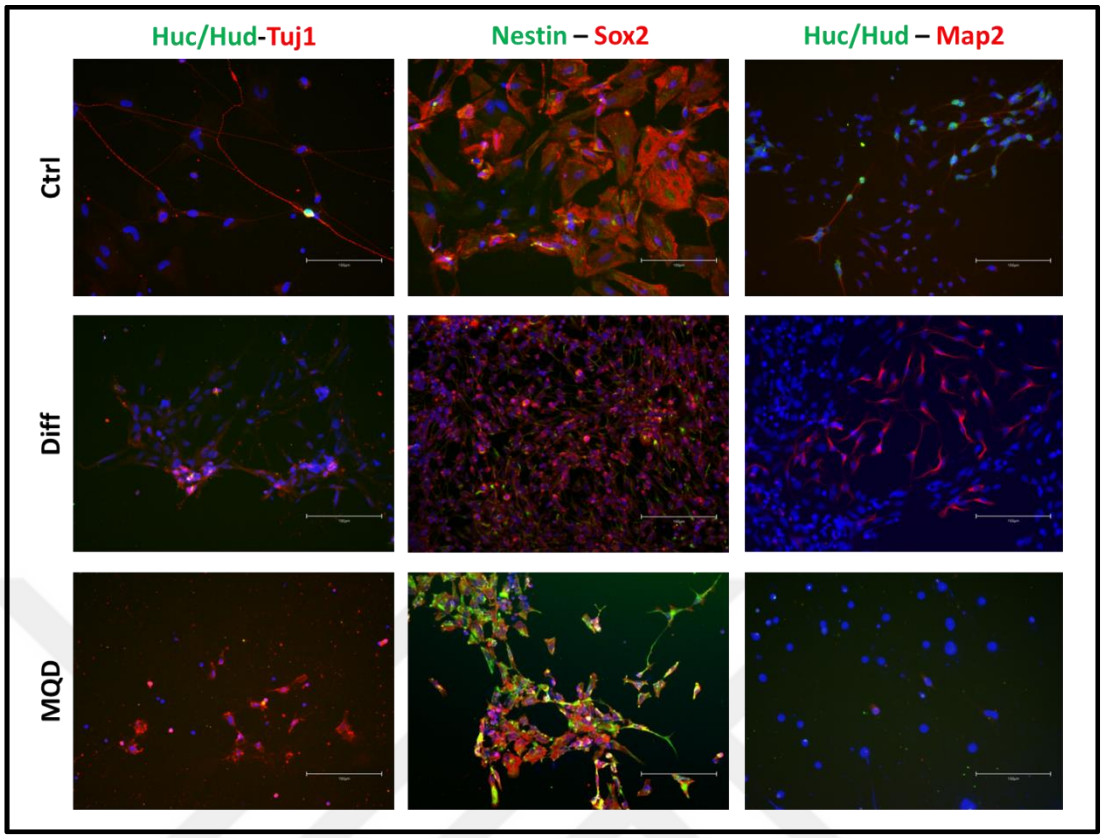

Figure 3.23. Immunofluorescent staining image of neural stem cells differentiated from iPSC

3.4. Nanomaterials Treatment and Cytotoxicity Test

Single iPS cells (5,000 cells/well) were seeded in a 96-well plate. After overnight incubation, cells were treated with MQD material at concentrations of 2.5, 5, 10, 20, 50, 100 ug/mL for 4 hours. LDH assay (Thermo) was performed at 24 hours according to kit instructions. A graph showing the percentage of cell viability was then plotted. According to this graph, the MQD material was found to be non-toxic **Figure 3.24**.

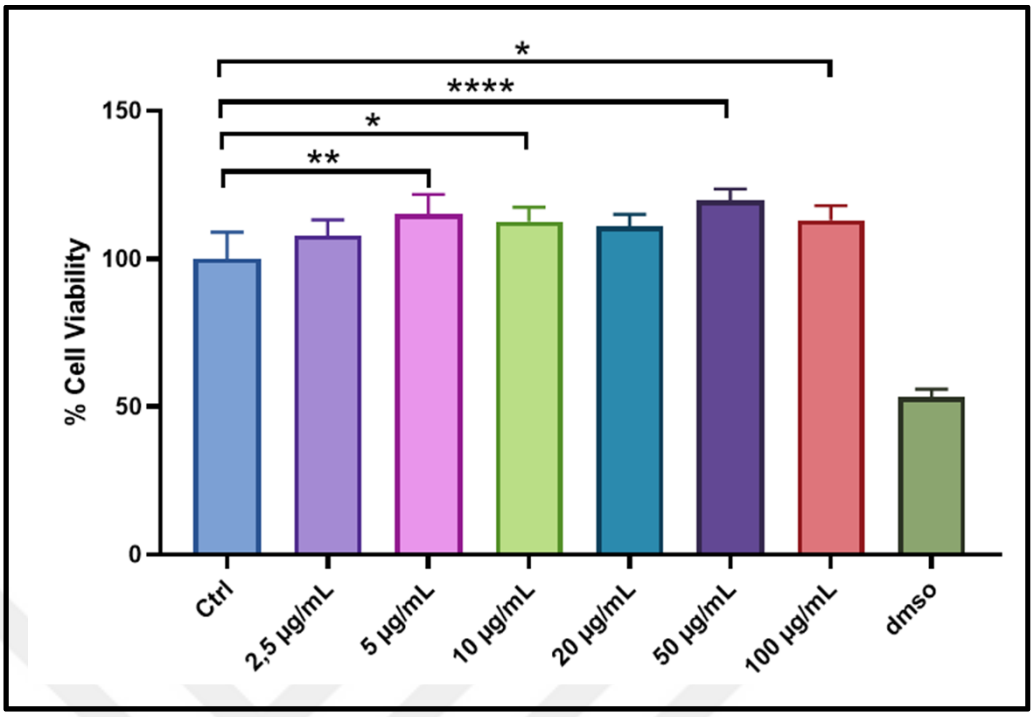

Figure 3.24. Cell viability analysis of iPS cells 24 hours after treatment with MQD. Normalized to control group $p<0.05$

3.5. 3D-Bioprinting Processes

3.5.1. Determination of the Effect of sGO and Electric Current Application on the Viability of Scaffolds Cultured with Mesenchymal Stem Cells by Live-Dead Staining Analysis

Non-toxic live-dead staining was performed to determine cell viability and mortality. Medium was removed; cells and scaffolds were washed with PBS. Cells and scaffold were then treated with the mixture from the Thermo-LIVE/DEAD Cell Viability Assay kit for 30 min at room temperature and visualized under an EVOS fluorescence microscope. Live and dead cell density was calculated. Accordingly, at the end of 14 days, a decrease in the number of viable cells was observed in the sGO and electrically treated groups **Figure 3.25**.

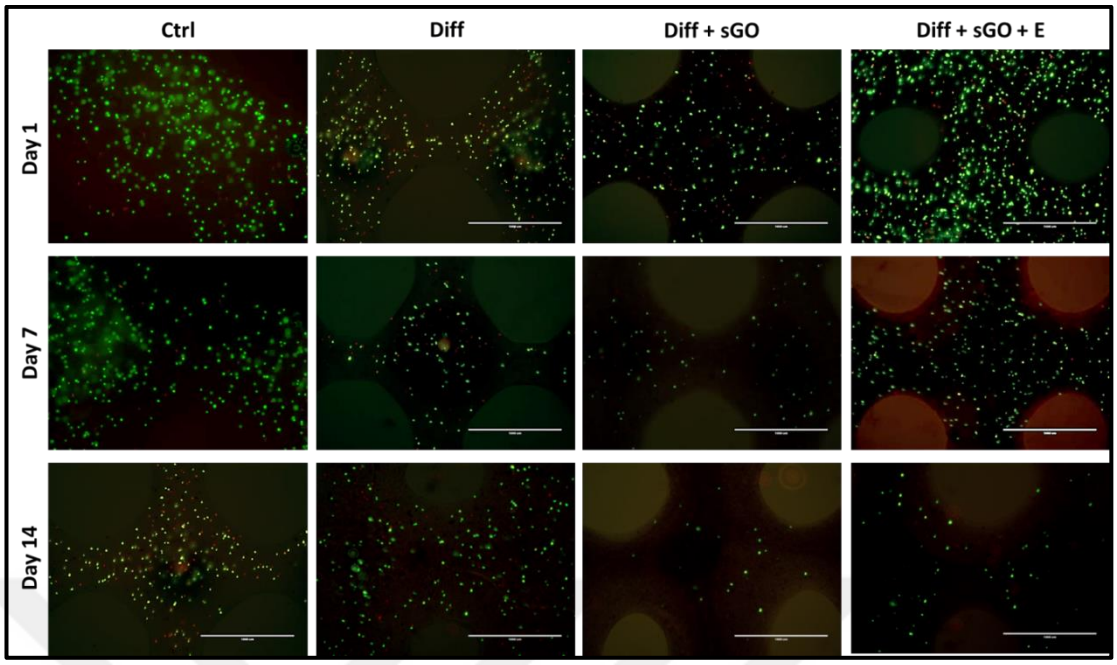

Figure 3.25. After 14 days, Live-Dead staining image of sGO and electrically treated scaffolds analyzing the number of viable cells

3.5.2. Determination of the Effect of sGO and Electric Current Application on Neural Markers in Scaffolds with Mesenchymal Stem Cells by Gene Expression (qRT-PCR) Analysis

Neural stem cells differentiated from MSCs were treated with electricity and sGO. At the end of the 14-day experiment, neural markers were analyzed by PCR. At the end of the 14th day, a significant increase in nestin and b-Tubulin III markers was observed in the electrically treated groups compared to the other groups **Figure 3.26**.

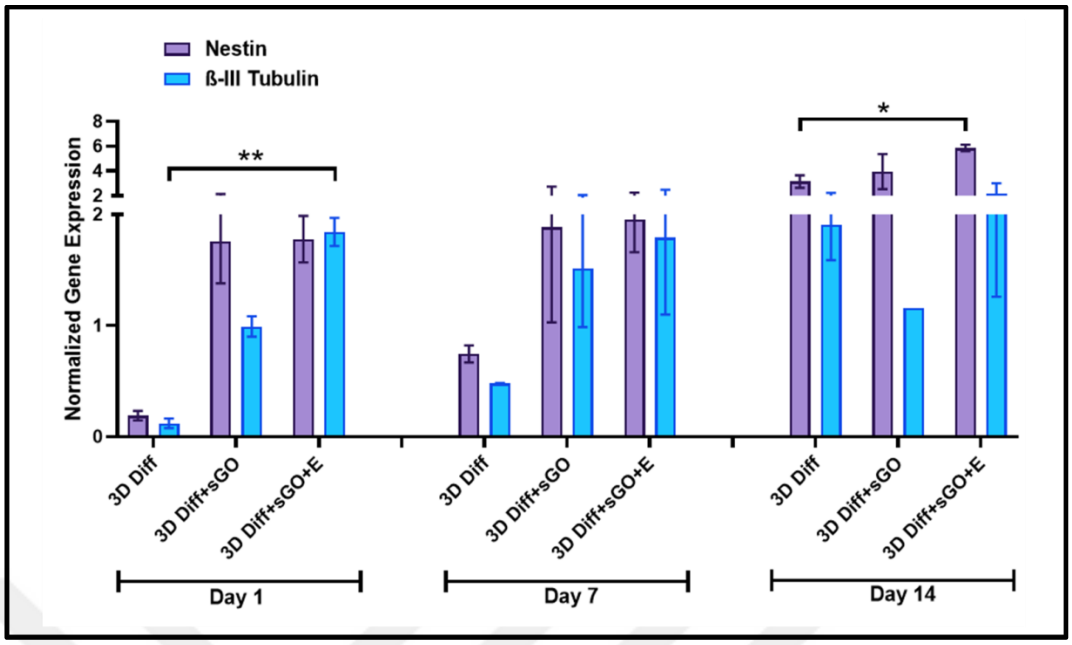

Figure 3.26. Real-time PCR analysis of MSC-derived neural stem cells isolated from scaffold on days 1, 7 and 14 after treatment with sGO and electric current. Gene expression levels were calculated and normalized to the control group $p<0.05$

3.5.3. Determination of The Morphological Properties of Neural Stem Cells Using Scanning Electron Microscope on Scaffolds

Scaffolds were printed with neural stem cells differentiated from iPSCs. They were treated with electricity, MQD and magnetic field. At the end of the 21-day experiment, SEM analysis was used to closely visualize the presence of neural cells in and on the scaffolds. According to the results, neural cells are thought to be present in the samples exposed to the magnetic field **Figure 3.27**.

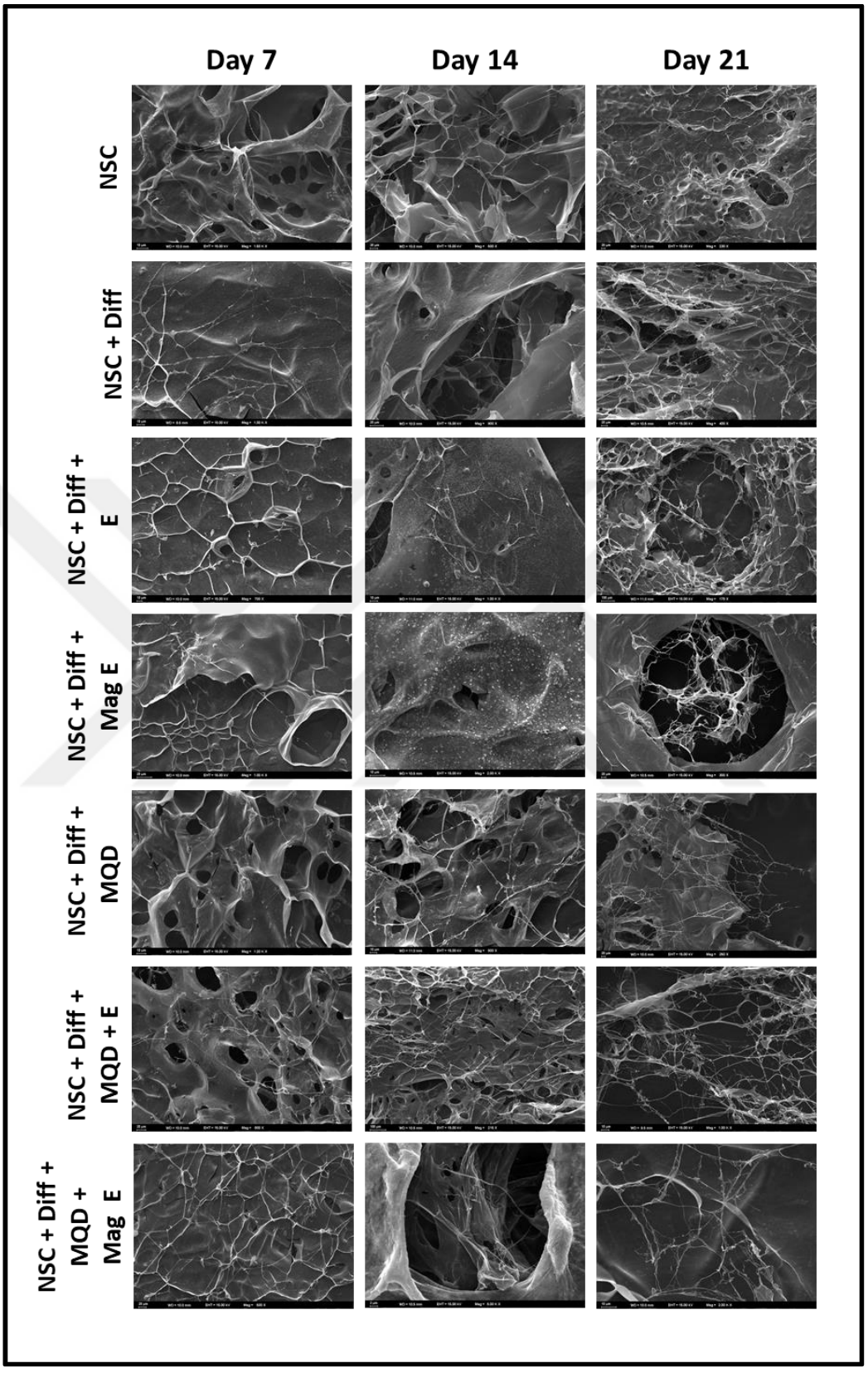

Figure 3.27. SEM images of scaffolds printed with neural stem cells

3.6. Animal Experiment Test Results

3.6.1. BBB Locomotor Test Results

A transparent plastic box with a non-slip floor was prepared for the BBB test. In this box, healthy animals and spinal cord injured animals were allowed to move freely before and after the operation to evaluate locomotor results. Two observers evaluated hind limb grasping skills, joint movements, paw placement, weight support and front/back limb coordination according to the BBB locomotion scale of 0-21 points for 4 min and were recorded on video at the same time. The BBB test was repeated every 2 weeks during the 8-week experiment. The assessment of functional motor recovery is thought to be an indicator of regeneration of the lesioned spinal cord. As a result of these observations, a score between 0-21 was made and comparison between the groups was made. According to these results, at the end of the 8th week, there was a significant increase in the BBB score of the group with spinal cord injury and exposed to MQD and electrical stimulation with neural stem cells **(Figure 3.28)**.

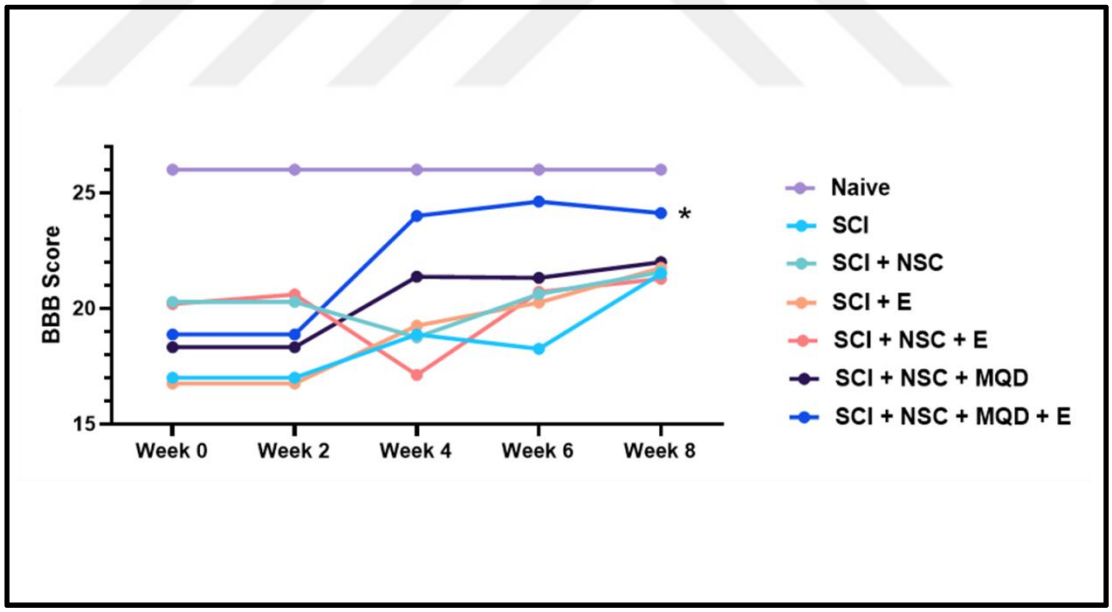

Figure 3.28. Analysis of the evaluation of functional motor recovery with the BBB score test

3.6.2. Hot Plate Locomotor Test Results

In the hot plate test, which measures pain response, the plate was heated to 58°C and fixed. This test was performed before and 1 week after spinal cord injury. The hot plate test was performed before and 1 week after spinal cord injury and was performed every 2 weeks during the 8-week experiment. The stopwatch was started as soon as the rat was placed on the hot plate and stopped when the rat showed jumping or hind paw licking behaviour. The time between the start and end was recorded. This time was compared between healthy animals and animals with spinal cord injury and behavioural movements related to recovery from spinal cord injury between groups were interpreted. Accordingly, at the end of the 8-week experiment, the group with spinal cord injury and exposed to neural stem cells, MQD and electrical stimulation showed significantly faster pain response than the other groups **Figure 3.29**. At the end of 8 weeks, the pain response rate of this group approached the pain response rate of the healthy group.

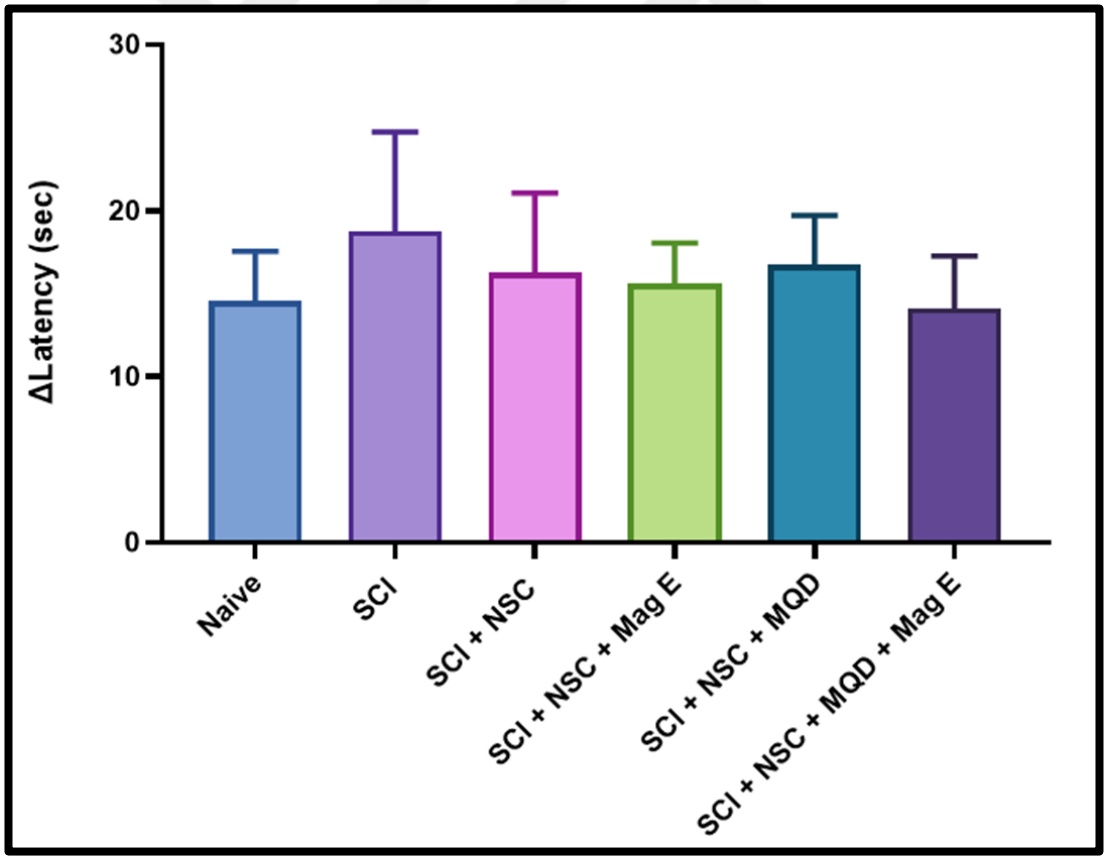

Figure 3.29. Analysis of hot plate test showing pain response

3.6.3. Electromyographi (EMG) Measurement Results

EMG measurements were recorded using LabChart at the end of the 8th week for each animal in the treatment group. Before EMG, the animals were anaesthetised using ketamine cocktail. Afterwards, the dorsal region of each animal was shaved. To obtain precise and reliable measurements, a surgical incision was made in the area between the shoulder blades starting 2 cm above the affected thoracic level (T7-T10). The measurement electrodes were placed above and below the incision, while the ground electrode was glued to the animal's tail and the animals were stimulated at the apex of the incision. In the LabChart interface, a filter was applied in the frequency range of 50-2000 Hz according to the information obtained from the literature. The pulse height was set to 4 V and the animals were subjected to repeated shocks at 0.1 s intervals **Figure 3.30**.

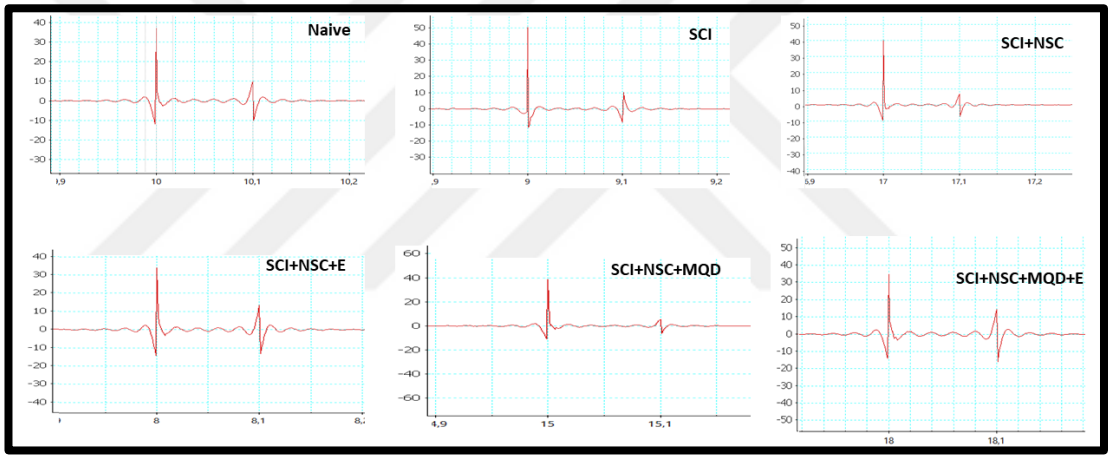

Figure 3.30. Peak image of the shock repeated at 0.1 s intervals to the experimental groups in the LabChart interface

The peak analysis feature of LabChart was used to analyse all responses in terms of peak amplitude and frequency. Accordingly, at the end of the 8-week experiment, the EMG frequency of the group with spinal cord injury and exposed to neural stem cells, MQD and electrical stimulation increased significantly compared to the EMG frequency of the healthy group **Figure 3.31**.

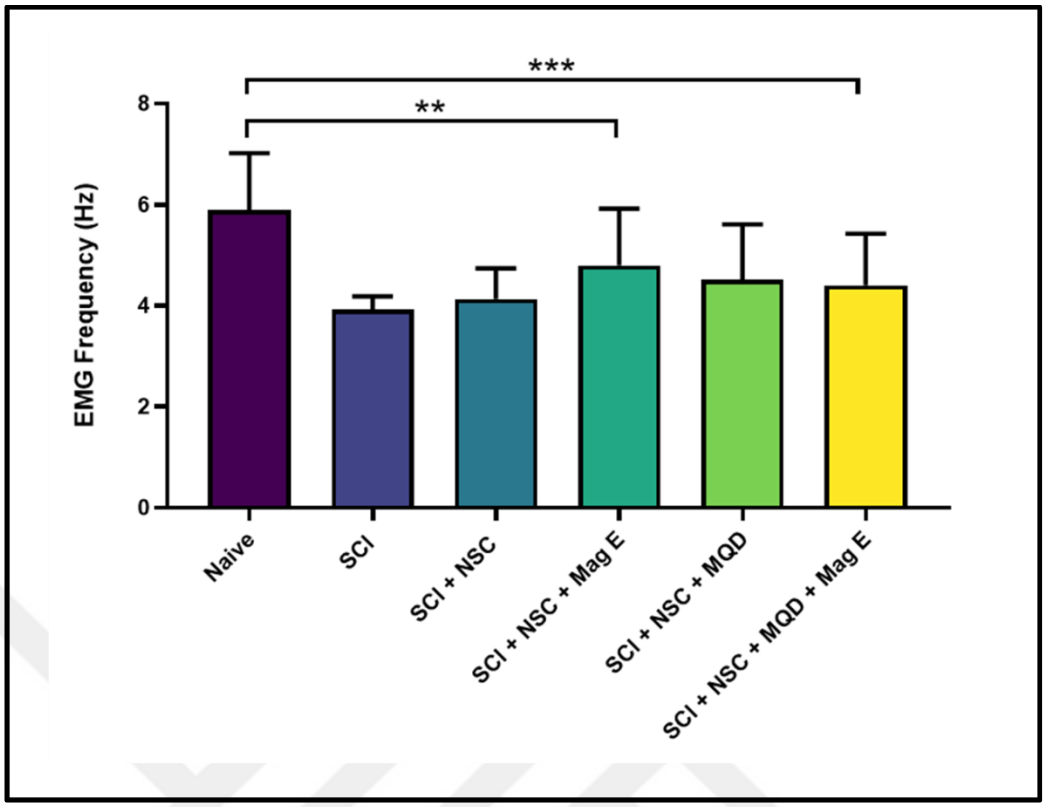

Figure 3.31. Analysis of the EMG frequency of the experimental groups by analyzing all responses in terms of peak amplitude and frequency using the peak analysis feature of the LabChart interface

3.6.4. Immunofluorescence Staining of Spinal Cord Tissue Obtained From Rats

The presented immunofluorescence images show the expression of key neural markers in spinal cord tissue sections following different treatment conditions. The analyzed markers include β-III Tubulin (B-III Tub, red) and S100 (green) for neuronal and glial identification, HuC/HuD (green) for neuronal cell presence, and MAP2 (red) and GFAP (green) for mature neurons and astrocytes, respectively. DAPI (blue) was used to stain cell nuclei, providing an overview of the overall cellular distribution within the spinal cord tissue. β-IIITubulin (B-III Tubulin) expressionβ-III Tubulin, a marker for immature neurons and neural differentiation, is observed at varying levels across sections **Figure 3.32**.

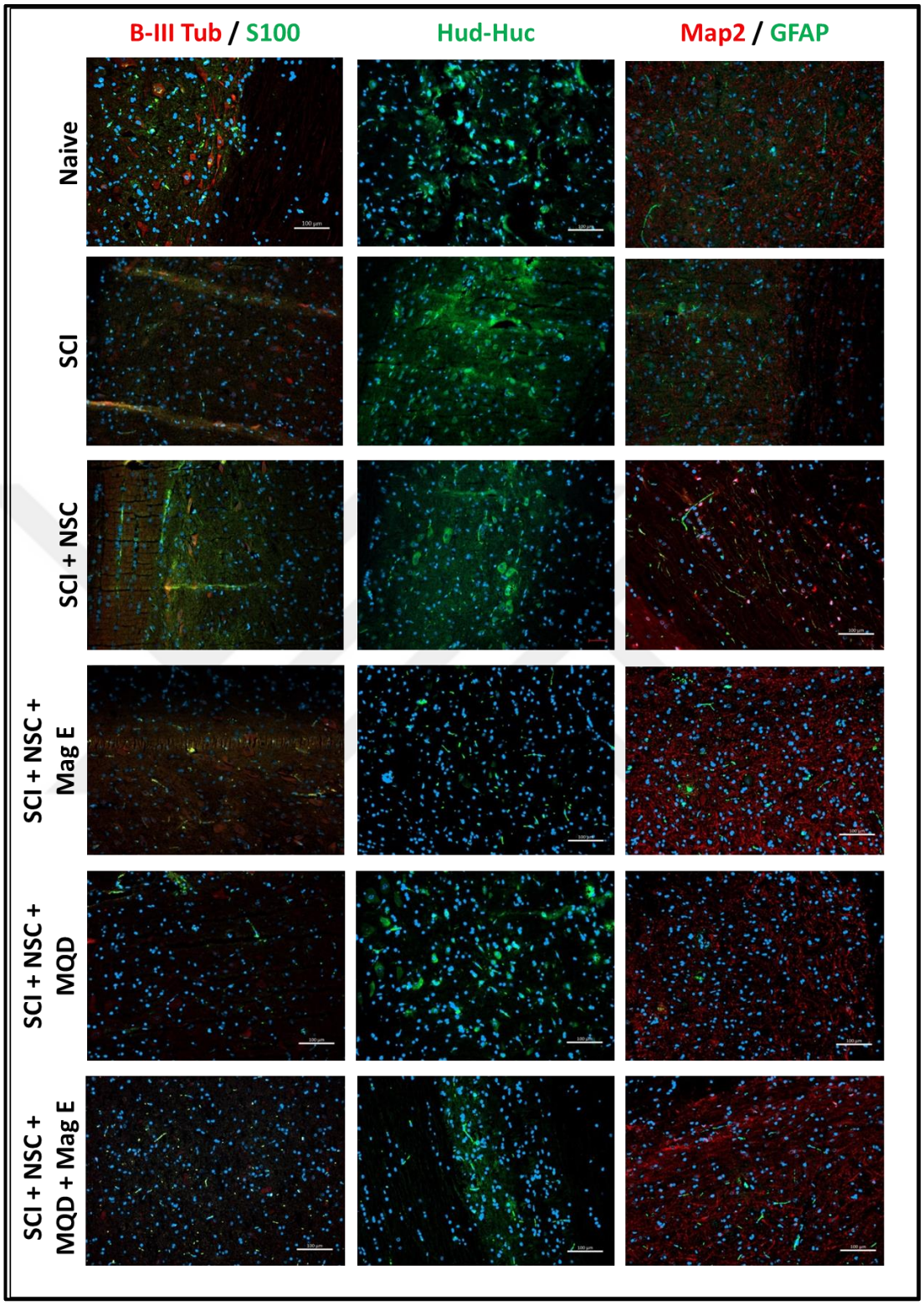

Figure 3.32. Immunofluorescence image of spinal cord tissue obtained from rats

4. DISCUSSION

Spinal cord injury (SCI) is a life-changing condition that affects millions of people worldwide. The global impact of SCI is significant, not only in terms of personal and family struggles, but also because of its economic burden on health systems and societies. It is estimated that between 250,000 and 500,000 people worldwide suffer a spinal cord injury each year. Exact figures may vary due to under-reporting and variability in the quality of data collection in different countries. Research suggests that the prevalence of spinal cord injury worldwide is between 40 and 80 cases per million people per year (Safdarian et al., 2023). The majority of new cases of spinal cord injury occur in young people between the ages of 16 and 30 (Chen et al., 2013). Spinal cord injury has a profound impact on the quality of life of those affected. People with spinal cord injury often experience significant physical and mental health problems, such as chronic pain, loss of bladder and bowel control and sexual dysfunction. The psychological impact can be equally severe, with many patients suffering from depression, anxiety and social isolation due to their physical limitations(Budd et al., 2022; Strøm et al., 2022) . The economic burden of SCI is also great. The cost of long-term care, rehabilitation and specialized medical equipment can be very high for both individuals and their families. In countries with inadequate health insurance, this often leads to financial hardship (Malekzadeh et al., 2022). In recent years, medical advances have improved the outlook for spinal cord injury patients. Treatments such asspinal cord stimulation, stem cell therapy and robotic exoskeletons show promise in helping patients regain some level of function or mobility. While these technologies are still in the experimental stage, they hold promise for the future of spinal cord injury recovery (Zeng, 2023). Research into nerve regeneration and neuroplasticity also has the potential to develop treatments that could eventually reverse the effects of spinal cord injury (Costăchescu et al., 2022; Punjani et al., 2023).

With millions affected worldwide, SCI has led to an urgent need for innovative therapies to improve outcomes for spinal cord injury patients. While traditional treatments focus on managing symptoms and preventing further damage, stem cell therapies have emerged as a promising frontier in regenerative medicine. Two of the most studied stem cell types for SCI are mesenchymal stem cells (MSCs) and induced pluripotent stem cells (iPSCs). Both offer exciting possibilities to repair spinal cord injury, potentially restoring lost function and improving recovery (Rahimi Darehbagh et al., 2024). Spinal cord injuries

cause damage to the nerves and tissues that transmit signals between the brain and the rest of the body. The result is loss of sensation, movement and autonomic functions below the level of injury. Unfortunately, the spinal cord has a limited ability to heal itself due to the complex structure of neurons and surrounding glial cells.

When the spinal cord is injured, a series of events occur. Primary damage causes direct destruction of neurons and glial cells. Secondary damage is exacerbated by a wave of inflammation, cell death and scarring in the hours and days following the injury. This further impairs the spinal cord's ability to repair itself. Stem cell therapies aim to intervene in both the primary and secondary damage stages, offering the possibility of cell replacement, regeneration and reduction of damaging inflammatory responses (Lima et al., 2022; Ortega et al., 2023; Shao et al., 2019).

MSC therapies are attractive because of their immunomodulatory properties . They can reduce inflammation and help the body's immune system to better respond to injury. Their ability to localize to injury sites and secrete factors that promote healing makes them ideal candidates for the treatment of spinal cord injuries (Fan et al., 2020). MSCs are primarily used to treat SCI due to their ability to secrete growth factors and anti-inflammatory molecules that help create a more favorable environment for recovery. They do not necessarily replace lost neurons but work by reducing inflammation, promoting tissue repair and neural survival. MSCs modulate the immune response, which can help minimize the secondary damage (inflammation) that occurs after an SCI. MSCs can stimulate surrounding cells to regenerate or repair themselves (promoting tissue repair). By creating a protective environment around the injury, they promote neuron survival and prevent further degeneration (Kim et al., 2021; Pang et al., 2023). Studies have shown that MSC transplantation can improve motor function and reduce scar formation that otherwise hinders recovery. Researchers are still investigating how to improve the ability of MSCs to directly replace damaged spinal cord cells, but their supportive role in recovery is well documented (Montoto-Meijide et al., 2023).

Induced pluripotent stem cells (iPSCs) are adult cells that have been genetically reprogrammed to revert to an embryonic stem cell-like state. This means that iPSCs are pluripotent, able to differentiate into any cell type in the body, including neurons and other cell types critical in spinal cord repair (Ye et al., 2013). iPSCs are created by adding specific genes to a mature cell (such as a skin cell) and “rebooting” it into a pluripotent state. The

major advantage of iPSCs is that they can be produced from the patient's own cells, reducing the risk of rejection by the immune system when used for treatments (G. Wang et al., 2022). iPSCs have great potential for treating SCI due to their capacity to regenerate neural tissue. By replacing damaged cells in the spinal cord, iPSCs can help restore lost functions and facilitate neural repair (Khazaei et al., 2014). Unlike MSCs, iPSCs offer the potential for direct neuronal replacement. Because iPSCs can develop into any cell type, they can be programmed to become neurons, oligodendrocytes (cells that form myelin around neurons) or astrocytes - all critical components in the spinal cord (Albert et al., 2021; Khazaei et al., 2014). iPSCs can help SCI recovery by replacing damaged neurons, restoring myelination, supporting synaptic connectivity. iPSCs can be differentiated into motor neurons or sensory neurons to replace those lost due to injury. They can enhance signal transmission in the damaged spinal cord by producing oligodendrocytes that help remyelinate (re-coat) axons. iPSCs can help form new neural connections that are essential for regaining motor and sensory functions (Hu et al., 2023; Khazaei et al., 2014; Li et al., 2024; Punjani et al., 2023).

Despite advances in medical treatments, there is still no fully effective therapy to repair damaged spinal cords. But recent advances in 3D bioprinting have raised hopes in the field of regenerative medicine. 3D bioprinting, the latest technology that enables the fabrication of complex biological structures, offers the potential to create personalized, functional tissue replacements for patients with spinal cord paralysis. Scientists aim to utilize this technology to repair damaged spinal cord tissues, potentially improving outcomes for those suffering from paralysis and other serious consequences of SCI (Kim et al., 2024).

3D bioprinting is an innovative process that involves the precise layer-by-layer creation of biological tissues using bio-inks composed of living cells, growth factors and biomaterials. Much like traditional 3D printing, where plastic or metal is deposited to create three-dimensional objects, bioprinting uses biological materials to print structures that mimic the tissues and organs of the human body. These printed tissues can act as scaffolds for cells to grow, regenerate and eventually integrate with the body's existing structures (Ghosh, 2024; Gu et al., 2020; Vanaei et al., 2021).

In the field of regenerative medicine, 3D bioprinting offers an unprecedented opportunity to create personalized tissue constructs that can replace damaged or lost tissues. The goal for SCI is to use bioprinting technology to develop functional nerve tissues that can integrate with the injured spinal cord and restore its ability to transmit signals between the

brain and the rest of the body. Bioprinting allows researchers to by precisely printing scaffolds that resemble the architecture of the spinal cord, bioprinted tissues can support the regeneration of neural networks. Bioprinted tissues can be tailored to each patient's specific injury, increasing the chances of successful integration and recovery. Printed scaffolds provide an environment that supports the growth of neural cells and promotes tissue repair (Liu et al., 2021).

The success of 3D bioprinting largely depends on the choice of biomaterials used to create the scaffolds. These materials, often referred to as bio-ink, must be biocompatible to allow cells to grow and function while providing the necessary structural support. The ingredients of common materials can be listed as follows. Hydrogels (water-based materials) can be loaded with cells and provide a soft, flexible environment similar to that of natural tissues. Extracellular matrix (ECM) materials are the natural scaffolding that surrounds cells in the body and using ECM-derived materials can promote better cell integration and function. Somebioprinting applications use synthetic materials that can be engineered to degrade over time as natural tissue regenerates (Chen et al., 2023). The choice of biomaterials is critical as materials need to support both cell growth and neural function, which is particularly challenging in spinal cord applications.

Spinal cord injuries (SCI) represent one of the most complex and challenging medical conditions to treat. Current therapies primarily focus on managing symptoms and limiting further damage, but few offer the possibility of reversing the injury or promoting significant neural regeneration. This is where nanotechnology has begun to offer new hope. Nanomaterials, due to their unique properties, have shown great potential in aiding spinal cord repair and regeneration. By interacting at the cellular and molecular levels, nanomaterials can target the specific needs of injured tissues, promote neural repair, reduce inflammation and deliver therapies directly to damaged areas. These properties make nanomaterials ideal candidates for medical applications, particularly regenerative medicine and tissue engineering. In regenerative medicine, nanomaterials are used to repair or replace damaged tissues and promote the body's natural healing processes. For SCI, nanomaterials can provide structural support to damaged areas, promote the growth of new neurons, deliver therapeutic agents and even modulate the immune response to reduce harmful inflammation. Their small size and customizable properties allow nanomaterials to interact with cells at the molecular level, which is essential for the complex task of spinal cord repair (Engel et al., 2008; Han et al., 2023).

Nanomaterials have the potential to promote spinal cord repair through several key mechanisms. First, nanomaterials can provide a scaffold or framework that supports and guides the growth of new nerve cells (neurons). These scaffolds mimic the natural environment of the spinal cord, encouraging neurons to elongate and reconnect with each other. Secondly, inflammation is a major challenge after SCI, as it can cause further damage. Nanomaterials can be designed to reduce inflammation by controlling the release of anti-inflammatory molecules or targeting immune cells to prevent excessive immune reactions. Third, one of the most promising uses of nanomaterials is their ability to deliver drugs, growth factors or other therapeutic molecules directly to the site of injury. For example, nanoparticles can be designed to cross the blood-spinal cord barrier, a natural barrier that often limits the effectiveness of conventional drug therapies (Aljabali et al., 2023; Hersh et al., 2022; Kaplan & Levenberg, 2022).

As summarized above, SCI is a disease that affects millions of people, has no complete treatment and has a heavy economic burden. Different studies are being tried in the literature for SCI, for which traditional medicine is currently helpless. In this PhD thesis, we aimed to address neural regeneration with a multidisciplinary approach. Neural stem cells differentiated from MSC, human NSC and human iPS cells were treated with neural growth factors and different nanomaterials and differentiated into neural cells in 2D culture medium. At the same time, a bioink containing neural stem cells and nanomaterials was used to create a scaffold from a 3D bioprinter and cultured with neural growth factors. Electric current was applied to both 2D and 3D cultures to increase the potential for neural differentiation. Thus, the effect of electrically conductive nanomaterials on neural differentiation was investigated and these scaffolds were used in rats with SCI. The results obtained are discussed below.

Initially, mesenchymal stem cells obtained from adipose tissue were tried to be differentiated with homemade neural differentiation media. For this, homemade medium was prepared in two steps. As a control group, only standard growth medium was given to the MSCs. In the first stage, induction medium was used and mesenchymal stem cells were cultured in this medium for 7 days. At the end of 7 days, we switched to differentiation medium. At this stage, sGO and 1mA electric current were applied to certain groups. This application continued for 14 days with differentiation medium. At the end of 14 days, live-dead, gene expression and protein expression of MSCs were analyzed. In the live-dead image of MSCs obtained from 2D culture, a decrease in viability was observed in the (differentiation medium + sGO + electric current) group. This decrease in the number of

viable cells was interpreted as the cells that could not differentiate into neural cells died and moved away from the medium, while the cells that could differentiate into neural cells remained alive and continued in culture. The remaining viable cells became morphologically thinner and longer compared to the control group, as previously shown (Lo Furno et al., 2018).

Neural cell markers were analyzed in gene expression analysis of MSCs obtained from 2D culture. On days 1, 7 and 14, the expression level of each gene was determined according to the reference GAPDH gene by qRT-PCR analysis and normalized to the control group during qRT-PCR analysis. Neural cell markers used were nestin (a neural stem cell marker) and b-III-tubulin (critical for neural activity). There was a significant increase in the nestin marker in the electric current treated groups, especially at the end of the 14th day. Based on these data, it was observed that MSCs begin to differentiate into neural cells (Park et al., 2017) and the efficiency of this differentiation is enhanced by the electrical effect.

Immunofluorescent staining was performed on 2D cultures to support qRT-PCR analysis. Primary antibodies for b-III-tubulin and nestin were used as neural markers. After incubation, they were stained using FITC and AF543-labeled secondary antibodies. Immunofluorescence staining clearly shows that cells in the day 14 (differentiation medium + sGO + electric current) group express nestin. It is also observed that the cell morphology becomes thinner and longer in this group compared to the other groups. In these studies (Jang et al., 2010; Khan et al., 2020; Urrutia et al., 2019), it was reported that adipose-derived MSCs can differentiate into neural precursors or mature neurons. Therefore, our data are supported by these studies in the literature.

When it was determined that MSCs could be differentiated into neural precursors, but it was not reproducible, cell lines with more efficient differentiation potential than MSCs were tested for more efficient and novel experiments planned later in this thesis. For this purpose, commercially purchased human neural stem cells (HNSCs) were differentiated to obtain neurons. However, the desired cell density could not be obtained from the culture of these HNSCs purchased in spheroid form. HNSCs were excluded from this thesis as sufficient cell numbers could not be obtained for future studies. Instead, it was decided to try human iPS cells, which have both high differentiation potential and high cell number.

PBMC cells isolated from blood were subjected to programming with Sendai viruses carrying OKSM programming factors (Sharma et al., 2018). After transduction, the cells started to attach to the surface. After about 10-15 days colonies started to form. These have the characteristics of typical pluripotent stem cell colonies mentioned in the literature: large nuclei, small cells, shiny colony wall. On days 15-20 of transduction, when the colonies were large enough to be picked, picking was performed under a microscope. To ensure colony multiplication, colonies were selected and a certain number of stock nitrogen was replicated from each colony. In parallel with the replication process, characterization studies were started. In order to prove the presence of viral transduction, it was analyzed whether the genes were expressed in the cells with the primer sets specified in the kit. For this purpose; total RNA was isolated from cells collected on the 2nd day following transduction and cDNA synthesis was performed. The PCR products obtained were run on agarose gel. After transduction, the presence of expression of virus transgenes in RNA isolated PBMC cells was observed and PCR gel image was shown. According to the PCR results obtained from different numbered colonies in the following passage cycles, pluripotency markers (SOX2, Oct4 and Nanog) were expressed. For colony number 4 passaged 16 times, it was analyzed whether the viral vectors were deleted and whether the genes were expressed in the cells with the primer sets specified in the kit. The reduced presence of viral vectors in the cells was demonstrated by analyzing the reduced gene expression of viral vectors.

Following gene expression analysis, the PSC4-Marker Immunocytochemistry Kit was used to confirm that the stem cell population remained pluripotent by confirming the expression of pluripotency markers. Oct4 is a transcription factor crucial for the maintenance of stem cell pluripotency. SSEA-4 is a surface glycoprotein usually expressed in pluripotent cells. TRA-1-60 and TRA-1-81 - surface markers associated with undifferentiated pluripotent stem cells (Sharma et al., 2018). Cells from the 4th colony, passaged 18 times and stained with the PSC4-Marker Immunocytochemistry Kit, were shown to express pluripotent genes of iPS cells derived from stained iPSC colonies. Alkaline phosphatase staining, which is commonly expressed in undifferentiated cells (such as iPSC), allowed for confirmation of pluripotency and non-destructive evaluation. With this method, all colonies were shown to express alkaline phosphatase enzymes, a marker of pluripotency, and the cells retained stem cell-like properties.

iPSCs form embryoid bodies to mimic early embryonic development, promote multi-stage differentiation and test their pluripotent potential. In the context of embryoid body (EB) formation, markers such as AFP, Brachury and FGF5 are important indicators of differentiation into the three germ layers (endoderm, mesoderm and ectoderm), respectively. Each of these markers reflects the commitment of cells to specific lineages during the differentiation process. AFP represents endodermal differentiation. Brachyury represents mesodermal differentiation. FGF5 represents ectodermal differentiation. These markers are critical in monitoring how embryoid bodies spontaneously differentiate into different germ layers during in vitro development, ensuring the proper formation of tissues representing early embryonic development. Based on the results of the qPCR assay, a significant increase in normalized AFP, Brachury and FGF5 expression was observed. The results of spontaneous differentiation immunofluorescence staining of EBs also supported the qPCR results.

Successful derivation and expansion of induced pluripotent stem (iPS) cells to serve as a source for neural differentiation has been achieved. Compact and tightly packed morphology is the hallmark of high-quality pluripotent stem cells. These observations are consistent with previously reported characteristics of iPS cell cultures, including dome-shaped colonies with smooth edges and high nucleus-to-cytoplasm ratios. These features are critical to ensure that the cells maintain their pluripotent state and ability to differentiate into neural lineages. Expansion of iPS cells to this stage is a prerequisite for their directed differentiation into neural lineages. High-quality iPS cells provide a reliable cell source to generate neural progenitors and mature neurons. Ensuring pluripotency of iPS cells at this stage is critical as any loss of stemness could compromise their differentiation potential (Fluri et al., 2012).

In this stage, the progression of neural induction from iPS-derived cells over a period of 7 days was demonstrated using a neural differentiation kit. This stage, known as neural induction, marks the first and critical step in directing pluripotent stem cells towards a neural lineage. The process of neural induction begins with iPS cells exhibiting dense colony-like structures (Day 0), typical of their pluripotent state. As neural induction progresses, marked morphological changes can be observed: 1-3. Days: Cells begin to spread and colony compaction decreases. This stage marks the deterioration of iPS cell morphology as they lose their pluripotency and begin to transition towards neural progenitor-like structures. 4-5. Days: A marked increase in cell-cell junctions and the appearance of neural rosette-like

formations become apparent. Neural rosettes are a hallmark of early neural progenitor cells and indicate the successful initiation of neural lineage commitment. 6-7. Days: Cells exhibit a uniform, flattened morphology with diffuse rosette-like patterns indicating advanced neural induction and a higher degree of neural progenitor cell enrichment. These morphological changes are consistent with previously reported features of neural induction in which iPS cells transition from pluripotent colonies to progenitor-like formations capable of differentiating into neurons, astrocytes and oligodendrocytes (Neaverson et al., 2022).

Gene expression profiles of neural stem cells differentiated from iPS cells after 21 days of treatment with MQD and electrical stimulation are shown by PCR data. The most prominent feature of the graph is that although MQD alone induces some neural marker expression, the levels are significantly lower than those observed in the combined treatment group. The effects of electrical stimulation alone appear to marginally increase differentiation (nestin and b-tub III). These findings are in line with previous studies suggesting that bioelectric cues and compounds such as MQD can act as external signals to drive lineage-specific differentiation by mimicking physiological conditions. MQD may function by enhancing cell signaling pathways or promoting epigenetic modifications that support neuronal gene activation. Electrical stimulation is also known to mimic physiological neural activity, modulating ion channels and intracellular signaling cascades that facilitate neural differentiation. The ability to modulate differentiation through MQD and electrical stimulation is supported by studies showing significant promise for therapeutic applications (Augustyniak et al., 2019; Innamorati et al., 2025).

The viability of neural stem cells (NSCs) differentiated from iPS cells was studied under electrical stimulation and MQD for a period of 21 days. The results revealed significant differences in cell viability between the groups and a significant decrease in viable cells, especially in the groups treated with electrical stimulation for a longer period of time. At Day 7, the majority of cells in all treatment groups exhibited high viability as evidenced by Live-Dead staining. This suggests that NSCs were initially able to tolerate both MQD and electrical stimulation. However, slight increases in red-stained dead cells were observed in the electrical stimulation group, indicating that even at this early stage, electrical currents can cause some degree of cellular stress. By Day 21, the effects of electrical stimulation on cell viability became even more pronounced. The electrical stimulation group exhibited widespread cell death. In contrast, only the MQD group showed sustained survival, while the MQD + electrical stimulation group maintained moderate viability, suggesting that

MQD may partially attenuate the cytotoxic effects of electrical stimulation. The observed results underline the need for careful optimization of electrical stimulation parameters, including intensity, duration and frequency, to balance its differentiation-promoting effects with the maintenance of cell survival. In contrast to the deleterious effects of electrical stimulation, MQD treatment appeared to promote NSC survival throughout the experiment. When combined with electrical stimulation, MQD partially attenuated the cytotoxic effects and improved survival compared to electrical stimulation alone. This suggests that MQD may serve as a protective agent in protocols involving bioelectrical cues (Pires et al., 2015).

Immunofluorescent staining for markers such as HuC/HuD, Tuj1, Nestin, Sox2 and Map2 provides insight into the progression of neural differentiation, highlighting distinct cell populations at various stages of maturation. Staining for HuC/HuD and Tuj1 (β-III tubulin) reveals the presence of mature and immature neurons. Cells with enlarged neurite-like projections were evident, showing cytoskeletal rearrangements required for neuronal connectivity. HuC/HuD expressing cells indicate postmitotic neurons, Tuj1 positivity indicates developing neurons and the formation of cytoskeletal structures necessary for neuronal function. The co-localization of these markers confirms successful neural differentiation with treatments that effectively promote the transition from neural progenitors to neurons. Nestin, a marker for neural progenitors, and Sox2, a pluripotency-related transcription factor, were evaluated to assess the status of progenitor populations. Nestin positive cells were observed, while co-expression of Sox2 suggests that some progenitor cells retain some degree of undifferentiated potential. The presence of Sox2+ cells alongside differentiated populations highlights the heterogeneity within the culture, with some cells not yet fully committed to the neural lineage. The persistence of nestin positive cells suggests the maintenance of a progenitor subpopulation that may provide a reservoir for continued differentiation into neurons or glial cells. Co-staining for HuC/HuD and Map2 (microtubule-associated protein 2) confirms advanced neural differentiation and maturation, but while most cells stain positive for HuC/HuD and Map2, the intensity and distribution of staining indicates some variability in the degree of maturation. This may be due to different responses to the treatments applied or to intrinsic heterogeneity within iPS-derived neural progenitors. Map2 is specifically associated with mature neurons and their dendritic structures. Its expression indicates that cells develop structural and functional properties of mature neurons. Despite heterogeneity, the expression of mature neuronal markers such as HuC/HuD and Map2 indicates the overall success of the differentiation protocol in generating functional neurons. Immunostaining results confirm that iPS-derived neural stem

cells successfully differentiate into neuronal populations with expression of both early and late stage neural markers. MQD treatments were effective in promoting neural lineage commitment and maturation, as evidenced by the expression of HuC/HuD, Tuj1 and Map2. Recent studies in the literature have shown that cell proliferation and differentiation are regulated simultaneously but independently of each other, that cells often begin to differentiate long before they stop dividing, and that the onset of differentiation is not restricted to any part of the cell cycle (Brown et al., 2003). These findings support the reason for the heterogeneity encountered in culture. Despite some heterogeneity, the overall results underline the potential of this differentiation protocol to generate functional neural cells, increasing its applicability in neurobiological research and therapeutic development (Peretz et al., 2016).

The cytotoxic effects of MQD material on iPS cells were assessed using an LDH assay as shown in the graph. Single iPS cells were seeded in 96-well plates, treated with various concentrations of MQD and cell viability was assessed 24 hours post-treatment. They show a consistent pattern of high cell viability at all MQD concentrations tested, with values near or above 100% of the untreated control group. This suggests that MQD does not cause significant cell membrane damage or cytotoxic effects even at the highest concentration of 100 µg/mL. This observation is in line with the hypothesis that MQD could potentially have bioactive properties that promote cell growth or protect against stress. The lack of cytotoxicity observed in this experiment emphasizes that MQD is a biocompatible material suitable for use in cellular applications. The high viability at all concentrations tested indicates that MQD does not disrupt cell membrane integrity as LDH release (a marker of cell lysis) remains low. MQD maintains its non-toxic profile even at high doses, making it safe for long-term exposure or higher concentration applications. These findings are crucial for future experiments in which MQD will be used in combination with electrical stimulation to influence neural differentiation. Ensuring the non-toxic nature of MQD provides confidence that any observed effects on differentiation or functionality will be due to its intended bioactive properties rather than cytotoxic stress (Kaja et al., 2017).

Live-Dead staining images reveal a clear distinction between live and dead cells under different experimental conditions. It shows that cells in the sGO and electrically treated groups exhibited a significant decrease in viability compared to the other groups over the 14-day culture period. The observed decrease in the number of viable cells suggests that the scaffold composition, particularly the presence of graphene oxide (GO), may have

exerted cytotoxic effects or altered the microenvironment in a way that affected cell survival. Possible factors contributing to reduced cell viability include surface roughness, oxidative stress induced by GO, or insufficient cell adhesion and proliferation on the scaffold material. The reduced viability of cells exposed to electrical stimulation suggests that prolonged exposure to electrical currents may have triggered cellular stress, potentially leading to apoptosis or necrosis. Electrical stimulation is known to affect cellular processes such as membrane potential and ion channel activity; however, suboptimal stimulation parameters (e.g. excessive intensity or duration) may have contributed to the observed decrease in cell survival. It is also possible that the combined effect of SGO and electrical stimulation may have created an environment that is not conducive to long-term cell viability. The Live-Dead staining results suggest that although sGO scaffolds and electrical stimulation have potential in neural tissue engineering, the current application parameters may lead to reduced cell viability during prolonged culture periods. Optimizing scaffold composition and electrical stimulation parameters will be critical to achieve an environment that promotes both cell survival and differentiation. These findings provide valuable insights for the development of improved biomaterial-based strategies for regenerative medicine applications (Lee et al., 2024).

The role of electrical stimulation in mimicking the physiological environment of neurons and promoting differentiation by enhancing intracellular signaling pathways is widely recognized (Rangarajan et al., 2014; Tominami et al., 2024). The observed increase in Nestin and β-Tubulin III expression in electrically stimulated groups suggests that electrical cues effectively promote neural connectivity and cytoskeleton development critical for neuronal function. Nestin is a well-known marker of neural progenitor cells. Its significant upregulation in the electrical stimulation group suggests that electrical cues enhance progenitor cell proliferation and maintenance, providing a stronger basis for further neuronal differentiation. The higher expression in the electrically treated group compared to the sGO-only group implies that electrical stimulation may act synergistically with biochemical cues to sustain progenitor cell populations for long-term differentiation. β-Tubulin III is an important cytoskeletal protein associated with mature neurons and axonal growth. Increased expression of this marker in the electrical stimulation group indicates accelerated differentiation towards mature neuronal phenotypes. This suggests that electrical stimulation not only promotes the initial commitment of the neural lineage but also promotes the development of functional neural cells by enhancing structural maturation. While the presence of sGO in culture medium showed moderate effects on neural differentiation

marker expression, it did not induce the same level of up-regulation observed with electrical stimulation. Despite its conductive properties, sGO alone may not provide sufficient bioelectrical cues needed to optimally guide differentiation. The interaction of cells with scaffold surfaces may influence gene expression patterns and further optimization of sGO composition may be required to increase its efficacy. The data suggest that combining sGO with electrical stimulation may enhance differentiation outcomes by taking advantage of both the conductive properties of the scaffold and the bioelectrical stimuli provided by the electric field. Electrical stimulation significantly increased the expression of Nestin and β-Tubulin III, important neural differentiation markers, in MSC-derived neural stem cells compared to sGO treatment alone. These findings highlight the important role of electrical stimulation in promoting both early and late stages of neural differentiation. While sGO offers a promising scaffold material, its combination with electrical stimulation may yield optimal results for neural tissue engineering and regenerative medicine applications (Geremia et al., 2007).

BBB scores ranging from 0 to 21 points were assessed at two-week intervals to evaluate motor function in hindlimb movement, joint coordination and weight support. The highest improvement in motor function was observed in the group receiving the combined treatment of NSCs, MQD and electrical stimulation, which achieved the highest BBB score among all groups at the end of week 8. This finding suggests that the combined treatment has a synergistic effect promoting neuroregeneration and functional recovery. The significant improvement in locomotor function implies improved neural connectivity, enhanced cell integration and restoration of spinal cord tracts. The superior functional outcomes observed in the SCI + NSC + MQD + E group can be attributed to the synergistic effects of the combined treatments. NSCs provide a source of new neurons and glial cells that can replace damaged tissue and restore lost function. They may contribute to reducing inflammation and creating a pro-regenerative microenvironment. By modulating cellular signaling pathways, MQD can promote cell survival, reduce oxidative stress and promote neural differentiation. It may enhance stem cell integration and improve synaptic plasticity, leading to functional recovery. Electrical stimulation is known to enhance axonal growth, modulate neuroplasticity and promote functional recovery by stimulating endogenous repair mechanisms (Scheff et al., 2002).

The latency to respond to thermal stimulus (hot plate) was analyzed to assess functional recovery and sensory improvements between the different treatment groups. The

SCI + NSC + MQD + E group exhibited the most significant improvement in sensory function, with response latencies approaching those of the healthy control group at the end of the experiment. The combination of NSCs, MQD and electrical stimulation appears to have a synergistic effect, facilitating neural repair, axonal regrowth and functional recovery of sensory pathways. The improved pain response observed in SCI + NSC + MQD + E group may be attributed to the combined effects of the treatments applied. NSCs provide support for cell replacement, neuroprotection and axonal regrowth in the injured spinal cord. Secrete neurotrophic factors that promote survival and differentiation of endogenous neurons. MQD facilitates functional restoration of sensory circuits, possibly by enhancing neurogenesis and reducing oxidative stress. It may promote the survival and integration of transplanted NSCs, enhancing their activity. Electrical stimulation increases neuronal excitability, promotes synaptic plasticity and stimulates sensory pathways, leading to faster pain perception and improved sensory-motor coordination. Contributes to improved sensory feedback by facilitating cellular signaling and axonal outgrowth. The combined effect of these interventions likely promotes axonal regeneration, remyelination and synaptic reconnection, leading to improved pain perception and functional recovery. The results of the hot plate test show that the combination of NSCs, MQD and electrical stimulation significantly improves sensory function in spinal cord injured animals, as evidenced by faster pain response delays. This group achieved levels of sensory recovery approaching those of healthy animals by the end of the 8-week period, highlighting the potential of multimodal therapeutic strategies in the treatment of spinal cord injury (Boido et al., 2014).

The most significant improvement was observed in the group receiving a combination of NSCs, MQD and electrical stimulation. The EMG frequencies in this group were higher than in the other SCI groups, indicating a synergistic effect facilitating the recovery of neuromuscular function. Despite this improvement, the values did not reach those of the healthy control group, suggesting that the functional recovery was partial rather than complete. The improvements in EMG frequencies observed in the SCI + NSC + MQD + E group may be attributed to the combined effects of the treatments applied. NSCs provide neuroprotection, replace lost cells and contribute to partial functional restoration by promoting synaptic connectivity. They facilitate the formation of new neural circuits and integration into existing pathways. MQD likely acts by enhancing neural repair mechanisms, reducing inflammation and providing a supportive environment for NSC survival and differentiation. Electrical stimulation promotes neuromuscular reactivation by increasing electrical excitability, improving synaptic plasticity and facilitating functional recovery of

motor circuits. The combined effects of these interventions can be supported by improved neural signaling and muscle responsiveness, as demonstrated by high EMG frequencies (Meilink et al., 2008).

Immunofluorescence staining of tissue sections from damaged spinal cord tissue revealed a higher density of β-III Tubulin-positive cells in some areas, indicating increased neuronal differentiation and axonal growth in response to treatment. The presence of HuC/HuD-positive cells, whose HuC/HuD expression indicates post-mitotic neurons, is evident in different sections, confirming neuronal survival and differentiation. The distribution model shows that neuronal differentiation is more pronounced in certain treated groups, indicating a positive response to interventions such as stem cell transplantation and electrical stimulation. Higher S100 expression indicates active glial support, potentially aiding neuronal regeneration by providing structural and metabolic support. GFAP, an astrocytic marker, is predominantly found in regions surrounding the injury site and indicates astrocyte reactivity. Elevated GFAP levels may indicate reactive gliosis, which is commonly observed in response to spinal cord injury, and may contribute to the formation of a glial scar that potentially inhibits neuronal integration. MAP2, a marker of mature neurons, shows moderate expression in certain regions, indicating the presence of differentiated neurons within the spinal cord tissue. The distribution of MAP2-positive cells is indicative of neuronal survival and potential integration within the host tissue. The presence of HuC/HuD-positive cells as well as MAP2 indicates the ongoing maturation and functional potential of newly integrated neurons. The results suggest that treatments involving neural stem cells, electrical stimulation and bioactive compounds such as MQD contribute to neuronal survival and differentiation as evidenced by the expression of β-III Tubulin, HuC/HuD and MAP2 markers (Dráberová et al., 2008).

This study demonstrates that the combination of neural stem cells (NSCs), nanomaterials (MQD), and electrical stimulation significantly enhances neural differentiation and functional recovery in spinal cord injury (SCI) models. Key findings reveal that electrical stimulation promotes neural differentiation by increasing the expression of neural markers such as Nestin and β-III Tubulin, while MQD supports cell viability and neuroprotection. Functional assessments, including BBB scoring, hot plate tests, and EMG analysis, indicate that the combined treatment leads to improved locomotor and sensory recovery compared to other groups. Immunofluorescence analysis confirms the presence of mature neurons in the injured spinal cord, suggesting successful integration of transplanted

cells. The study highlights the potential of this multidisciplinary approach in advancing SCI treatment by offering a promising strategy to enhance neuroregeneration and functional restoration.

5. CONCLUSION AND FUTURE ASPECTS

Spinal cord injury (SCI) remains one of the most challenging medical conditions, affecting millions of people worldwide with devastating physical, psychological, and financial consequences. Traditional treatments have focused primarily on managing symptoms and preventing further damage, but they offer limited potential for restoring lost functions. However, advances in regenerative medicine, including stem cell therapy, 3D bioprinting, and nanotechnology, are transforming the outlook for SCI patients.

Stem cell therapies, particularly mesenchymal stem cells (MSCs) and induced pluripotent stem cells (iPSCs), have shown promise in promoting neural regeneration and reducing inflammation, offering hope for functional recovery. Additionally, 3D bioprinting presents exciting possibilities for creating personalized scaffolds that can support tissue repair in the spinal cord. Nanotechnology, with its ability to deliver targeted therapies and provide structural support, further enhances the potential for SCI recovery.

In conclusion, this study highlights the promising potential of a multidisciplinary approach combining neural stem cells (NSCs), bioactive nanomaterials (MQD), and electrical stimulation for enhancing neural differentiation and promoting functional recovery in spinal cord injury (SCI) models. The results demonstrated that electrical stimulation significantly enhances neural differentiation by upregulating key neuronal markers, while MQD contributes to cell viability and neuroprotection. Functional assessments, including BBB scoring, hot plate tests, and EMG analysis, confirmed improved motor and sensory recovery in the combined treatment group, suggesting a synergistic effect of these interventions. Immunofluorescence and gene expression analyses further validated the successful differentiation of NSCs into mature neurons, supporting their integration into the injured spinal cord tissue. Despite these encouraging findings, several challenges remain to be addressed to facilitate the translation of this approach into clinical applications. Future research should focus on:

- Optimization of Treatment Protocols: Fine-tuning electrical stimulation parameters (intensity, duration, frequency) to achieve maximum neural differentiation without compromising cell viability. Determining the optimal concentration and delivery methods for MQD to enhance neural regeneration.

- Long-Term Efficacy and Safety Studies: Conducting extended follow-up studies to evaluate the sustainability of functional improvements and potential adverse effects. Investigating the effects of the treatment on different spinal cord injury severities and in larger animal models to assess scalability.

- Integration with Advanced Biomaterials and 3D Bioprinting: Utilizing advanced bioprinting techniques to fabricate personalized, biomimetic scaffolds that can support long-term neural regeneration. Exploring alternative bio-inks and scaffold compositions that can better support cell adhesion, differentiation, and functionality.

- Molecular Mechanisms and Pathways: Further exploration of the molecular pathways influenced by MQD and electrical stimulation to understand the mechanisms driving neural regeneration. Studying interactions between transplanted cells and the host spinal cord environment to improve integration and connectivity.

- Clinical Translation and Regulatory Considerations: Addressing immunogenicity, ethical considerations, and regulatory challenges to pave the way for human trials. Developing standardized protocols to ensure reproducibility and safety in clinical settings.

In summary, the combination of NSCs, MQD, and electrical stimulation presents a novel and promising strategy for treating spinal cord injuries. While the findings provide a solid foundation for further exploration, future studies should focus on optimizing and translating these approaches to achieve effective and scalable therapeutic solutions for SCI patients. While these technologies are still largely in the experimental phase, they represent a significant step toward finding more effective treatments for SCI. The combination of these innovations holds the potential to revolutionize spinal cord injury care, offering new hope to those affected by this life-altering condition. As research continues, the future of SCI treatment looks increasingly promising, with the potential to restore mobility, independence, and quality of life to millions of patients around the world.

REFERENCES

Adul-Rasool, A. A., Athair, D. M., Zaidan, H. K., Rheima, A. M., Al-Sharify, Z. T., Mohammed, S. H., & kianfar, E. (2024). 0,1,2,3D nanostructures, types of bulk nanostructured materials, and drug nanocrystals: An overview. *Cancer Treatment and Research Communications*, *40*, 100834. https://doi.org/https://doi.org/10.1016/j.ctarc.2024.100834

Ahuja, C. S., Wilson, J. R., Nori, S., Kotter, M. R. N., Druschel, C., Curt, A., & Fehlings, M. G. (2017). Traumatic spinal cord injury. *Nature Reviews Disease Primers*, *3*(1), 17018. https://doi.org/10.1038/nrdp.2017.18

Al Abbar, A., Ngai, S. C., Nograles, N., Alhaji, S. Y., & Abdullah, S. (2020). Induced Pluripotent Stem Cells: Reprogramming Platforms and Applications in Cell Replacement Therapy. *Biores Open Access*, *9*(1), 121-136. https://doi.org/10.1089/biores.2019.0046

Albert, K., Niskanen, J., Kälvälä, S., & Lehtonen, Š. (2021). Utilising Induced Pluripotent Stem Cells in Neurodegenerative Disease Research: Focus on Glia. *Int J Mol Sci*, *22*(9). https://doi.org/10.3390/ijms22094334

Ali, S., Ismail, P. M., Humayun, M., & Bououdina, M. (2025). Hexagonal boron nitride: From fundamentals to applications. *Desalination*, *599*, 118442. https://doi.org/https://doi.org/10.1016/j.desal.2024.118442

Alizadeh, A., Dyck, S. M., & Karimi-Abdolrezaee, S. (2019). Traumatic Spinal Cord Injury: An Overview of Pathophysiology, Models and Acute Injury Mechanisms. *Front Neurol*, *10*, 282. https://doi.org/10.3389/fneur.2019.00282

Aljabali, A. A., Obeid, M. A., Bashatwah, R. M., Serrano-Aroca, Á., Mishra, V., Mishra, Y., El-Tanani, M., Hromić-Jahjefendić, A., Kapoor, D. N., Goyal, R., Naikoo, G. A., & Tambuwala, M. M. (2023). Nanomaterials and Their Impact on the Immune System. *Int J Mol Sci*, *24*(3). https://doi.org/10.3390/ijms24032008

Altammar, K. A. (2023). A review on nanoparticles: characteristics, synthesis, applications, and challenges. *Frontiers in Microbiology*, *14*, 1155622. https://doi.org/10.3389/fmicb.2023.1155622

Amin, N., Tan, X., Ren, Q., Zhu, N., Botchway, B. O. A., Hu, Z., & Fang, M. (2019). Recent advances of induced pluripotent stem cells application in neurodegenerative diseases. *Progress in Neuro-Psychopharmacology and Biological Psychiatry*, *95*, 109674. https://doi.org/https://doi.org/10.1016/j.pnpbp.2019.109674

Augustyniak, J., Lenart, J., Lipka, G., Stepien, P. P., & Buzanska, L. (2019). Reference Gene Validation via RT-qPCR for Human iPSC-Derived Neural Stem Cells and Neural Progenitors. *Mol Neurobiol*, *56*(10), 6820-6832. https://doi.org/10.1007/s12035-019-1538-x

Bahmad, H., Hadadeh, O., Chamaa, F., Cheaito, K., Darwish, B., Makkawi, A.-K., & Abou-Kheir, W. (2017). Modeling Human Neurological and Neurodegenerative Diseases: From Induced Pluripotent Stem Cells to Neuronal Differentiation and Its Applications in Neurotrauma [Review]. *Frontiers in Molecular Neuroscience*, *10*. https://doi.org/10.3389/fnmol.2017.00050

Baig, N., Kammakakam, I., & Falath, W. (2021). Nanomaterials: a review of synthesis methods, properties, recent progress, and challenges [10.1039/D0MA00807A]. *Materials Advances*, *2*(6), 1821-1871. https://doi.org/10.1039/D0MA00807A

BASSO, D. M., BEATTIE, M. S., & BRESNAHAN, J. C. (1995). A Sensitive and Reliable Locomotor Rating Scale for Open Field Testing in Rats. *Journal of Neurotrauma*, *12*(1), 1-21. https://doi.org/10.1089/neu.1995.12.1

Bishop, E. S., Mostafa, S., Pakvasa, M., Luu, H. H., Lee, M. J., Wolf, J. M., Ameer, G. A., He, T. C., & Reid, R. R. (2017). 3-D bioprinting technologies in tissue engineering and regenerative medicine: Current and future trends. *Genes Dis*, *4*(4), 185-195. https://doi.org/10.1016/j.gendis.2017.10.002

Boido, M., Garbossa, D., Fontanella, M., Ducati, A., & Vercelli, A. (2014). Mesenchymal Stem Cell Transplantation Reduces Glial Cyst and Improves Functional Outcome After Spinal Cord Compression. *World Neurosurgery*, *81*(1), 183-190. https://doi.org/https://doi.org/10.1016/j.wneu.2012.08.014

Brown, G., Hughes, P. J., & Michell, R. H. (2003). Cell differentiation and proliferation--simultaneous but independent? *Exp Cell Res*, *291*(2), 282-288. https://doi.org/10.1016/s0014-4827(03)00393-8

Budd, M. A., Gater, D. R., Jr., & Channell, I. (2022). Psychosocial Consequences of Spinal Cord Injury: A Narrative Review. *J Pers Med*, *12*(7). https://doi.org/10.3390/jpm12071178

Byakodi, M., Shrikrishna, N. S., Sharma, R., Bhansali, S., Mishra, Y., Kaushik, A., & Gandhi, S. (2022). Emerging 0D, 1D, 2D, and 3D nanostructures for efficient point-of-care biosensing. *Biosensors and Bioelectronics: X*, *12*, 100284. https://doi.org/https://doi.org/10.1016/j.biosx.2022.100284

Castellanos-Gomez, A. (2015). Black Phosphorus: Narrow Gap, Wide Applications. *The Journal of Physical Chemistry Letters*, *6*(21), 4280-4291. https://doi.org/10.1021/acs.jpclett.5b01686

Chehelgerdi, M., Behdarvand Dehkordi, F., Chehelgerdi, M., Kabiri, H., Salehian-Dehkordi, H., Abdolvand, M., Salmanizadeh, S., Rashidi, M., Niazmand, A., Ahmadi, S., Feizbakhshan, S., Kabiri, S., Vatandoost, N., & Ranjbarnejad, T. (2023). Exploring the promising potential of induced pluripotent stem cells in cancer research and therapy. *Molecular Cancer*, *22*(1), 189. https://doi.org/10.1186/s12943-023-01873-0

Chen, X. B., Fazel Anvari-Yazdi, A., Duan, X., Zimmerling, A., Gharraei, R., Sharma, N. K., Sweilem, S., & Ning, L. (2023). Biomaterials / bioinks and extrusion bioprinting. *Bioactive Materials*, *28*, 511-536. https://doi.org/https://doi.org/10.1016/j.bioactmat.2023.06.006

Chen, Y., Tang, Y., Vogel, L. C., & Devivo, M. J. (2013). Causes of spinal cord injury. *Top Spinal Cord Inj Rehabil*, *19*(1), 1-8. https://doi.org/10.1310/sci1901-1

Costăchescu, B., Niculescu, A. G., Dabija, M. G., Teleanu, R. I., Grumezescu, A. M., & Eva, L. (2022). Novel Strategies for Spinal Cord Regeneration. *Int J Mol Sci*, *23*(9). https://doi.org/10.3390/ijms23094552

Davoodi, E., Sarikhani, E., Montazerian, H., Ahadian, S., Costantini, M., Swieszkowski, W., Willerth, S., Walus, K., Mofidfar, M., Toyserkani, E., Khademhosseini, A., & Ashammakhi, N. (2020). Extrusion and Microfluidic-based Bioprinting to Fabricate Biomimetic Tissues and Organs. *Adv Mater Technol*, *5*(8). https://doi.org/10.1002/admt.201901044

Deptuła, M., Zawrzykraj, M., Sawicka, J., Banach-Kopeć, A., Tylingo, R., & Pikuła, M. (2023). Application of 3D- printed hydrogels in wound healing and regenerative medicine. *Biomedicine & Pharmacotherapy*, *167*, 115416. https://doi.org/https://doi.org/10.1016/j.biopha.2023.115416

Dhamodharan, D., Al-Harthi, M. A., Ramya, B., Bafaqeer, A., & Alam, F. (2024). MXenes: A promising material with multifunctional applications. *Journal of Environmental Chemical Engineering*, *12*(2), 112316. https://doi.org/https://doi.org/10.1016/j.jece.2024.112316

Dorrian, R. M., Berryman, C. F., Lauto, A., & Leonard, A. V. (2023). Electrical stimulation for the treatment of spinal cord injuries: A review of the cellular and molecular mechanisms that drive functional improvements. *Front Cell Neurosci*, *17*, 1095259. https://doi.org/10.3389/fncel.2023.1095259

Dráberová, E., Del Valle, L., Gordon, J., Marková, V., Smejkalová, B., Bertrand, L., de Chadarévian, J. P., Agamanolis, D. P., Legido, A., Khalili, K., Dráber, P., & Katsetos, C. D. (2008). Class III beta-tubulin is constitutively coexpressed with glial fibrillary acidic protein and nestin in midgestational human fetal astrocytes: implications for phenotypic identity. *J Neuropathol Exp Neurol*, *67*(4), 341-354. https://doi.org/10.1097/NEN.0b013e31816a686d

Dumont, R. J., Okonkwo, D. O., Verma, S., Hurlbert, R. J., Boulos, P. T., Ellegala, D. B., & Dumont, A. S. (2001). Acute Spinal Cord Injury, Part I: Pathophysiologic Mechanisms. *Clinical Neuropharmacology*, *24*(5), 254-264. https://journals.lww.com/clinicalneuropharm/fulltext/2001/09000/acute_spinal_cord_injury,_part_i__pathophysiologic.2.aspx

Engel, E., Michiardi, A., Navarro, M., Lacroix, D., & Planell, J. A. (2008). Nanotechnology in regenerative medicine: the materials side. *Trends in Biotechnology*, *26*(1), 39-47. https://doi.org/https://doi.org/10.1016/j.tibtech.2007.10.005

Fan, X. L., Zhang, Y., Li, X., & Fu, Q. L. (2020). Mechanisms underlying the protective effects of mesenchymal stem cell-based therapy. *Cell Mol Life Sci*, *77*(14), 2771-2794. https://doi.org/10.1007/s00018-020-03454-6

Fluri, D. A., Tonge, P. D., Song, H., Baptista, R. P., Shakiba, N., Shukla, S., Clarke, G., Nagy, A., & Zandstra, P. W. (2012). Derivation, expansion and differentiation of induced pluripotent stem cells in continuous suspension cultures. *Nat Methods*, *9*(5), 509-516. https://doi.org/10.1038/nmeth.1939

Gao, G., Ahn, M., Cho, W. W., Kim, B. S., & Cho, D. W. (2021). 3D Printing of Pharmaceutical Application: Drug Screening and Drug Delivery. *Pharmaceutics*, *13*(9). https://doi.org/10.3390/pharmaceutics13091373

Geim, A. K., & Novoselov, K. S. (2007). The rise of graphene. *Nature Materials*, *6*(3), 183-191. https://doi.org/10.1038/nmat1849

George, J., & Bhattacharyya, D. (2023). Graphene: an introduction. In *Recent Advances in Graphene and Graphene-Based Technologies* (pp. 1-1-1-24). IOP Publishing. https://doi.org/10.1088/978-0-7503-3999-5ch1

Geremia, N. M., Gordon, T., Brushart, T. M., Al-Majed, A. A., & Verge, V. M. (2007). Electrical stimulation promotes sensory neuron regeneration and growth-associated gene expression. *Exp Neurol*, *205*(2), 347-359. https://doi.org/10.1016/j.expneurol.2007.01.040

Ghosh, P. K. (2024). Prospects of emerging 3D bioprinting technologies: major technology components, technology developers, and end users—Part I. *MGM Journal of Medical Sciences*, *11*(2), 331-339. https://doi.org/10.4103/mgmj.mgmj_96_24

Gu, Z., Fu, J., Lin, H., & He, Y. (2020). Development of 3D bioprinting: From printing methods to biomedical applications. *Asian J Pharm Sci*, *15*(5), 529-557. https://doi.org/10.1016/j.ajps.2019.11.003

Halevy, T., & Urbach, A. (2014). Comparing ESC and iPSC-Based Models for Human Genetic Disorders. *J Clin Med*, *3*(4), 1146-1162. https://doi.org/10.3390/jcm3041146

Han, F., Meng, Q., Xie, E., Li, K., Hu, J., Chen, Q., Li, J., & Han, F. (2023). Engineered biomimetic micro/nano-materials for tissue regeneration [Review]. *Frontiers in Bioengineering and Biotechnology*, *11*. https://doi.org/10.3389/fbioe.2023.1205792

Hersh, A. M., Alomari, S., & Tyler, B. M. (2022). Crossing the Blood-Brain Barrier: Advances in Nanoparticle Technology for Drug Delivery in Neuro-Oncology. *Int J Mol Sci*, *23*(8). https://doi.org/10.3390/ijms23084153

Hu, X., Xu, W., Ren, Y., Wang, Z., He, X., Huang, R., Ma, B., Zhao, J., Zhu, R., & Cheng, L. (2023). Spinal cord injury: molecular mechanisms and therapeutic interventions. *Signal Transduction and Targeted Therapy*, *8*(1), 245. https://doi.org/10.1038/s41392-023-01477-6

Innamorati, G., Sanchez-Petidier, M., Bergafora, G., Codazzi, C., Palma, V., Camera, F., Merla, C., André, F. M., Pedraza, M., Moreno Manzano, V., Caramazza, L., Colella, M., Marracino, P., Balucani, M., Apollonio, F., Liberti, M., & Consales, C. (2025). Characterization of Mesenchymal and Neural Stem Cells Response to Bipolar Microsecond Electric Pulses Stimulation. *International Journal of Molecular Sciences*, *26*(1), 147. https://www.mdpi.com/1422-0067/26/1/147

Jaatinen, L., Salemi, S., Miettinen, S., Hyttinen, J., & Eberli, D. (2015). The Combination of Electric Current and Copper Promotes Neuronal Differentiation of Adipose-Derived Stem Cells. *Annals of Biomedical Engineering*, *43*(4), 1014-1023. https://doi.org/10.1007/s10439-014-1132-3

Jang, S., Cho, H.-H., Cho, Y.-B., Park, J.-S., & Jeong, H.-S. (2010). Functional neural differentiation of human adipose tissue-derived stem cells using bFGF and forskolin. *BMC Cell Biology*, *11*(1), 25. https://doi.org/10.1186/1471-2121-11-25

Kaja, S., Payne, A. J., Naumchuk, Y., & Koulen, P. (2017). Quantification of Lactate Dehydrogenase for Cell Viability Testing Using Cell Lines and Primary Cultured Astrocytes. *Curr Protoc Toxicol*, *72*, 2.26.21-22.26.10. https://doi.org/10.1002/cptx.21

Kaplan, B., & Levenberg, S. (2022). The Role of Biomaterials in Peripheral Nerve and Spinal Cord Injury: A Review. *Int J Mol Sci*, *23*(3). https://doi.org/10.3390/ijms23031244

Khan, A. A., Huat, T. J., Al Mutery, A., El-Serafi, A. T., Kacem, H. H., Abdallah, S. H., Reza, M. F., Abdullah, J. M., & Jaafar, H. (2020). Significant transcriptomic changes are associated with differentiation of bone marrow-derived mesenchymal stem cells into neural progenitor-like cells in the presence of bFGF and EGF. *Cell & Bioscience*, *10*(1), 126. https://doi.org/10.1186/s13578-020-00487-z

Khan, I., Saeed, K., & Khan, I. (2019). Nanoparticles: Properties, applications and toxicities. *Arabian Journal of Chemistry*, *12*(7), 908-931. https://doi.org/https://doi.org/10.1016/j.arabjc.2017.05.011

Khazaei, M., Siddiqui, A. M., & Fehlings, M. G. (2014). The Potential for iPS-Derived Stem Cells as a Therapeutic Strategy for Spinal Cord Injury: Opportunities and Challenges. *J Clin Med*, *4*(1), 37-65. https://doi.org/10.3390/jcm4010037

Kim, D. Y., Liu, Y., Kim, G., An, S. B., & Han, I. (2024). Innovative Strategies in 3D Bioprinting for Spinal Cord Injury Repair. *International Journal of Molecular Sciences*, *25*(17), 9592. https://www.mdpi.com/1422-0067/25/17/9592

Kim, G. U., Sung, S. E., Kang, K. K., Choi, J. H., Lee, S., Sung, M., Yang, S. Y., Kim, S. K., Kim, Y. I., Lim, J. H., Seo, M. S., & Lee, G. W. (2021). Therapeutic Potential of Mesenchymal Stem Cells (MSCs) and MSC-Derived Extracellular Vesicles for the Treatment of Spinal Cord Injury. *Int J Mol Sci*, *22*(24). https://doi.org/10.3390/ijms222413672

Kim, H., Anasori, B., Gogotsi, Y., & Alshareef, H. N. (2017). Thermoelectric Properties of Two-Dimensional Molybdenum-Based MXenes. *Chemistry of Materials*, *29*(15), 6472-6479. https://doi.org/10.1021/acs.chemmater.7b02056

Kim, W. R., Kang, M., Park, H., Ham, H.-J., Lee, H., & Geum, D. (2017). Functional Test Scales for Evaluating Cell-Based Therapies in Animal Models of Spinal Cord Injury. *Stem Cells International*, *2017*(1), 5160261. https://doi.org/https://doi.org/10.1155/2017/5160261

Lee, S., Choe, G., Yi, J., Kim, J., Lee, S. H., Jeon, J., Yang, H. S., & Lee, J. Y. (2024). ROS-scavenging ultrasonicated graphene oxide/alginate microgels for mesenchymal stem cell delivery and hindlimb ischemia treatment. *Materials Today Bio*, *29*, 101289. https://doi.org/https://doi.org/10.1016/j.mtbio.2024.101289

Li, C., Luo, Y., & Li, S. (2024). The roles of neural stem cells in myelin regeneration and repair therapy after spinal cord injury. *Stem Cell Res Ther*, *15*(1), 204. https://doi.org/10.1186/s13287-024-03825-x

Li, X., Liu, B., Pei, B., Chen, J., Zhou, D., Peng, J., Zhang, X., Jia, W., & Xu, T. (2020). Inkjet Bioprinting of Biomaterials. *Chemical Reviews*, *120*(19), 10793-10833. https://doi.org/10.1021/acs.chemrev.0c00008

Lima, R., Monteiro, A., Salgado, A. J., Monteiro, S., & Silva, N. A. (2022). Pathophysiology and Therapeutic Approaches for Spinal Cord Injury. *International Journal of Molecular Sciences*, *23*(22), 13833. https://www.mdpi.com/1422-0067/23/22/13833

Liu, X., Hao, M., Chen, Z., Zhang, T., Huang, J., Dai, J., & Zhang, Z. (2021). 3D bioprinted neural tissue constructs for spinal cord injury repair. *Biomaterials*, *272*, 120771. https://doi.org/https://doi.org/10.1016/j.biomaterials.2021.120771

Lo Furno, D., Mannino, G., Giuffrida, R., Gili, E., Vancheri, C., Tarico, M. S., Perrotta, R. E., & Pellitteri, R. (2018). Neural differentiation of human adipose-derived mesenchymal stem cells induced by glial cell conditioned media. *Journal of Cellular Physiology*, *233*(10), 7091-7100. https://doi.org/https://doi.org/10.1002/jcp.26632

Lu, Y., Shang, Z., Zhang, W., Pang, M., Hu, X., Dai, Y., Shen, R., Wu, Y., Liu, C., Luo, T., Wang, X., Liu, B., Zhang, L., & Rong, L. (2024). Global incidence and characteristics of spinal cord injury since 2000-2021: a systematic review and meta-analysis. *BMC Med*, *22*(1), 285. https://doi.org/10.1186/s12916-024-03514-9

Luciani, M., Garsia, C., Beretta, S., Cifola, I., Peano, C., Merelli, I., Petiti, L., Miccio, A., Meneghini, V., & Gritti, A. (2024). Human iPSC-derived neural stem cells displaying radial glia signature exhibit long-term safety in mice. *Nat Commun*, *15*(1), 9433. https://doi.org/10.1038/s41467-024-53613-7

Malekzadeh, H., Golpayegani, M., Ghodsi, Z., Sadeghi-Naini, M., Asgardoon, M., Baigi, V., Vaccaro, A. R., & Rahimi-Movaghar, V. (2022). Direct Cost of Illness for Spinal Cord Injury: A Systematic Review. *Global Spine J*, *12*(6), 1267-1281. https://doi.org/10.1177/21925682211031190

Meilink, A., Hemmen, B., Seelen, H. A., & Kwakkel, G. (2008). Impact of EMG-triggered neuromuscular stimulation of the wrist and finger extensors of the paretic hand after stroke: a

systematic review of the literature. *Clin Rehabil*, *22*(4), 291-305. https://doi.org/10.1177/0269215507083368

Mekuye, B., & Abera, B. (2023). Nanomaterials: An overview of synthesis, classification, characterization, and applications. *Nano Select*, *4*(8), 486-501. https://doi.org/https://doi.org/10.1002/nano.202300038

Mendoza-Cerezo, L., Jesús, M. R., Macías-García, A., Marcos-Romero, A. C., & Díaz-Parralejo, A. (2023). Evolution of bioprinting and current applications. *Int J Bioprint*, *9*(4), 742. https://doi.org/10.18063/ijb.742

Mihaylova, A., Shopova, D., Parahuleva, N., Yaneva, A., & Bakova, D. (2024). (3D) Bioprinting-Next Dimension of the Pharmaceutical Sector. *Pharmaceuticals (Basel)*, *17*(6). https://doi.org/10.3390/ph17060797

Miller, L. W., & Perin, E. C. (2016). Chapter 1 - Introduction and Overview of Stem Cells. In E. C. Perin, L. W. Miller, D. A. Taylor, & J. T. Willerson (Eds.), *Stem Cell and Gene Therapy for Cardiovascular Disease* (pp. 3-11). Academic Press. https://doi.org/https://doi.org/10.1016/B978-0-12-801888-0.00001-1

Mimona, M. A., Rimon, M. I. H., Zohura, F. T., Sony, J. M., Rim, S. I., Arup, M. M. R., & Mobarak, M. H. (2025). Quantum dot nanomaterials: Empowering advances in optoelectronic devices. *Chemical Engineering Journal Advances*, *21*, 100704. https://doi.org/https://doi.org/10.1016/j.ceja.2025.100704

Mirshafiei, M., Rashedi, H., Yazdian, F., Rahdar, A., & Baino, F. (2024). Advancements in tissue and organ 3D bioprinting: Current techniques, applications, and future perspectives. *Materials & Design*, *240*, 112853. https://doi.org/https://doi.org/10.1016/j.matdes.2024.112853

Montoto-Meijide, R., Meijide-Faílde, R., Díaz-Prado, S. M., & Montoto-Marqués, A. (2023). Mesenchymal Stem Cell Therapy in Traumatic Spinal Cord Injury: A Systematic Review. *Int J Mol Sci*, *24*(14). https://doi.org/10.3390/ijms241411719

Moradi, S., Mahdizadeh, H., Šarić, T., Kim, J., Harati, J., Shahsavarani, H., Greber, B., & Moore, J. B. (2019). Research and therapy with induced pluripotent stem cells (iPSCs): social, legal, and ethical considerations. *Stem Cell Research & Therapy*, *10*(1), 341. https://doi.org/10.1186/s13287-019-1455-y

Moroni, L., Boland, T., Burdick, J. A., De Maria, C., Derby, B., Forgacs, G., Groll, J., Li, Q., Malda, J., Mironov, V. A., Mota, C., Nakamura, M., Shu, W., Takeuchi, S., Woodfield, T. B. F., Xu, T., Yoo, J. J., & Vozzi, G. (2018). Biofabrication: A Guide to Technology and Terminology. *Trends Biotechnol*, *36*(4), 384-402. https://doi.org/10.1016/j.tibtech.2017.10.015

National Institutes of Neurological Disorders and Stroke. (2025). https://www.ninds.nih.gov/health-information/disorders/spinal-cord-injury

Neaverson, A., Andersson, M. H. L., Arshad, O. A., Foulser, L., Goodwin-Trotman, M., Hunter, A., Newman, B., Patel, M., Roth, C., Thwaites, T., Kilpinen, H., Hurles, M. E., Day, A., & Gerety, S. S. (2022). Differentiation of human induced pluripotent stem cells into cortical neural stem cells. *Front Cell Dev Biol*, *10*, 1023340. https://doi.org/10.3389/fcell.2022.1023340

Okita, K., & Yamanaka, S. (2011). Induced pluripotent stem cells: opportunities and challenges. *Philos Trans R Soc Lond B Biol Sci*, *366*(1575), 2198-2207. https://doi.org/10.1098/rstb.2011.0016

Ortega, M. A., Fraile-Martinez, O., García-Montero, C., Haro, S., Álvarez-Mon, M., De Leon-Oliva, D., Gomez-Lahoz, A. M., Monserrat, J., Atienza-Pérez, M., Díaz, D., Lopez-Dolado, E., & Álvarez-Mon, M. (2023). A comprehensive look at the psychoneuroimmunoendocrinology of spinal cord injury and its progression: mechanisms and clinical opportunities. *Mil Med Res*, *10*(1), 26. https://doi.org/10.1186/s40779-023-00461-z

Ouyang, L., Armstrong, J. P. K., Lin, Y., Wojciechowski, J. P., Lee-Reeves, C., Hachim, D., Zhou, K., Burdick, J. A., & Stevens, M. M. (2020). Expanding and optimizing 3D bioprinting capabilities using complementary network bioinks. *Sci Adv*, *6*(38). https://doi.org/10.1126/sciadv.abc5529

Pang, Q.-M., Deng, K.-Q., Zhang, M., Wu, X.-C., Yang, R.-L., Fu, S.-P., Lin, F.-Q., Zhang, Q., Ao, J., & Zhang, T. (2023). Multiple strategies enhance the efficacy of MSCs transplantation for spinal cord injury. *Biomedicine & Pharmacotherapy*, *157*, 114011. https://doi.org/https://doi.org/10.1016/j.biopha.2022.114011

Panja, N., Maji, S., Choudhuri, S., Ali, K. A., & Hossain, C. M. (2022). 3D Bioprinting of Human Hollow Organs. *AAPS PharmSciTech*, *23*(5), 139. https://doi.org/10.1208/s12249-022-02279-9

Parent, S., Mac-Thiong, J. M., Roy-Beaudry, M., Sosa, J. F., & Labelle, H. (2011). Spinal cord injury in the pediatric population: a systematic review of the literature. *J Neurotrauma*, *28*(8), 1515-1524. https://doi.org/10.1089/neu.2009.1153

Park, J., Lee, N., Lee, J., Choe, E. K., Kim, M. K., Lee, J., Byun, M. S., Chon, M. W., Kim, S. W., Lee, C. J., Kim, J. H., Kwon, J. S., & Chang, M. S. (2017). Small molecule-based lineage switch of human adipose-derived stem cells into neural stem cells and functional GABAergic neurons. *Sci Rep*, *7*(1), 10166. https://doi.org/10.1038/s41598-017-10394-y

Peretz, Y., Eren, N., Kohl, A., Hen, G., Yaniv, K., Weisinger, K., Cinnamon, Y., & Sela-Donenfeld, D. (2016). A new role of hindbrain boundaries as pools of neural stem/progenitor cells regulated by Sox2. *BMC Biology*, *14*(1), 57. https://doi.org/10.1186/s12915-016-0277-y

Persaud, A., Maus, A., Strait, L., & Zhu, D. (2022). 3D Bioprinting with Live Cells. *Engineered Regeneration*, *3*(3), 292-309. https://doi.org/https://doi.org/10.1016/j.engreg.2022.07.002

Pires, F., Ferreira, Q., Rodrigues, C. A., Morgado, J., & Ferreira, F. C. (2015). Neural stem cell differentiation by electrical stimulation using a cross-linked PEDOT substrate: Expanding the use of biocompatible conjugated conductive polymers for neural tissue engineering. *Biochim Biophys Acta*, *1850*(6), 1158-1168. https://doi.org/10.1016/j.bbagen.2015.01.020

Protyai, M. I. H., & Bin Rashid, A. (2024). A comprehensive overview of recent progress in MXene-based polymer composites: Their fabrication processes, advanced applications, and prospects. *Heliyon*, *10*(17), e37030. https://doi.org/https://doi.org/10.1016/j.heliyon.2024.e37030

Punjani, N., Deska-Gauthier, D., Hachem, L. D., Abramian, M., & Fehlings, M. G. (2023). Neuroplasticity and regeneration after spinal cord injury. *N Am Spine Soc J*, *15*, 100235. https://doi.org/10.1016/j.xnsj.2023.100235

Rahimi Darehbagh, R., Seyedoshohadaei, S. A., Ramezani, R., & Rezaei, N. (2024). Stem cell therapies for neurological disorders: current progress, challenges, and future perspectives. *European Journal of Medical Research*, *29*(1), 386. https://doi.org/10.1186/s40001-024-01987-1

Rangarajan, S., Madden, L., & Bursac, N. (2014). Use of flow, electrical, and mechanical stimulation to promote engineering of striated muscles. *Ann Biomed Eng*, *42*(7), 1391-1405. https://doi.org/10.1007/s10439-013-0966-4

Rodríguez-Fernández, A., Lobo-Prat, J., & Font-Llagunes, J. M. (2021). Systematic review on wearable lower-limb exoskeletons for gait training in neuromuscular impairments. *J Neuroeng Rehabil*, *18*(1), 22. https://doi.org/10.1186/s12984-021-00815-5

Safdarian, M., Trinka, E., Rahimi-Movaghar, V., Thomschewski, A., Aali, A., Abady, G. G., Abate, S. M., Abd-Allah, F., Abedi, A., Adane, D. E., Afzal, S., Ahinkorah, B. O., Ahmad, S., Ahmed, H., Amanat, N., Angappan, D., Arabloo, J., Aryannejad, A., Athari, S. S., Atreya, A., Azadnajafabad, S., Azzam, A. Y., Babamohamadi, H., Banik, P. C., Bardhan, M., Bashiri, A., Berhie, A. Y., Bhat, A. N., Brown, J., Champs, A. P., Charalampous, P., Chukwu, I. S., Coberly, K., Dadras, O., Yada, D. Y., Dai, X., Dandona, L., Dandona, R., Dessalegn, F. N., Desta, A. A., Dhingra, S., Diao, N., Diaz, D., Dibas, M., Dongarwar, D., Dsouza, H. L., Ekholuenetale, M., El Nahas, N., Elhadi, M., Eskandarieh, S., Fagbamigbe, A. F., Fares, J., Fatehizadeh, A., Fereshtehnejad, S.-M., Fischer, F., Franklin, R. C., Garg, T., Getachew, M., Ghaffarpasand, F., Gholamrezanezhad, A., Gholizadeh Mesgarha, M., Ghozy, S., Golechha, M., Goleij, P., Graham, S. M., Gupta, V. K., Haagsma, J. A., Hamidi, S., Harlianto, N. I., Harorani, M., Hasanian, M., Hassan, A., Hassen, M. B., Hoveidaei, A. H., Iravanpour, F., Irilouzadian, R., Iwu, C. C. D., Jacob, L., Jaja, C. J., Joseph, N., Joshua, C. E., Jozwiak, J. J., Kadashetti, V., Kandel, A., Kantar, R. S., Karaye, I. M., Karkhah, S., Khader, Y. S., Khan, E. A., Khan, M. J., Khayat Kashani, H. R., Khonji, M. S., Khormali, M., Kim, G., Krishnamoorthy, V., Kumaran, S. D., Malekpour, M.-R., Meretoja, T. J., Mesregah, M. K., Mestrovic, T., Micheletti Gomide Nogueira de Sá, A. C., Miller, T. R., Mirahmadi, A., Mirghaderi, S. P., Mirza, M., Misganaw, A., Misra, S., Mohammad, Y., Mohammadi, E., Mokdad, A. H., Möller, H., Momtazmanesh, S., Moni, M. A., Mostafavi, E., Mulita, F., Naghavi, M., Nassereldine, H., Natto, Z. S., Nejati, K., Nguyen, H. L. T., Nguyen, V. T., Nogueira de Sá, A. T., Olagunju, A. T., Olufadewa, I. I., Omotayo, A. O., Owolabi, M. O., Patil, S., Pawar, S., Pedersini, P., Petcu, I.-R., Polinder, S., Pourbagher-Shahri, A. M., Qureshi, M. F., Raghav, P. R., Rahman, M., Rahnavard, N., Rajabpour-Sanati, A., Rashidi, M.-M., Rawaf, S., Roberts, N. L. S., Saddik, B., Saeed, U., Samadzadeh, S., Samy, A. M., Sarveazad, A., Seylani, A., Shafie, M., Shahbandi, A., Sharew, M. M. S., Sheikhi, R. A., Shetty, P. H., Yigit, A., Shobeiri, P., Shool, S., Shorofi, S. A., Sibhat, M. M., Sinaei, E., Singh, P., Singh, S., Solomon, Y., Sotoudeh, H., Tadesse, B. A., Umair, M., Valadan Tahbaz, S., Valdez, P. R., Venketasubramanian, N., Vu, L. G., Wickramasinghe, N. D., Zare, I., Yazdanpanah, F., Wu, A.-M., & Zhang, Z.-J. (2023). Global, regional, and national burden of spinal cord injury, 1990–2019: a systematic analysis for the Global Burden of Disease Study 2019. *The Lancet Neurology*, *22*(11), 1026-1047. https://doi.org/10.1016/S1474-4422(23)00287-9

Saini, G., Segaran, N., Mayer, J. L., Saini, A., Albadawi, H., & Oklu, R. (2021). Applications of 3D Bioprinting in Tissue Engineering and Regenerative Medicine. *J Clin Med*, *10*(21). https://doi.org/10.3390/jcm10214966

Scheff, S. W., Saucier, D. A., & Cain, M. E. (2002). A Statistical Method for Analyzing Rating Scale Data: The BBB Locomotor Score. *Journal of Neurotrauma*, *19*(10), 1251-1260. https://doi.org/10.1089/08977150260338038

Shao, A., Tu, S., Lu, J., & Zhang, J. (2019). Crosstalk between stem cell and spinal cord injury: pathophysiology and treatment strategies. *Stem Cell Research & Therapy*, *10*(1), 238. https://doi.org/10.1186/s13287-019-1357-z

Sharma, A., Mücke, M., & Seidman, C. E. (2018). Human Induced Pluripotent Stem Cell Production and Expansion from Blood using a Non-Integrating Viral Reprogramming Vector. *Curr Protoc Mol Biol*, *122*(1), e58. https://doi.org/10.1002/cpmb.58

Shiplu Roy, C., Yogeswaran, L., Law Jia, X., Fauzi Mh, B., Muhammad Dain, Y., Nadiah, S., Gargy, L., & Md Enamul, H. (2020). 3D Printed Bioscaffolds for Developing Tissue-Engineered Constructs. In Y. Evren, M. Mohsen, & S. Eleonora (Eds.), *Design and Manufacturing* (pp. Ch. 11). IntechOpen. https://doi.org/10.5772/intechopen.92418

Singh, N., Guha, L., & Kumar, H. (2024). From hope to healing: Exploring the therapeutic potential of exosomes in spinal cord injury. *Extracellular Vesicle*, *3*, 100044. https://doi.org/https://doi.org/10.1016/j.vesic.2024.100044

Srivastava, M., Banerjee, S., Bairagi, S., Singh, P., Kumar, B., Singh, P., Kale, R. D., Mulvihill, D. M., & Ali, S. W. (2024). Recent progress in molybdenum disulfide (MoS2) based flexible nanogenerators: An inclusive review. *Chemical Engineering Journal*, *480*, 147963. https://doi.org/https://doi.org/10.1016/j.cej.2023.147963

Strøm, V., Månum, G., Arora, M., Joseph, C., Kyriakides, A., Le Fort, M., Osterthun, R., Perrouin-Verbe, B., Postma, K., & Middleton, J. (2022). Physical Health Conditions in Persons with Spinal Cord Injury Across 21 Countries Worldwide. *J Rehabil Med*, *54*, jrm00302. https://doi.org/10.2340/jrm.v54.2040

Thakur, N., Kumar, P., Sati, D. C., Neffati, R., & Sharma, P. (2022). Recent advances in two-dimensional MXenes for power and smart energy systems. *Journal of Energy Storage*, *50*, 104604. https://doi.org/https://doi.org/10.1016/j.est.2022.104604

Thanaskody, K., Jusop, A. S., Tye, G. J., Wan Kamarul Zaman, W. S., Dass, S. A., & Nordin, F. (2022). MSCs vs. iPSCs: Potential in therapeutic applications. *Front Cell Dev Biol*, *10*, 1005926. https://doi.org/10.3389/fcell.2022.1005926

Tominami, K., Kudo, T. A., Noguchi, T., Hayashi, Y., Luo, Y. R., Tanaka, T., Matsushita, A., Izumi, S., Sato, H., Gengyo-Ando, K., Matsuzawa, A., Hong, G., & Nakai, J. (2024). Physical Stimulation Methods Developed for In Vitro Neuronal Differentiation Studies of PC12 Cells: A Comprehensive Review. *Int J Mol Sci*, *25*(2). https://doi.org/10.3390/ijms25020772

Tripathi, S., Mandal, S. S., Bauri, S., & Maiti, P. (2023). 3D bioprinting and its innovative approach for biomedical applications. *MedComm (2020)*, *4*(1), e194. https://doi.org/10.1002/mco2.194

Urrutia, D. N., Caviedes, P., Mardones, R., Minguell, J. J., Vega-Letter, A. M., & Jofre, C. M. (2019). Comparative study of the neural differentiation capacity of mesenchymal stromal cells from different tissue sources: An approach for their use in neural regeneration therapies. *PLOS ONE*, *14*(3), e0213032. https://doi.org/10.1371/journal.pone.0213032

Vanaei, S., Parizi, M. S., Vanaei, S., Salemizadehparizi, F., & Vanaei, H. R. (2021). An Overview on Materials and Techniques in 3D Bioprinting Toward Biomedical Application. *Engineered Regeneration*, *2*, 1-18. https://doi.org/https://doi.org/10.1016/j.engreg.2020.12.001

Ventura, R. D. (2021). An Overview of Laser-assisted Bioprinting (LAB) in Tissue Engineering Applications. *Medical Lasers*, *10*(2), 76-81. https://doi.org/10.25289/ML.2021.10.2.76

Wang, G., Heimendinger, P., Ramelmeier, R. A., & Wang, W. (2022). Pluripotent stem cell-based cell therapies: Current applications and future prospects. *Current Opinion in Biomedical Engineering*, *22*, 100390. https://doi.org/https://doi.org/10.1016/j.cobme.2022.100390

Wang, J., Shen, M., Liu, Z., & Wang, W. (2022). MXene materials for advanced thermal management and thermal energy utilization. *Nano Energy*, *97*, 107177. https://doi.org/https://doi.org/10.1016/j.nanoen.2022.107177

Wang, Y., Che, H., Qu, L., Lu, X., Dong, M., Sun, B., & Guan, H. (2024). The role of nanomaterials in revolutionizing ischemic stroke treatment: Current trends and future prospects. *iScience*, *27*(12), 111373. https://doi.org/https://doi.org/10.1016/j.isci.2024.111373

Wobus, A. M. (2001). Potential of embryonic stem cells. *Mol Aspects Med*, *22*(3), 149-164. https://doi.org/10.1016/s0098-2997(01)00006-1

Xia, Z., Jin, S., & Ye, K. (2018). Tissue and Organ 3D Bioprinting. *SLAS Technology*, *23*(4), 301-314. https://doi.org/https://doi.org/10.1177/2472630318760515

Ye, L., Swingen, C., & Zhang, J. (2013). Induced pluripotent stem cells and their potential for basic and clinical sciences. *Curr Cardiol Rev*, *9*(1), 63-72. https://doi.org/10.2174/157340313805076278

Yu, J., Park, S. A., Kim, W. D., Ha, T., Xin, Y.-Z., Lee, J., & Lee, D. (2020). Current Advances in 3D Bioprinting Technology and Its Applications for Tissue Engineering. *Polymers*, *12*(12), 2958. https://www.mdpi.com/2073-4360/12/12/2958

Zeng, C.-W., & Zhang, C.-L. (2023). Neuronal regeneration after injury: a new perspective on gene therapy [Opinion]. *Frontiers in Neuroscience*, *17*. https://doi.org/10.3389/fnins.2023.1181816

Zeng, C. W. (2023). Advancing Spinal Cord Injury Treatment through Stem Cell Therapy: A Comprehensive Review of Cell Types, Challenges, and Emerging Technologies in Regenerative Medicine. *Int J Mol Sci*, *24*(18). https://doi.org/10.3390/ijms241814349

APPENDIXS

Appendix-1

	Technical Universal Verification Belgelendirme Laboratuvar Eğitim Ve Sağlık Hizmetleri San. Tic. Ltd. Şti.	Doküman Kodu/ Document Code	FR.94
		Yürürlük Tarihi/ Effective date	05.05.2022
		Revizyon No/ Revision No	01
		Revizyon Tarihi/ Revision Date	26.01.2023
		Sayfa/ Page	1/1
HAYVAN DENEYLERI YEREL ETIK KURUL KARARI ONAY FORMU/ ANIMAL EXPERIMENTS LOCAL ETHICS COMMITTEE DECISION PERMISSION FORM			

Technical Universal Verification Yerel Etik Kurulu Yönergesi'ne göre aşağıda belirtilen kapsamda bahsi geçen çalışmanın yapılmasına oy çokluğu / oy birliği ile karar verilmiştir.

Toplantı Tarihi/ Meeting Date	21.06.2023
Toplantı No/ Meeting No	0020/2023
Etik Kurul No/ Ethical Committee No	EKN.0028/2023/01
Karar No/ Decision No	KN.0028/2023/01
Çalışmanın Adı/ Name of The Research	İnsan uPK Hücrelerinden Farklılaştırılmış Nöral Kök Hücreler ve Farklı Nanomalzemelerin 3-Boyutlu Biyobaskılanması ile Elde Edilen Doku İskelelerinin Nöral Rejenerasyonda Kullanımı
Çalışmanın Yürütücüsü/ Coordinator of The Research	Doç. Dr. Açelya YILMAZER AKTUNA
Çalışmanın Talep Edildiği Kurum-Kuruluş/ Institution-Organization Where The Research is Requested	Ankara Üniversitesi Mühendislik Fakültesi, Biyomedikal Mühendisliği
Çalışmada Kullanılacak Hayvanın Türü/ The Species of The Animal To Be Used in The Research	Sıçan (Wistar Albino)
Çalışmada Kullanılacak Hayvanın Cinsiyeti/ Gender of The Animal To Be Used in The Research	Erkek ve Dişi (4-6 haftalık)
Çalışmada Kullanılacak Hayvanın Sayısı/ Number of The Animals To Be Used in The Research	100
Geçerlilik Süresi/ Period of Availability	1 yıl

ETİK KURUL ÜYELERİ / MEMBERS OF ETHIC COMMITTEE			
Adı-Soyadı/ Name-Surname	**Unvanı/** Title	**Görevi/** Position	**İmzası/** Signature
Gizem ARALAN	Dr. Veteriner Hekim	Etik Kurul Başkanı	
Serdar AYYILDIZ	Genel Müdür	Etik Kurul Başkan Yrd.	
Ahmet Çevik TUFAN	Prof. Dr.	Etik Kurul Başkan Yrd.	
Gülben AKCAN	Dr. Biyolog	In Vivo Sorumlusu	
Betül ÇAĞLIOĞLU	Genel Koordinatör/Biyolog	Üye	
Tuğba ŞİMŞİR	Biyolog	Üye	
Murat Ekin ERDOĞAN	İç Mimar	STK Üyesi	

Appendix-2

İNSAN ARAŞTIRMALARI ETİK KURULU KARAR FORMU

ETİK KURULUN ADI	ANKARA ÜNİVERSİTESİ TIP FAKÜLTESİ İNSAN ARAŞTIRMALARI ETİK KURULU
AÇIK ADRES	Ankara Üniversitesi Tıp Fakültesi Morfoloji Binası 06100 Sıhhıye/ANKARA
TELEFON	0312 595 82 27
E-POSTA	tipinsanetik@ankara.edu.tr

BAŞVURU BİLGİLERİ	ARAŞTIRMANIN AÇIK ADI	Başvuru No: 2024000363(2024/363) İnsan uPK Hücrelerinden Farklılaştırılmış Nöral Kök Hücreler ve Farklı Nanomalzemelerin 3-Boyutlu Biyobaskılanması ile Elde Edilen Doku İskelelerinin Nöral Rejenerasyonda Kullanımı	
	KOORDİNATÖR/SORUMLU ARAŞTIRMACI ÜNVANI/ADI/SOYADI	Doç. Dr. Açelya YILMAZER AKTUNA	
	PROJE YÜRÜTÜCÜSÜ UNVANI/ADI/SOYADI (TÜBİTAK vb. gibi kaynaklardan destek alanlar için)		
	KOORDİNATÖR/SORUMLU ARAŞTIRMACININ UZMANLIK ALANI	Tıbbi Biyoloji ve Genetik	
	KOORDİNATÖR/SORUMLU ARAŞTIRMACININ BULUNDUĞU MERKEZ	Ankara Üniversitesi Biyomedikal Mühendisliği	
	ARAŞTIRMAYA KATILAN MERKEZLER	TEK MERKEZ ☒	ÇOK MERKEZLİ ☐

KARAR BİLGİLERİ	**Karar No:İ06-415-24**	**Tarih: 13 Haziran 2024**
	Yukarıda bilgileri verilen başvuru dosyası ile ilgili belgeler araştırmanın/çalışmanın gerekçe, amaç, yaklaşım ve yöntemleri dikkate alınarak incelenmiş ve uygun bulunmuş olup araştırmanın/çalışmanın başvuru dosyasında belirtilen merkezde gerçekleştirilmesinde etik ve bilimsel sakınca bulunmadığına toplantıya katılan etik kurul üye tam sayısının salt çoğunluğu ile karar verilmiştir.	

İNSAN ARAŞTIRMALARI ETİK KURULU	
ÇALIŞMA ESASI	İyi Klinik Uygulamaları Kılavuzu
BAŞKANIN UNVANI / ADI / SOYADI:	Prof.Dr.Hakan ERGÜN

Unvanı/Adı/Soyadı	Uzmanlık Alanı	Kurumu	Araştırma ile ilişki		İmza
Prof.Dr.Hakan ERGÜN	Tıbbi Farmakoloji	A.Ü. Tıp Fakültesi	E ☐	H ☒	
Prof.Dr.Berna ARDA	Tıp Tarihi ve Etik	A.Ü. Tıp Fakültesi	E ☐	H ☒	
Prof.Dr.Hatice ILGIN RUHİ	Tıbbi Genetik	A.Ü. Tıp Fakültesi	E ☐	H ☒	
Prof.Dr.Sevim AYDIN	Histoloji ve Embriyoloji	A.Ü. Tıp Fakültesi	E ☐	H ☒	
Prof.Dr.Berna SAVAŞ	Tıbbi Patoloji	A.Ü. Tıp Fakültesi	E ☐	H ☒	
Prof.Dr.Yüksel ÜRÜN	Tıbbi Onkoloji	A.Ü.Tıp Fakültesi	E ☐	H ☒	
Prof.Dr.Başak Ceyda MEÇO	Anesteziyoloji ve Reanimasyon	A.Ü. Tıp Fakültesi	E ☐	H ☒	
Doç.Dr.Emel OKULU	Çocuk Sağlığı ve Hastalıkları	A.Ü. Tıp Fakültesi	E ☐	H ☒	
Doç.Dr.Zahide Çiler BÜYÜKATALAY YALDIZ	Kulak, Burun ve Boğaz Hastalıkları	A.Ü. Tıp Fakültesi	E ☐	H ☒	
Doç.Dr.Rezzak YILMAZ	Nöroloji	A.Ü. Tıp Fakültesi	E ☐	H ☒	
Doç.Dr.Serkan AKBULUT	Cerrahi Onkoloji	A.Ü. Tıp Fakültesi	E ☐	H ☒	
Doç.Dr.Miraç YILDIRIM	Çocuk Sağlığı ve Hastalıkları	A.Ü. Tıp Fakültesi	E ☐	H ☒	
Dr.Öğr.Üyesi Can Yahya BOZTUĞ	Genel Cerrahi	A.Ü. Tıp Fakültesi	E ☐	H ☒	
Dr.İrem KAR	Biyoistatistik	A.Ü. Tıp Fakültesi	E ☐	H ☒	

Appendix-3

Criteria Used for BBB Analysis

BBB Score	BBB Criteria
0	No observabie hindlimb (HL) movement
1	Sight movement of one or two joints, usualy the hip and/or knee
2	Extensive movement of one joint ox extensive movement of one joint and sight movement of one other jpoint
3	Extensive movement of two joints
4	Sight movement of al three joints of the HL
5	Sight movement of two joints and extensive movement of the third
6	Extensive movement of of two joints and stight movement of the third
7	Extensive movement of all three jpints of the HL
8	Sweeping with no weight support ox plantar placement of tihe paw with no weight support
9	Plantar placement of the paw with weight support in stance ony f,e, when stationary) or ocasional, frequent, ar consistent weight-supported dorsal stepping and no plantar stepping
10	Occasional weight-supported plantar steps; no FL-HL coordination
11	Frequent to consistent weight-supported plantar steps and no FL-HL coordination
12	Frequent to consistent weight-supported plantar steps and occasional FL-HL coordination
13	Frequent to consistent weight-supported plantar steps and frequent FL-HL coordination
14	Consistent weight-supported plantar steps, consistent FL-HL coordination, and predorminant paw position during locomotion is rotated (internaly or exteraly) when it makes initial contact with the surface as wel as just before it lifted off at the end of stance: or requent plantar stepping, consistent FL-HL cooxdination, and occasional dorsal stepping
15	Consistent plantar stepping, consistent FL-HL coordination, and no toe clearance or occasional toe clearance during foward limb advancement; predorminant parw position is pararelle to the body at initial contact
16	Consistent plantar stepping, consistent FL-HL coordination, and toe clearance occurs frequently during forward imb advancement: predorminant paw position is pararelle at initial contact and rotated at Ift off
17	Consistent plantar stepping, consistent FL-HL coordination, and toe clearance occurs frequentiy during lorward imb advancement: predorminant paw position is pararelle at nitial contact and ift off
18	Consistent plantar stepping, consistent FL-HL coordination, toe clearance occurs consistently during forward imb advancement; predorminant paw position is pararelle at initial contact and rotated at ift off
19	Consistent plantar tepping, consistent FL-HL coordination, toe clearance occurs frequentily during fonward Imb advancement: predominant paw position is pararelle at initial contact and ift of, and tal is down part or al of the time
20	Consistent plantar stepping and consistent coordinated gait, consistent toe clearance, predominant paw position is pararele at initial contact and lift off, and turn instability; tall consistently up
21	Consistent plantar stepping and consistent FL-HL coordination during gait; and toe clearance occurs frequently during forward limb advancement; predominant paw position is parallel at initial contact and rotated at lift off